Macromolecular Crowding Effects on Globular Protein Stability

Andrew C. Miklos

A dissertation submitted to the faculty of the University of North Carolina at Chapel Hill in partial fulfillment of the requirements for the degree of Doctor of Philosophy in the Department of Chemistry

Chapel Hill
2010

Approved by:

Max Berkowitz

Matthew Redinbo

Andrew Lee

Gary Pielak

Michael Rubinstein

Abstract

Andrew C. Miklos: Macromolecular Crowding Effects on Globular Protein Stability
(Under the direction of Professor Gary J. Pielak, Ph.D.)

Macromolecular crowding inside cells is proposed to change many aspects of proteins compared to dilute solution. As such, it is an increasingly studied topic, both theoretically and experimentally. However, the difficulty of both theoretically modeling the intracellular milieu and manipulating its contents experimentally present roadblocks to a full picture of crowding inside cells. *In vitro* studies of macromolecular crowding allow us to study the effects of crowding agent identity, size, and concentration on globular protein stability in a highly controllable fashion. I used NMR-detected amide proton exchange to study the effects of poly(vinylpyrrolidone) at varying molecular weights and concentrations on the stability of chymotrypsin inhibitor 2. This residue-level study is the first to reveal both volume exclusion and weak interaction effects as contributors to protein stability in crowded conditions. I also studied the effects of a microgel crowder on the stability and dynamics of chymotrypsin inhibitor 2, displaying an upper limit to the size effect of crowding agents. This study also revealed no link between protein stability and ps-ns timescale backbone dynamics. Amide proton exchange was also used to study the effects of bovine serum albumin and lysozyme as crowding agents on chymotrypsin inhibitor 2.

This is the first reported study of protein stability when subjected to crowding by another protein, and provides some important implications for the stability of proteins inside cells.

Acknowledgements

As with any sufficiently complex system, this work could not have been completed without the assistance of many people whose efforts lay both inside and outside the realm of “scientific contribution.” To my parents: You have always been supportive of my decisions and have provided me with valuable advice, useful resources, and endless care packages. To my brother, Aleksandr: You have constantly been forging the path that I later tread, and in doing so, have made my travels infinitely easier. Hopefully I can repay the favor down the line by starting down a path you want to follow. To the Fellowship: Your friendship has always been the mold to which I compare to all others. Wherever we may be, it is never too far away to keep in touch. To Brian: Our lunch breaks have always been a welcome change of pace to the day and our conversations have always been illuminating, whether scientific or not. To Pam: Thanks for doing all the worrying about my dissertation for me. I’m sure your dissertation will be less stressful. I would also like to thank Gary Pielak for helping me through the process, and the entire Pielak lab for their assistance throughout.

Table of Contents

List of Tables

List of Figures

List of Abbreviations and Symbols

BSA	bovine serum albumin
c*	overlap concentration
CD	circular dichroism
CI2	chymotrypsin inhibitor 2
CLEANEX-PM	phase-modulated CLEAN chemical EXchange
CRABP	cellular retinoic acid binding protein
FPLC	fast protein liquid chromatography
$\Delta G_{op}^{0'}$	standard state free energy of opening
HSQC	heteronuclear single quantum correlation
IPTG	isopropyl β-D-1-thiogalactopyranoside
k_{cl}	rate of closing
$K_{op}^{0'}$	equilibrium constant for opening
k_{int}	intrinsic rate of exchange
k_{obs}	overall rate of exchange
k_{op}	rate of opening
LB	Luria broth
$\overline{M}_N$	number average molecular weight
$\overline{M}_W$	weight average molecular weight
MALLS	multi-angle laser light scattering
NIPAm-AAc	poly(*N*-isopropylacrylamide-*co*-acrylic acid)
NMR	nuclear magnetic resonance

NOE	nuclear Overhauser effect
NOESY	nuclear Overhauser enhancement spectroscopy
NOESY-HEX	NOESY-detected amide proton exchange
PEG	poly(ethylene glycol)
PVDF	poly(vinylidene fluoride)
PVP	poly(vinylpyrrolidone)
QELS	quasielastic light scattering
R_1	longitudinal relaxation rate
R_2	transverse relaxation rate
R_H	hydrodynamic radius
R_G	radius of gyration
S^2	order parameter
SE	Stokes-Einstein
SED	Stokes-Einstein-Debye
SPHERE	server program for hydrogen exchange rate estimation
T_1	longitudinal relaxation time
T_2	transverse relaxation time
τ_e	timescale of internal motion
TMAO	trimethylamine N-oxide
$\bar{v}_2$	partial specific volume

1 Introduction

1.1 Background and Motivation

Macromolecules can reach concentrations up to 400 g/L inside cells.[1-3] The effects of macromolecular crowding, which cannot be replicated in dilute solution, can have implications for intracellular protein function. As discussed below, previous work has shown effects on protein structure, association, aggregation, diffusion, enzyme activity, and stability. My work focuses on the effects of macromolecular crowding on stability and dynamics, and addresses the differences between hard and soft interactions present in crowded environments. Hard interactions arise from impenetrability of two particles in solution, and are also known as volume exclusion effects. Soft interactions encompass most other effects, and arise from through-distance attractive and repulsive chemical interactions in solution. To depict the current depth and breadth of knowledge of crowding, I present here a summary of selected experimental results from the last ten years.

Our group demonstrated that crowding inside cells can induce structure in the disordered protein FlgM,[4] and later found that crowding can maintain compact disordered states.[5] Roque *et al.* presented similar results, noting an induced molten globular state of a disordered domain in histone H1 upon adding synthetic polymer crowding agents.[6] Confined spaces have also been seen to

induce structural changes. Eggers and Valentine noticed that apomyoglobin became unfolded when embedded in sol-gel matrices,[7] while Peterson *et al.* saw proteins that were normally unfolded in dilute solution gain structure when confined within reverse micelles.[8] Lu and Deutsch detected compaction using a nascent chain polypeptide confined inside the ribosome exit tunnel.[9] A comprehensive study of crowding-induced structural changes by Homouz *et al.* demonstrated that a crowded solution of Ficoll 70 induces structural changes in VlsE, changing it from an oblong spheroid to either a "bean" or a sphere.[10] This result shows that crowding-induced changes can cause proteins to assume shapes inaccessible in dilute solution, suggesting that proteins crowded inside cells have functions that cannot be replicated in dilute solution.

Association is another protein function that is altered in crowded conditions. Generally, enhanced association is expected in environments with large amounts of volume exclusion. Such increases are seen for apomyoglobin dimerization in solutions crowded by RNase A,[11] bovine pancreatic trypsin inhibitor decamer formation in the presence of high concentrations of dextran,[12] and chymotrypsin A association induced by self-crowding.[13] Phillip *et al.,* however, have reported high concentration synthetic polymer systems that exhibit minimal effects on association.[14] Protein crowders have also been shown to enhance the binding affinity of RepA for DNA.[15] Akin to association, protein assembly and aggregation are also expected to be favored by crowding.

Formation of protein assemblies and aggregates is expected to be enhanced in crowded solutions, as it alleviates the problem of accessible

solution. To distinguish the two, assemblies generally have a biological function, whereas aggregates are typically associated with sequestration of protein rather than incorporation into a functional form. As seen in the work of del Alamo *et al.*[16] and Fu *et al.*,[17] solutions crowded by synthetic polymers enhance assembly rates of HIV and bacteriophage capsids, respectively. In the case of aggregation, α-synuclein is known to fibrillize faster in the presence of several crowding agents.[18] For proteins that do not exhibit association, assembly, or aggregation, it is also possible to study crowding effects on diffusion.

Diffusion in crowded conditions is expected to be slower than diffusion in dilute solution. Specifically, the Stokes-Einstein (SE) and Stokes-Einstein-Debye (SED) laws predict that in certain conditions, diffusion rates are time-independent, and are related to the viscosity of the solution.[19] Because crowding agents increase the viscosity of solution, it is predicted that they should decrease diffusion rates. Work has shown, however, that the constituents of the crowding environment can lead to deviations from this law. Our lab used Nuclear Magnetic Resonance (NMR) to determine that synthetic polymer crowders cause proteins to diffuse at faster rates than SE/SED would predict, and that protein and lysate crowders actually slow diffusion compared to SE/SED.[19, 20] These studies showed a fundamental difference between the effects of crowding by synthetic polymers and crowding by proteins. Others have investigated a phenomenon known as anomalous diffusion in crowded environments. Anomalous diffusion involves diffusion rates that are time-dependent, as opposed to constant diffusion rates in the case of SE/SED.[21] Guigas *et al.* used

fluorescence correlation spectroscopy in mammalian cells and found that the cytoplasm and nucleoplasm both exhibit anomalous diffusion.[22] Similarly, this phenomenon has been observed by Banks and Fradin in solutions crowded by dextran, a synthetic polymer.[23] In keeping with studying diffusion and association, enzyme activity has been a topic of interest in the crowding community.

Because of the multiple steps required for enzymatic activity, predictions of crowding effects vary depending on rate limits.[24] For instance, enzyme activity may decrease with crowder concentration, or it may show an initial increase in activity with crowder concentration and then drop upon further crowder addition. Recent results showcase both effects. Derham and Harding observed a constant decrease in activity for urease, pyruvate decarboxylase, and glutamate decarboxylase in concentrated solutions of dextran and poly(ethylene glycol) (PEG).[25] For protein crowders, however, the latter trend is noted, pointing again to differences between crowding-induced effects of proteins and synthetic polymers. It is possible that this difference is also present when studying globular protein stability in crowded conditions.

Among the subcategories of crowding effects, equilibrium thermodynamic stability of globular proteins is the most divisive. Some believe that crowding exhibits a strong stabilizing effect (up to 3 kcal/mol stabilization), while others think that the effect is more modest (less than 1 kcal/mol stabilization). Until recently, however, no one has suggested that crowding can be destabilizing. Results can be found to support all these beliefs. Due to the nature of techniques used to study protein stability (discussed later), no study has been conducted to

determine the effect of protein crowders on test protein stability. Evidence for strong crowding-induced stabilization can be seen in work performed by our group using chymotrypsin inhibitor 2 (CI2; PDB 2CI2) crowded by poly(vinylpyrrolidone) (PVP), resulting in CI2 stabilization upwards of 3 kcal/mol (a 50% increase from dilute solution stability for the variant used).[26] Additionally, 300 g/L dextran has been shown to increase the mechanical stability of ubiquitin by 20%,[27] Ficoll stabilizes the secondary structure of VlsE and flavodoxin,[28, 29] and PEG can return RNase A to its native fold in 2.4 M urea.[30] Others have noted a more modest stabilizing effect. For instance, Qu and Bolen report only a 1 kcal/mol increase in stability for ribonuclease T_1 in 400 g/L dextran.[31] Similarly, the stability of λ repressor was studied in cells, and showed no change from dilute solution.[32] Experiments in cells[33] and in Ficoll[34] even show mild destabilization of cellular retinoic acid binding protein (CRABP). With results that range from large stabilization to mild destabilization, it would seem difficult to come to a consensus about crowding effects on protein stability.

As shown in the past decade, the field of crowding is a veritable alphabet soup of test proteins and crowding agents, with no agreed-upon “perfect model” system to characterize crowding effects. Also, few systematic studies have been undertaken, so despite the glut of data, integration of the work into general knowledge is difficult due to the significant breadth but inadequate depth of study. Even the theory behind crowding has multiple models with conflicting accounts for the magnitude of proposed effects on proteins. Much of the theoretical framework arises from work over 50 years old by Ogsten and

Laurent,[35, 36] which focuses on the effect of excluded volumes on protein properties.

Theoretical treatments of volume exclusion involve a simple model of the crowded environment, which is addressed in two different ways. The crowding agent, in solution, can either present the test particle with a high concentration of impenetrable hard spheres, or a network of confining spaces. Both models rely solely on hard interactions between test particle and crowder. That is, volume exclusion is the result of impenetrable crowding agents occupying solvent space, removing volume otherwise accessible to the test particle.[37] In the crowded environment, particles are subjected to an entropic penalty if they have a large covolume with the crowder. The covolume can be thought of as the volume in which the center of mass of the test particle cannot exist due to the presence of the crowder.[38] No attractive forces exist in this system, and the most compact species of test particle is favored. Next, I discuss the implications of volume exclusion on protein stability.

The stability of globular proteins is defined as the position of the equilibrium between a native, structural state and an unfolded, thermodynamic state.[39] Because globular proteins are biologically active only in the native, folded state, any change in stability can alter their activity within cells. When considering crowding, unfolded states have larger covolumes because of their larger hydrodynamic radii (R_H) compared to the native state.[40] This results in a larger entropic penalty for the unfolded state. As a result, volume exclusion is expected to only increase protein stability, and does so by destabilizing the denatured

state. This topic will be revisited in chapter 2, focusing on local openings. However, the specifics of the two major exclusion models, hard particle exclusion and confinement, result in different predictions for the effects of crowding agent size and concentration on protein stability.

For volume exclusion by hard particle spheres, the key parameters are sphere size and number density. These parameters correspond directly to the variables of molecular weight and concentration of the crowding agent, respectively. In the case of independent hard sphere crowders, it is expected that stability will increase with increasing crowder concentration, but larger crowding agents should have less of a stabilizing effect.[41] For confinement, the shape and size of the confining space are key parameters, but these parameters do not correspond directly to molecular weight and crowder concentration. Nevertheless, increasing the concentration of the crowding agents should decrease the average size of a confining space, resulting in more stabilization. The molecular weight of a crowder, however, is not expected to change the size or shape of confining spaces, and should have no effect on stability. There is disagreement on the magnitude and relative contribution of these two models. Specifically, some claim that confinement has a larger effect on protein stability, while others believe that hard particle exclusion can be just as effective.

The conflicting theories and experimental results pose major questions about the relationship between stability and crowding. First and foremost, why do in-cell results of stability show destabilization while most *in vitro* studies show stabilization? Is it due to the difference between synthetic polymer crowding and

protein crowding? Second, do synthetic polymers provide an accurate model for the crowded environment in cells? Finally, are there important factors that cannot be captured by pure volume exclusion models? The studies that I have performed should help inform these questions, and lead us to improved theoretical models. With regards to these theoretical improvements, some progress has already been made involving soft interactions.

Both types of volume exclusion (hard particle exclusion and confinement) can be present inside cells, as globular proteins can be represented by hard particles, whereas cytoskeletal elements and chaperonins can provide confining spaces. In addition to hard particles and confining spaces, the inside of a cell is rife with through-distance, chemical interactions between proteins. These "soft" chemical interactions (as opposed to hard particle interactions) can have stabilizing or destabilizing effects, and have not been explicitly addressed in any theoretical treatment of crowding until recently. Previously, soft terms have been incorporated into hard particle crowding by changing the size of the crowding particle or otherwise parameterizing the system, resulting in a semi-empirical model that does not have predictive capability.[42] In 2010, McGuffee and Elcock provided a theoretical treatment of crowding effects that includes weak interactions and uses realistic concentrations and structures of actual proteins present in cells.[43] Thusfar, the work of McGuffee and Elcock is the most comprehensive simulation of crowding inside cells, and provides a model that can be compared to results from in-cell studies of protein stability. To further

validate this work, more studies must be conducted in physiologically relevant conditions.

Direct determination of protein stability inside cells, however, is difficult. Only two quantitative studies have been reported on equilibrium thermodynamic protein stability *in vivo*. Ghaemmaghami and Oas used mass spectrometry to determine the in-cell stability of λ repressor,[32] while Ignatova *et al.* chose fluorescence spectrometry to study the stability of CRABP.[33] These seminal studies found that the proteins tested had either unchanged or slightly lower stabilities in cells. These results hint at the previously mentioned difference between synthetic polymer crowders and protein crowders seen in diffusion and enzyme activity. In both cases, the complexity of the intracellular environment precludes systematic studies that determine the effect of crowder concentration and identity in a controlled fashion. Most troublesome, however, is the fact that both studies require the use of denaturants to assess stability. For fluorescence studies, a transition from native state to denatured state must be induced using a perturbant (temperature or denaturant), and results must be extrapolated to the absence of perturbant to obtain stability values. For mass spectrometry, denaturants are not necessary, but can be used in a similar fashion. Denaturants are excellent in dilute solution systems with only protein and denaturant, but can become problematic when more components are added.

Adding adulterants to a crowded system can confound stability analysis. The change in stability upon addition of a denaturant such as urea could be the result of a direct interaction between urea and the protein studied, or an effect

mediated by an interaction between urea and a crowding agent in solution. Interactions between synthetic polymers and common denaturants have been reported.[44] In the case of protein crowders, it is apparent that analysis can become difficult, as the crowding agent can experience drastic changes in properties as it denatures. A model system for studying crowding effects should not only avoid the use of denaturants, but also facilitate systematic, reductionist studies.

The use of macromolecular crowding agents for *in vitro* reductionist studies allows tight control of the environment experienced by the protein being studied (pH, temperature, concentration, identity of crowder). Additionally, this reduced system is simpler to model, allowing future correlation of theoretical frameworks with experimental results. For stability, these results can quantify the effect of concentration, molecular weight, and chemical identity of the crowder. Ideally, the technique used to study stability in crowded conditions should allow for reductionist experiments to be performed without the use of adulterants. NMR-detected amide proton exchange is such a technique.

I used NMR-detected amide proton exchange to study crowding effects on globular protein stability in three systems. I performed a systematic study of the effects of PVP crowding on CI2 and assessed volume exclusion effects in terms of both hard particle exclusion and confinement, also finding evidence for weak native-state binding. I performed a study using a gigantic tunable microgel to establish an upper limit on crowder size for notable crowding effects. Finally, I performed the first extensive study of globular protein stability in an environment

crowded by other proteins, with implications for weak destabilizing interactions that compete with the stabilizing effect of volume exclusion. A review of the techniques used to perform these experiments and the necessary controls follows.

1.2 References

1. Luby-Phelps, K. (2000) Cytoarchitecture and physical properties of cytoplasm: Volume, viscosity, diffusion, intracellular surface area, *Int. Rev. Cytol.* **192**, 189-221.

2. Malmström, J., Beck, M., Schmidt, A., Lange, V., Deutsch, E. W., and Aebersold, R. (2009) Proteome-wide cellular protein concentrations of the human pathogen Leptospira interrogans, *Nature* **460**, 762-765.

3. Zimmerman, S. B., and Trach, S. O. (1991) Estimation of macromolecule concentrations and excluded volume effects for the cytoplasm of *Escherichia coli*, *J. Mol. Biol.* **222**, 599-620.

4. Dedmon, M. M., Patel, C. N., Young, G. B., and Pielak, G. J. (2002) FlgM gains structure in living cells, *Proc. Natl. Acad. Sci. U.S.A.* **99**, 12681-12684.

5. McNulty, B. C., Young, G. B., and Pielak, G. J. (2006) Macromolecular crowding in the Escherichia coli periplasm maintains alpha-synuclein disorder, *J. Mol. Biol.* **355**, 893-897.

6. Roque, A., Ponte, I., and Suau, P. (2007) Macromolecular crowding induces a molten globule state in the C-terminal domain of histone H1, *Biophys. J.* **93**, 2170-2177.

7. Eggers, D. K., and Valentine, J. S. (2001) Molecular confinement influences protein structure and enhances thermal protein stability, *Protein Sci.* **10**, 250-261.

8. Peterson, R. W., Anbalagan, K., Tommos, C., and Wand, A. J. (2004) Forced folding and structural analysis of metastable proteins, *J. Am. Chem. Soc.* **126**, 9498-9499.

9. Lu, J., and Deutsch, C. (2005) Folding zones inside the ribosomal exit tunnel, *Nat. Struct. Mol. Biol.* **12**, 1123-1129.

10. Homouz, D., Perham, M., Samiotakis, A., Cheung, M. S., and Wittung-Stafshede, P. (2008) Crowded, cell-like environment induces shape changes in aspherical protein, *Proc. Natl. Acad. Sci. U.S.A.* **105**, 11754-11759.

11. Zorrilla, S., Rivas, G., Acuna, A. U., and Lillo, M. P. (2004) Protein self-association in crowded protein solutions: A time-resolved fluorescence polarization study, *Protein Sci.* **13**, 2960-2969.

12. Snoussi, K., and Halle, B. (2005) Protein self-association induced by macromolecular crowding: A quantitative analysis by magnetic relaxation dispersion, *Biophys. J.* **88**, 2855-2866.

13. Fernández, C., and Minton, A. P. (2009) Static light scattering from concentrated protein solutions II: Experimental test of theory for protein mixtures and weakly self-associating proteins, *Biophys. J.* **96**, 1992-1998.

14. Phillip, Y., Sherman, E., Haran, G., and Schreiber, G. (2009) Common Crowding Agents Have Only a Small Effect on Protein-Protein Interactions, *Biophysical Journal* **97**, 875-885.

15. Diaz-Lopez, T., Davila-Fajardo, C., Blaesing, F., Lillo, M. P., and Giraldo, R. (2006) Early events in the binding of the pPS10 replication protein RepA to single iteron and operator DNA sequences, *J. Mol. Biol.* **364**, 909-920.

16. del Alamo, M., Rivas, G., and Mateu, M. G. (2005) Effect of macromolecular crowding agents on human immunodeficiency virus type 1 capsid protein assembly *in vitro*, *J. Virol.* **79**, 14271-14281.

17. Fu, C. Y., Morais, M. C., Battisti, A. J., Rossmann, M. G., and Prevelige, P. E. (2007) Molecular dissection of O29 scaffolding protein function in an *in vitro* assembly system, *J. Mol. Biol.* **366**, 1161-1173.

18. Munishkina, L. A., Ahmad, A., Fink, A. L., and Uversky, V. N. (2008) Guiding protein aggregation with macromolecular crowding, *Biochemistry* **47**, 8993-9006.

19. Wang, Y., Li, C., and Pielak, G. J. (2010) Effects of proteins on protein diffusion, *J. Am. Chem. Soc.*, 9392–9397.

20. Li, C. G., Wang, Y. Q., and Pielak, G. J. (2009) Translational and rotational diffusion of a small globular protein under crowded conditions, *J. Phys. Chem. B* **113**, 13390-13392.

21. Havlin, S., and Benavraham, D. (1987) Diffusion in disordered media, *Adv. Phys.* **36**, 695-798.

22. Guigas, G., Kalla, C., and Weiss, M. (2007) The degree of macromolecular crowding in the cytoplasm and nucleoplasm of mammalian cells is conserved, *FEBS Lett.* **581**, 5094-5098.

23. Banks, D. S., and Fradin, C. (2005) Anomalous diffusion of proteins due to molecular crowding, *Biophys. J.* **89**, 2960-2971.

24. Minton, A. P. (1981) Excluded volume as a determinant of macromolecular structure and reactivity, *Biopolymers* **20**, 2093-2120.

25. Derham, B. K., and Harding, J. J. (2006) The effect of the presence of globular proteins and elongated polymers on enzyme activity, *Biochim. Biophys. Acta* **1764**, 1000-1006.

26. Charlton, L. M., Barnes, C. O., Li, C., Orans, J., Young, G. B., and Pielak, G. J. (2008) Macromolecular crowding effects on protein stability at the residue level, *J. Am. Chem. Soc.* **130**, 6826-6830.

27. Ping, G. H., Yang, G. L., and Yuan, H. M. (2006) Depletion force from macromolecular crowding enhances mechanical stability of protein molecules, *Polymer* **47**, 2564-2570.

28. Homouz, D., Sanabria, H., Waxham, M. N., and Cheung, M. S. (2009) Modulation of calmodulin plasticity by the effect of macromolecular crowding, *J. Mol. Biol.* **391**, 933-943.

29. Homouz, D., Stagg, L., Wittung-Stafshede, P., and Cheung, M. S. (2009) Macromolecular crowding modulates folding mechanism of a/b protein apoflavodoxin, *Biophys. J.* **96**, 671-680.

30. Tokuriki, N., Kinjo, M., Negi, S., Hoshino, M., Goto, Y., Urabe, I., and Yomo, T. (2004) Protein folding by the effects of macromolecular crowding, *Protein Sci.* **13**, 125-133.

31. Qu, Y. X., and Bolen, D. W. (2002) Efficacy of macromolecular crowding in forcing proteins to fold, *Biophys. Chem.* **101**, 155-165.

32. Ghaemmaghami, S., and Oas, T. G. (2001) Quantitative protein stability measurement *in vivo*, *Nat. Struct. Biol.* **8**, 879-882.

33. Ignatova, Z., and Gierasch, L. M. (2004) Monitoring protein stability and aggregation *in vivo* by real-time fluorescent labeling, *Proc. Natl. Acad. Sci. U.S.A.* **101**, 523-528.

34. Hong, J., and Gierasch, L. M. Macromolecular Crowding Remodels the Energy Landscape of a Protein by Favoring a More Compact Unfolded State, *Journal of the American Chemical Society* **132**, 10455-10452.

35. Ogston, A. G. (1958) The Spaces in a Uniform Random Suspension of Fibres, *Transactions of the Faraday Society* **54**, 1754-1757.

36. Laurent, T. C., and Ogston, A. G. (1963) Interaction between Polysaccharides and Other Macromolecules .4. Osmotic Pressure of

Mixtures of Serum Albumin and Hyaluronic Acid, *Biochemical Journal* **89**, 249-253.

37. Zhou, H. X., Rivas, G. N., and Minton, A. P. (2008) Macromolecular crowding and confinement: Biochemical, biophysical, and potential physiological consequences, *Annu. Rev. Biophys.* **37**, 375-397.

38. Davis-Searles, P. R., Saunders, A. J., Erie, D. A., Winzor, D. J., and Pielak, G. J. (2001) Interpreting the effects of small uncharged solutes on protein-folding equilibria, *Ann. Rev. Biophys. Biomol. Struct.* **30**, 271-306.

39. Lumry, R., Biltonen, R., and Brandts, J. F. (1966) Validity of the "two-state" hypothesis for conformational transitions of proteins, *Biopolymers* **4**, 917-944.

40. Miller, W. G., and Goebel, C. V. (2002) Dimensions of protein random coils, *Biochemistry* **7**, 3925-3935.

41. Minton, A. P. (1983) The effect of volume occupancy upon the thermodynamic activity of protein: Some biochemical consequences, *Mol. Cell. Biochem.* **55**, 119-140.

42. Elcock, A. H. (2010) Models of macromolecular crowding effects and the need for quantitative comparisons with experiment, *Curr. Opin. Struct. Biol.* **20**, 196-206.

43. McGuffee, S. R., and Elcock, A. H. (2010) Diffusion, crowding & protein stability in a dynamic molecular model of the bacterial cytoplasm, *PLoS Comput. Biol.* **6**, e1000694.

44. Güven, O., and Eltan, E. (1981) Molecular association in aqueous solutions of high molecular weight poly(N-vinyl-2-pyrrolidone), *Makromol. Chem.* **182**, 3129-3134.

2 NMR-Detected Amide Proton Exchange for Determination of Globular Protein Stability

The material in this chapter is from:

Miklos AC, Li C, Pielak GJ. **2009.** *Methods in Enzymology*, 466, 1-18.

2.1 Introduction

There are a number of ways to determine the stability of a protein in solution. For many techniques, however, it can be difficult to detect the target protein in crowded environments, as the crowding agent's weight concentration can be up to two orders of magnitude higher than that of the target protein. Additionally, these methods typically require perturbation of the system to detect unfolded states. As discussed previously, crowding agent interactions with denaturing agents can also hamper certain studies of protein stability, and thermal denaturation can prove just as problematic due to temperature-sensitive properties of some crowding agents. It is also useful to determine the extent of soft interactions present between the crowding agent and the target protein. This information can provide valuable insight regarding the contribution of hard and soft interactions. For full studies of protein stability under crowded conditions, a tool that can detect proteins in high concentrations of crowder to assess stability and interactions is necessary.

Solution-state, high-resolution NMR spectroscopy is that tool. Because only NMR-active nuclei are detected, I can use isotopic enrichment of the target protein not only to remove background signals due to crowding agents, but also to simplify protein spectra.[1] For the work described here, the NMR-active isotope is ^{15}N. NMR-detected backbone amide proton exchange is a technique that allows residue-level stability determination without the use of perturbants.[2] Other experiments discussed below allow us to determine the extent of interaction between protein and crowding agent. For amide proton exchange experiments, ^{15}N-^{1}H Heteronuclear Single Quantum Correlation (HSQC) spectra are obtained.[3, 4] These spectra correlate the chemical shift of an ^{15}N nucleus with its attached proton. The result is a crosspeak for each non-proline backbone amide bond and for most nitrogen-containing side chains. Figure 2.1 depicts a characteristic HSQC spectrum for CI2 with some residues labeled. I will focus on the backbone amide resonances. The volume of a crosspeak corresponds to the concentration of the N-H group. Knowledge of the ^{15}N and ^{1}H chemical shift assignments for these residues is a prerequisite for amide proton exchange. As described below, the exchange of the amide proton for a deuteron can be used to assess protein stability.

2.2. Mechanism and Limits of Amide Proton Exchange

Consider a short unstructured peptide in aqueous solution. Its amide protons react reversibly with hydroxide ions and then H_2O, with the net result that the amide protons exchange with protons from H_2O. The kinetics of exchange

are pseudo first order, and can be catalyzed by both acid and base (Figure 2.2).[2] When placed into D_2O, the amide protons exchange for deuterons. NMR-detected amide proton exchange exploits this reaction in two ways. First, ^2H (D) is not detected in ^1H NMR. Second, the concentration of ^2H from the D_2O is hundreds to thousands-fold higher than any exchangeable ^1H, making the exchange essentially irreversible. These properties make exchange experiments amenable for study by using NMR.

To start exchange, the peptide or protein of interest is usually lyophilized from H_2O and dissolved in a solution containing D_2O. Using NMR, the exponential decay in the volume of each amide proton crosspeak on an HSQC spectrum can be used to obtain a rate constant for exchange, k_{obs}, provided the reaction is slow enough to be monitored. Approaches to measuring k_{obs} under crowded conditions are discussed in section 2.6. Once measured, k_{obs} values can be correlated to protein stability.

Hvidt and Nielsen connected protein stability to amide proton exchange rates, using arguments that parallel those for global stability.[5] Each amide region in the protein can be in one of two states: open or closed. Amide proton exchange only occurs from the open state, such that the irreversible exchange reaction can be described as

$$cl\text{–}{}^1H \underset{k_{cl}}{\overset{k_{op}}{\rightleftharpoons}} op\text{–}{}^1H \xrightarrow{k_{\text{int}}} op\text{–}{}^2H \underset{k_{op}}{\overset{k_{cl}}{\rightleftharpoons}} cl\text{–}{}^2H$$

(I)

where cl and op are the open and closed states, k_{op} and k_{cl} are the associated rate constants, and k_{int} is the exchange rate from the open state. The open states are ensembles whose subpopulations range from small, low amplitude fluctuations of the native state to rare, globally unfolded forms. As shown by Frost and Pearson, the overall rate constant, k_{obs}, for such a reaction is:[6]

$$k_{obs} = \frac{(k_{op}+k_{cl}+k_{int}) - \sqrt{(k_{op}+k_{cl}+k_{int})^2 - 4k_{op}k_{int}}}{2} \quad (1)$$

With the addition of some assumptions, the equation can be simplified to link k_{obs} and stability. First, the protein is assumed to be stable *i.e.* $k_{cl} \gg k_{op}$. Given this assumption, there are two limiting extremes. First, if $k_{int} \gg k_{cl}$, then the exchange is said to occur under an EX1 limit, and the equation simplifies to:

$$k_{obs} = k_{op} \quad (2)$$

The EX1 limit is typically associated with less stable or slow folding proteins[7] and doesn't provide information about stability. The EX2 limit occurs when $k_{cl} \gg k_{int}$, that is, when exchange from the open state is the rate determining step. In this instance, the equation simplifies to:

$$k_{obs} = \frac{k_{op}}{k_{cl}} k_{int} \quad \text{and} \quad \frac{k_{op}}{k_{cl}} = K_{op}^{0'} \quad (3)$$

where $K_{op}^{0'}$ is the equilibrium constant for opening the amide backbone at that residue. As noted by this equation, evalution of $K_{op}^{0'}$ requires values for k_{obs} (determined from overall exchange rate) and k_{int}.

The base-catalyzed amide proton exchange rate in an unstructured peptide, k_{int}, is directly proportional to the hydroxide-ion concentration. The minimum rate constant for exchange, ~1 sec^{-1}, occurs near pH 4, and increases

to ~10^{10} sec^{-1} at pH 12 (Figure 2.2). The rate is also proportional to the amide proton's acidity, K_a (~10^{-18}).[8] The non-additivity of peptide backbone solvation[9] means that K_a, and hence the exchange rate of a particular amide proton, depends on primary structure. Molday and Englander conducted the classical studies on the exchange of amide ^1H for ^2H in D_2O.[10] Their results have been refined in Englander's laboratory, and an easy to use computer program (SPHERE) for calculating these values is available on-line from the Roder Lab (http://www.fccc.edu/research/labs/roder/sphere/sphere.html).[11] My approach to estimate k_{int} values under crowded conditions is discussed in section 2.5.5 With knowledge of k_{ex} and k_{int}, $K_{op}^{0'}$ can be determined, and both local and global stability of a globular protein can be assessed.

2.3 Globular Protein Stability

Global protein stability is defined as the free-energy change, $\Delta G^{0'}$, for the following reaction,

$$N \rightleftharpoons D$$

(II)

where N represents the native, biologically-active structural state and D represents the denatured (or non-native) thermodynamic state.[12] This simple two-state reaction applies to many single-domain globular proteins. The strongest evidence for this behavior is the correspondence between the indirectly measured van 't Hoff denaturation enthalpy and the directly measured

calorimetric denaturation enthalpy.[13] The two-state nature is further confirmed when all probes used to monitor reversible denaturation yield similar thermodynamic values.[14]

A variety of probes, including circular dichroism spectropolarimetry,[15] absorbance,[16] and fluorescence[17] spectroscopies, and differential scanning calorimetry[16] are used to assess the equilibrium constant for global denaturation, $K_{eq(den)}^{0'} = \frac{[D]}{[N]}$, in dilute solution. Values of $\Delta G_{den}^{0'}$ can then be obtained from $K_{eq(den)}^{0'}$ and the Gibbs equation,

$$\Delta G_{den}^{0'} = -RTln(K_{eq(den)}^{0'}) \quad (4)$$

where *R* is the gas constant and *T* is the absolute temperature. As previously stated, backbone amide proton exchange can be used to assess $K_{op}^{0'}$ at the level of individual protein backbone amides. Likewise, these values can be converted into an opening free energy, defined as

$$\Delta G_{op}^{0'} = -RTln(K_{op}^{0'}) \quad (5)$$

These $\Delta G_{op}^{0'}$ values need not be uniform for a two-state unfolding model. Local unfolding events that are not indicative of full denaturation can occur, and have $\Delta G_{op}^{0'}$ values that are smaller than $\Delta G_{den}^{0'}$.[2] However, some residues only exchange when the entire protein is unfolded, and for these global unfolding events, $\Delta G_{op}^{0'} = \Delta G_{den}^{0'}$. In this way, both local and global protein stability can be assessed by amide proton exchange. In chapter 3, I will discuss how this picture of local and global stability changes as a result of the crowded environment. Just as amide proton exchange has requirements to link exchange to protein stability,

NMR detection of exchange events in crowded conditions creates restrictions on the test system.

2.4 Requirements for Candidate Systems

The ability to acquire a high-resolution solution NMR spectrum of a globular protein depends on its rotational diffusion, which is determined by the protein's molecular weight and by the viscosity of the sample.[18] As protein molecular weight and solution viscosity increase, the quality of NMR spectra decreases. Techniques exist for examining larger proteins, but conventional heteronuclear studies of amide proton exchange are usually restricted to monomeric globular proteins up to ~40 kDa in size. Crowded solutions decrease this value because of their increased viscosities. Luckily, the relationship between viscosity and rotational diffusion in macromolecular crowding conditions leads to a higher diffusion rate than the Stokes-Einstein-Debye equation predicts.[18, 19] With the proper conditions, exchange experiments are possible under crowded conditions.

NMR tubes come in a variety of sizes, but typical 5-mm diameter tubes require a volume of ~0.4 to 1.0 mL, and measuring the diminution of an amide proton crosspeak accurately requires a protein concentration of ~1 mM. Given these parameters, each exchange experiment requires ~10 mg of CI2. Of course, the protein must remain soluble at that concentration for the duration of the experiment.

The instrument time required for an exchange experiment is always a compromise. Longer acquisition times allow quantification of larger $\Delta G_{op}^{0'}$ values, but also risk precipitation of protein. I found that 24 h strikes a balance between these factors for my system. To ensure accurate determination of k_{obs}, only crosspeak volumes that decay by a factor of two are analyzed. This requirement gives a lower limit for k_{obs} value of ~8 x 10^{-6} s^{-1}. The largest observable k_{obs} values must also be considered.

It takes 60 min to acquire a high-quality HSQC spectrum, and 3-4 points above the baseline are needed to perform a regression. These requirements set the upper limit for k_{obs} values at ~1 x 10^{-4} s^{-1}. Using another experiment called SOFAST,[20] acquisition time can be reduced to only 7 minutes per spectrum, which moves the upper limit to ~3 x 10^{-3} s^{-1}. For my experiments (pH 5.4 or 6.5, 37 °C or 20 °C), this detection window corresponds to $\Delta G_{op}^{0'}$ values between 1 kcal/mol and 8 kcal/mol. Because the observation window is related to both k_{int} and protein stability, the window can be altered by mutagenesis, temperature changes, and pH alterations. With these time and stability constraints in mind, the crowding agent must also be selected with care.

There are two kinds or macromolecular crowding agents that I will address, polydisperse polymers and natural proteins. Whichever crowding agent is chosen, it must have the same key property as the test protein; solubility over the length of time required to collect the data. In addition, the crowding agent must be reasonably pure and should be inexpensive. Consider a crowder that is 99% pure by weight. A 300 g/L exchange sample will contain impurities at

weight concentrations rivaling that of the test protein. Expense is a factor for the crowding agent because tens to hundreds of grams are necessary for characterization and to perform detailed exchange studies. Many polydisperse polymers satisfy these requirements.

Polydisperse crowders include synthetic polymers, and naturally occurring polymers such as polysaccharides. One advantage of choosing synthetic polymers is that they are often available in a range of molecular weights. For instance, PVP is available in molecular weights from 10 kDa to 1.3 MDa. This property allows exploration of volume exclusion with regards to molecular weight without changing the underlying monomer. A second advantageous property is that a model for the monomer is often available and can be used to probe the importance of the crowder's polymeric nature. Our lab used *N*-ethylpyrrolidone as the model for PVP to show that the polymeric nature of PVP was the factor that increased CI2 stability.[21] In fact, our lab was able to show that the monomer model destabilized the protein. Polymeric crowding, however, does come with disadvantages.

One potential disadvantage is that synthetic polymers are polydisperse. One might overcome this problem by using disordered proteins, such as FlgM, which are random coil-like, but are monodisperse.[22] Another disadvantage involves physiological significance: If one is only interested in understanding stability, synthetic polymers are fine, but cells do not contain synthetic polymers. Instead, they are crowded with monodisperse, and mostly globular, proteins.

Globular proteins are the most physiologically relevant crowding agents. Furthermore, they all approximate a spherical shape which scales in radius rather smoothly with the number of residues between about 50 and 200 amino acids in length.[23] They also have drawbacks. For instance, the surface features of proteins can vary wildly because they are composed of 20 types of subunits. The result is that it is difficult to vary the size of the crowder while maintaining its surface properties. Second, at concentrations up to 300 g/L, most globular proteins will aggregate, which means the crowding molecules will tend to interact with each other and with the test protein. I will revisit the differences between these two types of systems upon discussion of my experimental findings. Knowing all the requirements for a successful amide proton exchange experiment, controls and characterizations can be performed to find an acceptable candidate system.

2.5 Preliminary Experiments

Before any system can be used to assess protein stability under crowded conditions, a number of exploratory experiments must be performed. These experiments will ensure that the results obtained from an amide proton exchange experiment are valid and indicative of a real change in protein stability upon addition of crowder.

2.5.1 Aggregation Studies

To avoid wasting time and ^{15}N-enriched protein, some preliminary experiments can be performed with unenriched samples. First, it is important to know whether the protein aggregates in the presence of the crowder, because aggregation confounds analysis of hydrogen exchange experiments. Specifically, aggregation and amide proton exchange both reduce the amide proton signal, and cannot be separated. Preliminary aggregation studies are performed by making 1-mL solutions containing 1-mM test protein with varying concentrations of crowding agent up to the highest concentration desired in the experiment. The samples are stored in sealed tubes at the desired temperature. After 24 h, the tubes are centrifuged at 16,000 x g for 5 min and inspected for pellets. Although precipitation is easy to detect, there are more subtle problematic interactions, the detection of which requires more sophisticated methods.

2.5.2 Protein – Crowder Interactions

Soluble aggregates will not be detected in the centrifugation experiment. Furthermore, high concentrations of crowding agents can promote nonspecific interactions between crowding agent and test protein. These interactions can induce structural changes, especially in loop regions.[21] NMR can be used to detect soluble aggregates, nonspecific interactions, and structural changes. To determine the presence of soluble aggregates, HSQC spectra are analyzed for alterations in crosspeak volume and linewidth (width at half-peak height) under non-exchange conditions as functions of time.

An increase in crosspeak linewidth in the presence of crowding agents results from an increase in the rotational correlation time of the protein.[24] Such an effect is induced by the increase in the apparent molecular weight of the test protein from an increase in viscosity, aggregation, or from binding to a larger species. In our previous study of the stability of CI2 in 300 g/L of 40 kDa PVP, we assessed the aggregation state of CI2 by monitoring changes in linewidths and crosspeak volume with time.[21] Neither linewidth broadening nor crosspeak volume changes were observed. These data are consistent with the monomeric nature of the protein in both dilute and crowded solutions. However, the width of the crosspeaks increased in 40 kDa PVP compared to dilute solution as a result of increased viscosity and, perhaps, protein-crowder interactions. Analysis of chemical shift changes in crowded condition will also provide information about changes in protein structure and help identify weak protein-crowder interaction.

NMR chemical shifts are highly sensitive, empirical indicators of the chemical environment of the nucleus being studied. Therefore, changes in this environment induced by binding or alteration in protein structure can result in significant chemical shift changes and even crosspeak disappearance due to severe line-broadening. Our lab found that 300 g/L 40 kDa PVP induced changes in ^{1}H and ^{15}N backbone chemical shifts in the loops and turns of CI2. Such small changes are expected because crowding causes compaction, and these regions are not maximally compact.[21] This observation is consistent with other studies showing that crowding can force unstructured regions into more compact states.[25, 26] Of course, the chemical shift changes could also reflect

weak interactions between 40 kDa PVP and these surface areas. The existence of weak interactions can be assessed quantitatively by using a more advanced experiment.

Our lab has shown that non-specific interactions between the test protein and crowding agents can be characterized by using the product of the transverse and longitudinal relaxation rates, R_1 and R_2, respectively.[24] This product is sensitive to nonspecific binding brought about by high crowder concentrations, but is insensitive to the crowder-induced increases in viscosity. This method was first tested in a model system comprising CI2 in 200 g/L bovine serum albumin (BSA). CI2 not only interacts with BSA, but also forms a small amount of homodimer in BSA. Having established the suitability of the protein-crowder combination for NMR-detected amide proton exchange experiments, exchange limits must be examined.

2.5.3 Exchange Limit Determination

As mentioned in section 2.2, there are two extreme exchange limits: EX1 and EX2. The EX2 limit is necessary to correlate exchange rates to stabilities. Two generally accepted methods for determining the exchange limit are analysis of the pH dependence of k_{obs} and Nuclear Overhauser Enhancement Spectroscopy (NOESY) crosspeak analysis.

The pH dependence of k_{obs} can be used if pH changes do not affect protein stability. pH meter readings from D_2O-containing solutions should be listed as pH_{read} because pD differs from pH,[27] but I forego this convention here.

For most proteins, physiologically relevant conditions exist in the base-catalyzed region for amide proton exchange (Figure 2.2). For EX2 exchange, the exchange event (represented by k_{int}) is rate determining [Eq. (4)]. As a result, a plot of log k_{obs} of a given residue *versus* pH will yield a line of unitary slope with a non-zero intercept. The same result is expected for a plot of log k_{obs} for individual residues for one value of pH *versus* a second value. In this instance, the intercept will equal the difference in pH values.

When the test protein exchanges via the EX1 limit, and rate of opening (k_{op}) is not pH dependent, k_{int} is not the rate determining step for exchange. The pH should not affect log k_{obs}. Likewise, a plot of log k_{obs} for individual residues for one value of pH *versus* a second value will result in a line of unitary slope and an intercept of zero.

Using the pH dependence of k_{obs} to determine the exchange limit is well-established for dilute solution studies[28, 29] and has yielded success in macromolecular crowding conditions[21] in which the stability of the protein remained constant over the pH range studied. The size or surface characteristics of some crowding agents depend on pH, which can result in a stability change for the target protein. In this case, another technique can be used.

NOESY creates a correlation between NMR-active nuclei that are spatially close to one another. Wagner and Wütrich showed that the exchange limit can be determined by analyzing the disappearance of an NOE signal from a partially exchanged sample for which exchange has been halted.[30] Time-resolved NOESY-detected exchange experiments (NOESY-HEX) are now possible.[28] For

the purposes of this experiment, there are three types of crosspeaks of interest: an amide – amide crosspeak corresponding to the combined decay of two amide protons with rate $k_{obs(A,B)}$, and two amide – aliphatic crosspeaks corresponding to each proton's individual decay, with rates $k_{obs(A)}$and $k_{obs(B)}$. For the EX1 limit,

$$k_{obs(A,B)} = k_{obs(A)} = k_{obs(B)} \quad (8)$$

For an EX2 limit, the exchanges should be independent events, and

$$k_{obs(A,B)} = k_{obs(A)} + k_{obs(B)} \quad (9)$$

To determine the exchange limit, the relationship between these exchange rates must be analyzed.

An exchange sample is prepared with ^{15}N-enriched protein. Consecutive ^{15}N-filtered ^{1}H-^{1}H NOESY spectra[31-33] are then obtained over the course of 12 h. The ^{15}N filtering removes a significant portion of signals from C_α protons and other aliphatic protons. The resulting spectra are analyzed to identify NOE crosspeaks in the amide – amide and amide – aliphatic regions that correspond to amide backbone proton resonances. Crosspeak volumes are plotted as a function of time, and a first-order rate constant is obtained from fits to a single exponential function. This amide-amide "linked" decay is then compared to the individual proton decays from the amide – aliphatic crosspeaks to determine exchange limit. My results for CI2 in dilute solution are shown in Table 2.1. The data show that the k_{obs} value for a given amide – amide crosspeak corresponds to the sum of the k_{obs} values of the corresponding amide – aliphatic crosspeaks. Furthermore, the correspondence between the rate constants measured from the NOESY spectra and the HSQC spectra lends confidence to the conclusion that

CI2 exchanges under the EX2 limit in 50 mM sodium acetate buffer at 37 °C, pH 5.4. This conclusion also agrees with a previous study.[28] Having established an EX2 limit, one final control experiment is needed.

2.5.4 Intrinsic Exchange Rate

The value of the intrinsic exchange rate (k_{int}) depends not only on the acidity and solvation of the amide nitrogens,[9] but may also be affected by the behavior of water.[34] High concentrations of crowding agents could alter these parameters either directly or indirectly by affecting the pK_a of H_2O. If this were to occur, k_{int} values from SPHERE would no longer be applicable to crowded conditions.

Our group attempted to measure the effect of 40 kDa PVP on k_{int}[21] using methods described in Bai *et al.*.[35] The experiment involved the exchange of L-alanyl-L-alanine under crowded conditions, but the results suggest a strong interaction between the peptide and PVP, obviating the measurement, so another method was used.

CI2 contains an extended loop between residues 33 and 44 that is not maximally compacted. Our group assumed this loop mimics an unstructured peptide, and resolved to measure k_{int} through determination of the rapid exchange rates of these residues.[21] A water-saturation transfer experiment, phase-modulated CLEAN chemical EXchange (CLEANEX-PM),[36] was used. In contrast to the protocol described in section (2.6), CLEANEX-PM does not require fully deuterated solutions, and can measure rates for exchanges that are

too fast (3-55 s^{-1}) to be detected using traditional amide ^1H exchange (8 x 10^{-6} – 3 x 10^{-3} s^{-1}).

Two experiments were performed. A control sample of lyophilized protein dissolved in buffer was analyzed to determine dilute solution k_{int} values. These values were compared to values from SPHERE.[11] A second sample of lyophilized protein dissolved in buffered crowding solution was then analyzed. The presence of the crowding agent did not affect k_{int}.[21] With the knowledge that the intrinsic exchange rate is not changed by the experimental setup, amide ^1H exchange experiments can proceed.

2.6 A Protocol for Amide Proton Exchange

There are two methods to prepare a sample for amide proton exchange. Buffer exchange can be achieved by using centrifugal filter devices, but the viscosity of crowded solutions makes buffer exchange difficult. Alternatively, lyophilized protein can be added to prepared solutions. The latter method is greatly preferred for the sake of time and convenience. For these reasons, I used samples made from lyophilized protein. Two samples are prepared. The first sample is used to adjust the shims. This sample contains a low ionic strength solution (< 150 mM) with 10-20% D_2O (to lock the spectrometer) at the desired pH, and contains 1 mM protein, but has no crowding agent. The second sample is an exchange sample, and comprises 100% D_2O buffered solution at the same ionic strength and pH with crowding agent at the desired concentration. Enough lyophilized protein to bring the exchange sample to a final concentration of 1 mM

is brought to the spectrometer. The protein is not mixed into the sample until later.

After shim optimization, the lyophilized protein is added to the exchange sample and mixed. This complete sample is then immediately spun in a microcentrifuge at 16000 x g for 1 min to remove any insoluble aggregates. The supernatant is transferred to an NMR tube, which is immediately placed in the magnet. The 90° pulse width is optimized by examining the first increment of a ^{15}N-^{1}H HSQC spectrum.[3, 4] Multiple (20-24) sequential ^{15}N-^{1}H HSQC spectra are obtained using the established parameters. Upon completion, the sample tube is again examined for aggregates and the pH is checked. The HSQC data are then processed, making sure to use the same processing parameters for each spectrum, to yield a list of residue numbers with crosspeak volumes as a function of time. To determine k_{obs}, each peak decay plot is fitted to a three parameter exponential function. Some crosspeaks overlap, which creates difficulties. To overcome this problem, both peaks are measured together and a five parameter, double exponential function can be used. Care must be taken to determine which of the two peaks is the faster-exchanging species. I find that the uncertainties in k_{obs} from curve fitting are of equal magnitude or lower than those of reproducing the experiment. To convert the k_{obs} values into $K_{op}^{0'}$ values, the k_{int} value for each residue must be known.

Section 2.5.4 describes the methods for determining whether k_{int} values calculated from SPHERE can be used for the crowded solutions. If this is not possible, k_{int} values in crowded conditions can be quantified by using the

technique described by Bai, *et al*..[35] An alternative would be to adjust k_{int} values as determined by the CLEANEX-PM experiment. This method has not been tested, and its use assumes that the alterations to k_{int} in the loop region of a protein uniformly apply to all residues.

2.7 Summary

Amide ^{1}H exchange provides a valuable tool to investigate the stability of proteins. NMR techniques add to its utility by providing residue-level interrogation. When coupled with *in vitro* experiments using macromolecular crowding agents, valuable information about the combination of excluded volume effects and nonspecific interactions can be obtained. Although I have focused on macromolecular crowding, the methods should be applicable to any solvent additive, whether stabilizing[21] or destabilizing.[37] *In vitro* studies should provide insight as to how crowded environments like cell interiors affect protein properties. To understand macromolecular crowding fully, however, it is necessary to design experiments that distinguish between hard excluded volume effects and soft interactions in a more quantitative way. To this end, I performed a systematic study of PVP crowding effects on the stability of CI2.

2.8 Figures and Tables

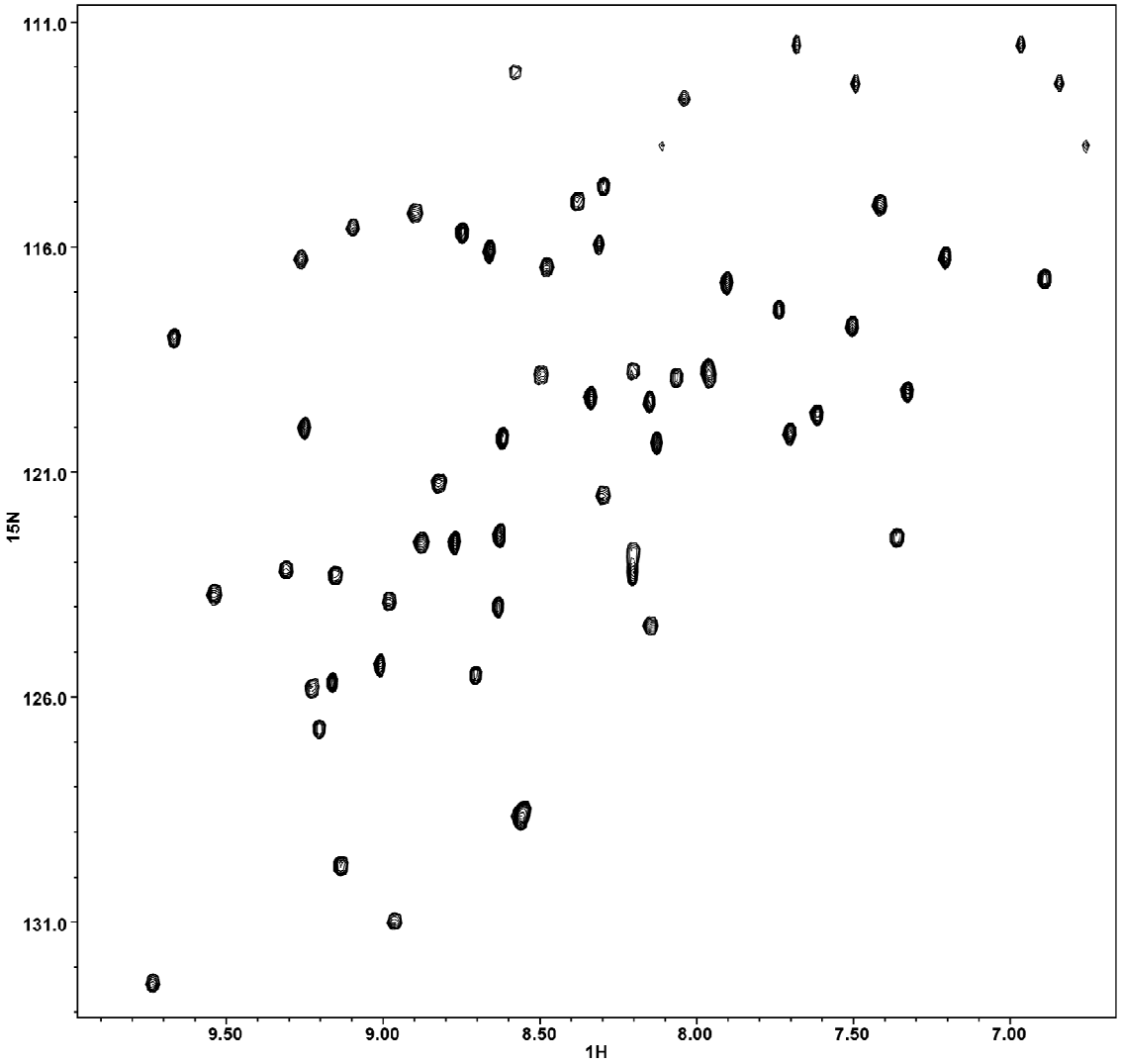

Figure 2.1 ^{1}H-^{15}N HSQC spectrum of CI2 in dilute solution

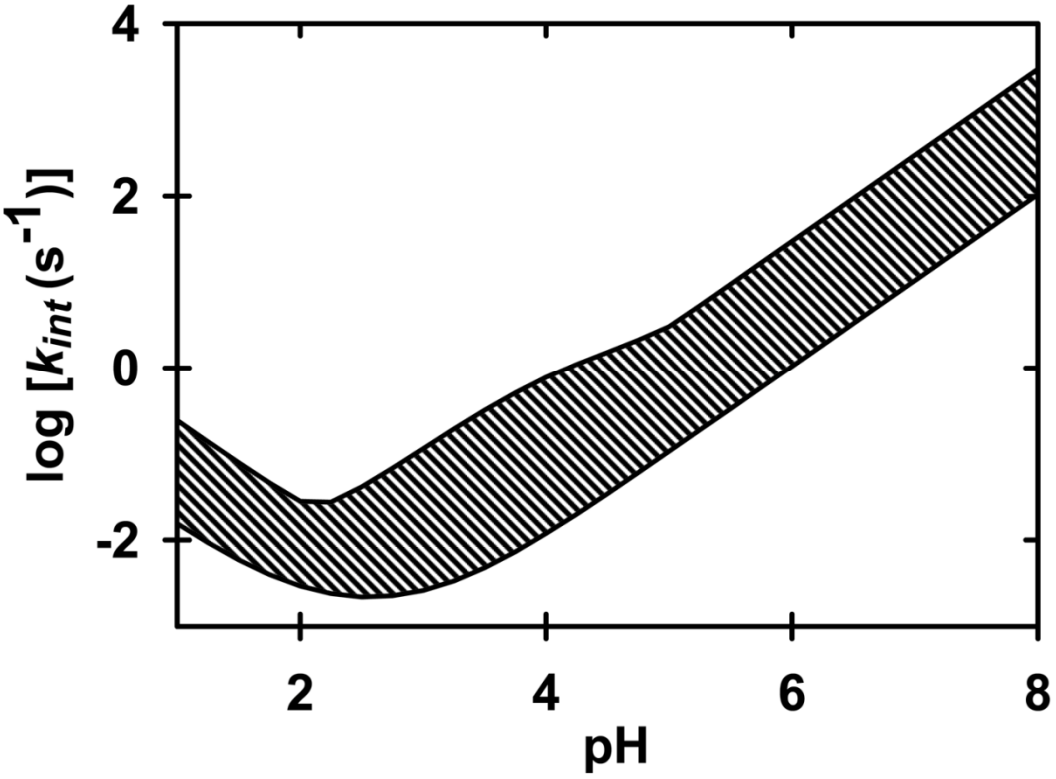

Figure 2.2 pH dependence of k_{int}

The shaded area corresponds to the range of k_{int} values for CI2 at 37 °C. Rate constants are calculated using the SPHERE program.[11]

Residue(s)	k_{obs} NOESY (s^{-1} x 10^5)	k_{obs} HSQC (s^{-1} x 10^5)
Leu8	5	5
Val9	3	3
Leu8 + Val9[a]	8	8
Leu8, Val9[b]	8	—
Lys17	66	74
Lys18	35	29
Lys17 + Lys18[a]	101	103
Lys17 , Lys18[b]	77	N/A
Ala58	6	7
Glu59	5	5
Ala58 + Glu59[a]	11	12
Ala58 , Glu59[b]	10	—

Table 2.1 NOESY-HEX results

k_{obs} values from NOESY-detected amide proton exchange and HSQC-detected amide proton exchange for CI2 in 50 mM sodium acetate buffer, pH 5.4, 37 °C.

[a] Sum of values from individual crosspeak decays
[b] Exchange rate of amide-amide NOESY crosspeak

2.9 References

1. Serber, Z., and Dötsch, V. (2001) In-cell NMR spectroscopy, *Biochemistry* **40**, 14317-14323.

2. Englander, S. W., and Kallenbach, N. R. (1983) Hydrogen exchange and structural dynamics of proteins and nucleic acids., *Q. Rev. Biophys.* **16**, 521-655.

3. Bodenhausen, G., and Ruben, D. J. (1980) Natural abundance nitrogen-15 NMR by enhanced heteronuclear spectroscopy, *Chem. Phys. Lett.* **69**, 185-189.

4. Kay, L., Keifer, P., and Saarinen, T. (1992) Pure absorption gradient enhanced heteronuclear single quantum correlation spectroscopy with improved sensitivity, *J. Am. Chem. Soc.* **114**, 10663-10665.

5. Hvidt, A. A., and Nielsen, S. O. (1966) Hydrogen exchange in proteins, *Adv.Prot.Chem.* **21**, 287-386.

6. Frost, A. A., and Pearson, R. G. (1953) *Kinetics and Mechanism*, John Wiley & Sons, New York, NY, USA.

7. Ferraro, D. M., Lazo, N. D., and Robertson, A. D. (2004) EX1 hydrogen exchange and protein folding, *Biochemistry* **43**, 3756-3756.

8. Molday, R. S., and Kallen, R. G. (1972) Substituent effects on amide hydrogen-exchange rates in aqueous-solution, *J. Am. Chem. Soc.* **94**, 6739-6745.

9. Avbelj, F., and Baldwin, R. L. (2009) Origin of the change in solvation enthalpy of the peptide group when neighboring peptide groups are added, *Proc. Natl. Acad. Sci. U.S.A.* **106**, 3137-3141.

10. Molday, R. S., Englander, S. W., and Kallen, R. G. (1972) Primary structure effects on peptide group hydrogen exchange, *Biochemistry* **11**, 150-158.

11. Zhang, Y.-Z. (1995) Protein and peptide structure and interactions studied by hydrogen exchange and NMR, in *Structural Biology and Molecular Biophysics*, University of Pennsylvania, PA, USA.

12. Lumry, R., Biltonen, R., and Brandts, J. F. (1966) Validity of the "two-state" hypothesis for conformational transitions of proteins, *Biopolymers* **4**, 917-944.

13. Privalov, P. L., and Khechinashvili, N. N. (1974) A thermodynamic approach to the problem of stabilization of globular protein structure: A calorimetric study, *J. Mol. Biol.* **86**, 665-684.

14. Huang, G. S., and Oas, T. G. (1995) Structure and stability of monomeric *l* repressor: NMR evidence for two-state folding, *Biochemistry* **34**, 3884-3892.

15. Doyle, D. F., Waldner, J. C., Parikh, S., Alcazar-Roman, L., and Pielak, G. J. (1996) Changing the transition state for protein (un)folding, *Biochemistry* **35**, 7403-7411.

16. Cohen, D. S., and Pielak, G. J. (1994) Stability of yeast iso-1-ferricytochrome *c* as a function of pH and temperature, *Protein Sci.* **3**, 1253-1260.

17. Betz, S. F., and Pielak, G. J. (1992) Introduction of a disulfide bond into cytochrome *c* stabilizes a compact denatured state, *Biochemistry* **31**, 12337-12344.

18. Pielak, G. J., Li, C., Miklos, A. C., Schlesinger, A. P., Slade, K. M., Wang, G., and Zigoneanu, I. G. (2008) Protein NMR under physiological conditions, *Biochemistry* **48**, 226–234.

19. Kuttner, Y. Y., Kozer, N., Segal, E., Schreiber, G., and Haran, G. (2005) Separating the contribution of translational and rotational diffusion to protein association, *J. Am. Chem. Soc.* **127**, 15138-15144.

20. Schanda, P., and Brutscher, B. (2005) Very fast two-dimensional NMR spectroscopy for real-time investigation of dynamic events in proteins on the time scale of seconds, *J. Am. Chem. Soc.* **127**, 8014-8015.

21. Charlton, L. M., Barnes, C. O., Li, C., Orans, J., Young, G. B., and Pielak, G. J. (2008) Macromolecular crowding effects on protein stability at the residue level, *J. Am. Chem. Soc.* **130**, 6826-6830.

22. Dedmon, M. M., Patel, C. N., Young, G. B., and Pielak, G. J. (2002) FlgM gains structure in living cells, *Proc. Natl. Acad. Sci. U.S.A.* **99**, 12681-12684.

23. Richards, F. M. (1977) Areas, volumes, packing, and protein structure, *Annu. Rev. Biophys. Bioeng.* **6**, 151-176.

24. Li, C., and Pielak, G. J. (2009) Using NMR to distinguish viscosity effects from nonspecific protein binding under crowded conditions *J. Am. Chem. Soc.* **131**, 1368–1369.

25. Perham, M., Stagg, L., and Wittung-Stafshede, P. (2007) Macromolecular crowding increases structural content of folded proteins, *FEBS Lett.* **581**, 5065-5069.

26. Stagg, L., Zhang, S.-Q., Cheung, M. S., and Wittung-Stafshede, P. (2007) Molecular crowding enhances native structure and stability of α/β protein flavodoxin, *Proc. Natl. Acad. Sci. U.S.A.* **104**, 18976-18981.

27. Schowen, B. K., Schowen, R. L., and Daniel, L. P. (1982) Solvent isotope effects on enzyme systems, *Methods Enzymol.* **87**, 551-606.

28. Neira, J. L., Itzhaki, L. S., Otzen, D. E., Davis, B., and Fersht, A. R. (1997) Hydrogen exchange in chymotrypsin inhibitor 2 probed by mutagenesis, *J. Mol. Biol.* **270**, 99-110.

29. Qu, Y. X., and Bolen, D. W. (2003) Hydrogen exchange kinetics of RNase A and the urea:TMAO paradigm, *Biochemistry* **42**, 5837-5849.

30. Wagner, G. (1980) A novel application of nuclear Overhauser enhancement (NOE) in proteins: Analysis of correlated events in the exchange of internal labile protons, *Biochem. Biophys. Res. Commun.* **97**, 614-620.

31. Kim, S., and Szyperski, T. (2003) GFT NMR, a new approach to rapidly obtain precise high-dimensional NMR spectral information, *J. Am. Chem. Soc.* **125**, 1385-1393.

32. Kupce, E., and Freeman, R. (2003) Projection-reconstruction of three-dimensional NMR spectra, *J. Am. Chem. Soc.* **125**, 13958-13959.

33. Kupce, E., and Freeman, R. (2004) Projection-reconstruction technique for speeding up multidimensional NMR spectroscopy, *J. Am. Chem. Soc.* **126**, 6429-6440.

34. LeMaster, D. M., Anderson, J. S., and Hernandez, G. (2006) Role of native-state structure in rubredoxin native-state hydrogen exchange, *Biochemistry* **45**, 9956-9963.

35. Bai, Y., Milne, J. S., Mayne, L., and Englander, S. W. (1993) Primary structure effects on peptide group hydrogen exchange, *Proteins: Struct., Funct., Genet.* **17**, 75-86.

36. Hwang, T.-L., van Zijl, P. C. M., and Mori, S. (1998) Accurate quantitation of water-amide exchange rates using the phase-modulated CLEAN

chemical EXchange (CLEANEX-PM) approach with a fast-HSQC (FHSQC) detection scheme, *J. Biomol. NMR* **11**, 221-226.

37. Bai, Y. W., Sosnick, T. R., Mayne, L., and Englander, S. W. (1995) Protein folding intermediates: Native-state hydrogen exchange, *Science* **269**, 192-197.

3 Volume Exclusion and Soft Interaction Effects on Protein Stability under Crowded Conditions

The material in this chapter is from:

Miklos AC, Li C, Sharaf NG, Pielak GJ. **2010.** *Biochemistry*, 49, 6987-6991.

3.1 Introduction

Studies in dilute solution have yielded essential information about the biophysical properties of globular proteins. As suggested in Chapter 1, The complex milieu inside cells can change these properties.[1-4] Studying the nature and magnitude of these changes should bring us closer to understanding how proteins function in their native environments. The following experiments focus on NMR-based approaches that quantify the effects of macromolecular crowding on equilibrium protein stability. I examine the stability of CI2 as a function of both the concentration and the molecular weight of a synthetic polymer. Studies such as these can provide both evidence for the importance of crowding in biological systems and quantitative results useful for verifying and refining predictions of crowding effects.[5]

As mentioned in Chapter 1, stability is the difference in free energy between the unfolded state ensemble (U) and the native state (N).[6] In Chapter 2, local stabilities were also covered, but without reference for how these values are changed in a crowded environment. When a protein goes from dilute to crowded conditions, a transfer free energy from dilute solution to crowded conditions must

be considered for both states (Figure 3.1). The transfer results in a new standard state with a new free energy of opening, $\Delta G_{op}^{0^*}$, for each residue. These values reflect both local and global unfolding events, and the largest values reflect global protein stability, $\Delta G_{N\rightarrow U}^{0^*}$.[7] Using techniques described in Chapter 2, global and local stability values can be determined in dilute solution, and in crowded conditions.

As mentioned in Chapter 1, hard interactions are predominantly used to explain the effects of crowding on $\Delta G_{op}^{0^*}$. Hard interactions are separated into two major models, hard particle exclusion and confinement.[8, 9] Hard particle exclusion arises when macromolecular crowders act as independent particles. The change in stability caused by independent particles is expected to exhibit both a concentration and a molecular weight dependence.[10] Confinement arises when the crowders create a space from which proteins rarely escape. The stability change in this instance is based on the size and shape of the cavity.[9] These models are not completely accurate when describing synthetic polymer crowders, but can be used as a first approximation. For synthetic polymer crowders, a transition from hard particle crowding to confinement is expected above the polymer's overlap concentration (c*), defined as the concentration above which the polymer molecules no longer act as individual particles. At this concentration, the solution moves from the dilute to semidilute regime, and polymers begin to overlap and create confining spaces.[11]

Hard particle crowding and confinement, however, can only explain part of the observed effect, because these models assume that the crowding agent is

inert. Few, if any, crowders exhibit such ideal behavior. Instead, crowding agents are expected to interact chemically with the protein.[12] These soft chemical interactions, as opposed to purely volume exclusion effects, must be considered.

As mentioned in Chapter 1, soft interactions affect both entropy and enthalpy, and can be stabilizing or destabilizing. These interactions take into account the chemical nature of the molecules involved as opposed to treating them as hard spheres. We divide soft interactions into two types, nonspecific interactions and native-state interactions. Interactions involving urea, trimethylamine N-oxide (TMAO), and ligand binding provide three familiar examples of different types of soft interaction between proteins and small molecules.

The effects of urea and TMAO have a common source, the protein backbone. These small molecules have nonspecific interactions with protein, but have differing effects on stability. Urea has a favorable weak interaction with protein backbone.[13] As unfolded states expose more backbone to urea solutions than native states, urea destabilizes globular proteins. Conversely, the protein backbone interacts more favorably with H_2O than with TMAO, resulting in stabilization.[14] These types of nonspecific interactions are commonly considered in studies involving proteins and cosolutes, but native-state interactions can also have an effect in crowded conditions.

Some small molecules stabilize proteins by specifically binding the native state, as seen in stabilization by ligand binding.[15] Unlike nonspecific interactions, native-state interactions often lead to changes in chemical environment for a

specific region of the protein. Native-state binding is also possible for crowding agents, if the crowder has a favorable interaction with a specific protein structural element or region. Both volume exclusion and soft interactions play a role in crowding effects, and NMR can be used to assess soft interactions, even if they are weak.

I use the I29A;I37H variant of CI2 as my test protein. It is a small (7.4 kDa) globular protein with two-state folding properties.[16] CI2 (Figure 3.2) has a compact core containing its sole α-helix (Ser12-Lys24), two major β-sheet regions (Gln28-Val34 and Asp45-Asp52), an extended loop (Gly35-Ile44), and several turns. Dilute solution NMR-detected amide proton exchange experiments show that Lys11, Ile20, Leu21, Ile30, Val47, Leu49, Phe50, and Val51 are on the global unfolding path, which means they only become exchange-competent when the entire protein unfolds.[17] These properties allow hydrogen exchange experiments to probe both local and global stabilities upon adding a crowding agent. We also use R_1R_2 and changes in chemical shifts to interpret changes in $\Delta G_{op}^{0^*}$ brought about by crowding effects.

I approach crowding systematically by varying the concentration and molecular weight of the crowding agent. Such reductionism is not feasible in the complex intracellular environment. For tight control of concentration and molecular weight, I use the polymeric crowding agent PVP.[18] PVP (Figure 3.1) has four advantageous properties. It is highly soluble (up to 300 g/L) and is available in several molecular weights (Table 3.1). The partial specific volume of PVP (0.80 mL/g) allows physiological volume occupancy to be obtained, and

PVP interacts only weakly with proteins.[19, 20] Furthermore, this polymer can be studied both above and below c* (Table 3.1) allowing me to explore both hard particle crowding and confinement, respectively. These properties make PVP an excellent choice for my experiments.

This system has been previously used in studies of macromolecular crowding effects. Ladurner and Fersht used guanidinium chloride as a denaturant and intrinsic fluorescence as a detection method to assess the stability of CI2 in PVP.[21] They found that CI2 is destabilized by 0.8 kcal/mol in 50 g/L 10 kDa PVP. In contrast, Charlton *et al.* used NMR-detected amide proton exchange to determine the effects of 40 kDa PVP at 300 g/L on CI2 stability and found a maximal stabilization of 3 kcal/mol.[19] The apparent difference between these two results arises from the differences in the two approaches.

Detection methods such as fluorescence and circular dichroism (CD) spectroscopies allow determination of stability through the observation of structure. These techniques probe global stability. NMR detected amide proton exchange experiments yield comparable global stabilities.[19] NMR experiments, however, allow residue level determination of stability, providing a tool to study both global and local unfolding. These local unfolding events can often be as important as global events, and NMR is the only technique that can probe these effects throughout the protein in a single experiment. Most importantly, fluorescence and CD detection require perturbation of the system, whether by temperature changes or by adding a denaturant to detect folding or unfolding. NMR-detected amide proton exchange does not have these constraints, and

allows determination of stability without perturbing the system. As discussed in Chapter 1, components of the system that react to changes in temperature or addition of denaturants can affect analysis. Denaturant induced perturbations are especially important in crowding experiments, as the temperature and denaturant sensitive components exist at concentrations of 100 g/L and greater.

The difference between the two results[19, 21] can be explained in terms of denaturant induced perturbations. It has been shown that guanidinium salts and urea alter the properties of PVP.[22] Specifically, guanidinium salts can induce chain collapse in PVP, resulting in smaller crowding particles. This suggests that the two results cannot be compared. In essence, PVP-CI2-guanidinium chloride is a different system than PVP-CI2. For this reason, native-state hydrogen exchange,[23] which requires solutions containing both PVP and urea, was not used. Instead, NMR-detected amide proton exchange was performed without the addition of denaturants, as a function of PVP molecular weight and concentration.

The data obtained by Charlton *et al.*[19] showed the feasibility of using NMR−detected amide proton exchange to assess the effects of crowding on protein stability, but were inadequate to detect the nuances of concentration and molecular weight dependences. The results presented here quadruple the number of observations made previously.[19] These new data allow the determination of concentration-dependent stability trends and molecular weight-dependent trends. The data also reveal new information about weak

crowder-protein interactions and facilitated observation of hard particle volume exclusion and confinement in the same experimental system.

3.2 Materials and Methods

3.2.1 PVP Characterization

PVP-10, -29, -40, and -55 (Fisher or Sigma) were used without purification. For light scattering experiments, a solution containing 8 mg/mL PVP in 50 mM sodium acetate buffer, pH 5.4 was prepared. A 100 µL sample of this solution was injected onto a size exclusion column (Superdex 200 10/300 GL, GE Healthcare) connected to an AKTA fast protein liquid chromatography (FPLC) system (GE Healthcare) in tandem with a light scattering system. The system comprises a DAWN-EOS unit with a QELS attachment (Wyatt Technologies) and an Optilab DSP (Wyatt) for refractive index measurements. Prior to injection, the column was equilibrated with 50 mM sodium acetate buffer, pH 5.4, containing 0.02% NaN_3. Data were analyzed with *ASTRA* software (Wyatt). Analysis of the data yields values for the weight average molecular weight ($\bar{M}_W$), the number average molecular weight ($\bar{M}_N$), the polydispersity ($\bar{M}_W/\bar{M}_N$), and the hydrodynamic radius (R_H). The radius of gyration (R_G) is equal to $1.5 * R_H$.[11] Calculations of c^* were made by using $\bar{M}_W$, R_G, and the equation:[11]

$$c^* = \frac{4}{3}\frac{\bar{M}_W}{R_G^3 N_A}$$

where N_A is Avogadro's number.

To determine partial specific volumes ($\bar{v}_2$), PVP samples were dried at 37 °C for 72 h and dissolved in distilled, deionized water to the desired weight concentration. The density of each solution was measured by using an Anton Paar DMA 5000 density meter. Experiments were performed in triplicate. A linear relation between the weight fraction and inverse density was used to obtain $\bar{v}_2$.[24]

3.2.2 Protein Expression and Purification

The plasmid containing CI2 was donated by the Andrew Lee lab (UNC), and was altered by site-directed mutagenesis to produce the I29A;I37H variant of CI2 used in these studies. Mutagenesis was performed by Charlton *et al.*[19] The variant protein was prepared as follows. The plasmid is transformed into BL-21(DE3-Gold) *Escherichia coli* bacterial cells. Transformed cells are plated onto Luria Broth (LB) agar plates containing 60 µg/mL kanamycin and incubated at 37 °C overnight. A single colony is picked from the agar plate and transferred into a 250 mL baffled flask containing 100 mL of ^{15}N-enriched Spectra 9 media (Cambridge Stable Isotopes) and 60 µg/mL kanamycin. This inoculated culture incubates at 37 °C with shaking overnight. The following morning, the culture is transferred into a 6 L flask containing 900 mL of ^{15}N-enriched Spectra 9 media (Cambridge Stable Isotopes) and 60 µg/mL kanamycin. This culture is incubated at 37 °C with shaking. When the absorbance of the culture at 600 nm reaches 0.8, isopropyl β-D-1 thiogalactopyranoside (IPTG) is added to a final concentration of 1 mM to induce protein expression. Expression proceeds under

shaking and incubation at 37 °C for 5 hours. The culture is then transferred to a 1L centrifuge bottle and centrifuged at 6500 x g for 30 minutes. The supernatant is decanted, and the pellet is frozen overnight.

The pellet is resuspended in a total of 25 mL of 25 mM tris(hydroxymethyl)aminomethane (Tris) buffer, pH 8.0, and transferred into two small centrifuge tubes. Lysis is performed using a Fisher model 500 sonic dismembrator with a 1/8" tip. The samples are pulsed at 20% amplitude for 2 s at a time with 2 s rest periods. The samples are then centrifuged at 14000 x g for 30 minutes and the supernatant is pooled. To precipitate DNA, 250 mg of streptomycin sulfate is added to the supernatant and stirred on ice for 30 minutes. This sample is then centrifuged at 14000 x g for 30 minutes. The supernatant is sterilized using a 0.22 μM PVDF filter (Millipore) and further purified with FPLC.

The sample is purified first using a Q sepharose anion exchange column (GE Healthcare) with low salt buffer comprising 25 mM Tris, pH 8.0, and high salt buffer comprising 25 mM Tris, 1M sodium chloride, pH 8.0. CI2 does not have an affinity for the Q column, and comes out in the wash step. High salt buffer is used primarily for cleaning the column. The fractions containing CI2 are dialyzed in water overnight, and purified further on a Superdex 75 size exclusion column (GE Healthcare) using water for elution. The fractions containing CI2 are lyophilized and stored in a dessicator.

3.2.3 NMR

Amide proton exchange experiments were performed as described in Chapter 2 on a 500 MHz spectrometer with a cold probe (Varian) at a ^{1}H sweep width of 8401.6 Hz and a ^{15}N sweep width of 2200 Hz. Buffers containing 50 mM acetate were used. I limited the ionic strength of the sample to take full advantage of the cold probe.[25] Processing was performed with nmrPipe.[26] Assignments have been described.[19] Crosspeak volumes were quantified, plotted against time, and fitted to exponential decays by using NMRViewJ.[27] Examples of such curves can be seen in Figure 3.3.

Values for k_{int} were determined as described by Hwang *et al.*[28] for 1 mM I29A:I37H variant in 50 mM sodium acetate buffer, pH 5.4, 37 °C containing 0 g/L and 300 g/L PVP-40. Experiments were performed on a 600 MHz spectrometer (Varian) at a ^{1}H sweep width of 10000 Hz and a ^{15}N sweep width of 2000 Hz. The water signal remained constant with mixing times from 0 to 53 ms. $R_{1B,app}$ was therefore chosen to be 0.01 s^{-1}. As expected,[29] the value of $R_{1B,app}$ did not alter the results.

NOESY-detected amide proton exchange experiments were performed as described in Chapter 2 on the 500 MHz spectrometer at a ^{1}H sweep width of 8401.6 Hz. The sample comprised 1 mM I29A:I37H variant in 50 mM sodium acetate buffer, pH 5.4, 37 °C with 50 g/L PVP-10. Processing and exponential decay fitting were performed as described for the exchange experiments, but assignments were made by matching amide-amide crosspeaks to ^{1}H shifts from the HSQC assignment corresponding to pairs of proximal amide protons.

R_1R_2 data were acquired and processed as described by Li and Pielak.[30]

Samples for determining chemical shift changes comprised 1 mM I29A:I37H variant in 50 mM sodium acetate buffer, pH 5.4, 37 °C with 15% D_2O and either 10 g/L or 100 g/L PVP-55. One HSQC spectrum was acquired for each sample. The data were processed with nmrPipe. Peaks were picked with NMRViewJ and compared to dilute solution peak positions. The chemical shift changes (δ_{av}) were calculated with the equation:[31]

$$\delta_{av} = \left[\left(\Delta\, ^1H\ ppm \right)^2 + \frac{\left(\Delta^{15}N\ ppm\ \times 0.154 \right)^2}{2} \right]^{\frac{1}{2}}$$

3.3 Results

3.3.1 PVP Characterization

Light scattering and density measurements were used to quantify the properties of the polydisperse PVP samples. We performed this analysis for two reasons. First, we wanted to ensure that $\bar{M}_W$ values provided by the manufacturer were correct. Second, we wanted to ensure that our samples did not have excessive amounts of low molecular weight polymer. Values for $\bar{M}_W$, $\bar{M}_N$, polydispersity, R_H, the partial specific volume ($\bar{v}_2$), and c^* were determined (Table 3.1). Experiments yielded linear fits for $\bar{v}_2$ with R^2 values greater than 0.997. A comparison of our values to results for 10 kDa PVP[24] indicate that our $\bar{v}_2$ values are accurate to three decimal places. Analysis of other PVP sizes yields similar precision.

3.3.2 Stability under Crowded Conditions

I determined $\Delta G_{op}^{0^*}$ values in triplicate for 33 CI2 residues under 13 conditions (0, 100., 200., and 300. g/L solutions of PVP-10, -29, -40, and -55). One experiment was also performed in 50 g/L of PVP-10. A total of 1339 $\Delta G_{op}^{0^*}$ values were obtained, resulting in 430 average $\Delta G_{op}^{0^*}$ values. Tables of all average $\Delta G_{op}^{0^*}$ values with standard errors can be found in Appendix A. For comparison, Charlton *et al.* analyzed results from 170 $\Delta G_{op}^{0^*}$ values and 34 average $\Delta G_{op}^{0^*}$ values with only PVP-40.[19] In PVP solutions, almost all residues exhibit an increase in $\Delta G_{op}^{0^*}$ compared to dilute solution. The exceptions are $\Delta G_{op}^{0^*}$ values that are the same in the presence and absence of PVP.

I confirmed the conclusions from Charlton *et al.*[19] that $k_{cl} \gg k_{int}$ [*i.e.*, exchange occurs in the EX2 regime[23, 32]] and that PVP does not affect k_{int}. I confirmed that $k_{cl} \gg k_{int}$ by performing a NOESY-HEX experiment in 50 g/L PVP-10,[33, 34] a separate technique from the pH dependence of exchange in 300 g/L PVP-40 performed by Charlton *et al.*[19] The NOESY-HEX data show that the k_{obs} value for the combined amide-amide decay matches the sum of the individual decays (Table 3.2), which is expected when $k_{cl} \gg k_{int}$.[34] To determine k_{int}, I repeated the CLEANEX-PM experiments in 0 and 300 g/L PVP-40.[19] For the fully exposed loop residue His37, k_{int} was the same in 300 g/L PVP-40 and in dilute solution (Figure 3.4). The CLEANEX-PM results also confirm that the activity of water is not changed between dilute solution and crowded conditions, because k_{int} depends on water activity.[35]

Trends in stability were defined by linearly regressing plots of $\Delta G_{op}^{0^*}$ against either PVP molecular weight or PVP concentration for each of the 33 residues for which I could obtain exchange rates. The mean of the slopes indicated a presence or absence of trend. First, I examined trends arising from PVP molecular weight. For 100 g/L solutions of PVP, the mean slope for all observable residues was −3.0 ± 0.8 cal/(mol kDa), indicating the presence of a trend. For 200 and 300 g/L solutions of PVP, the mean slopes were 0.9 ± 0.7 cal/(mol kDa) and 1 ± 2 cal/(mol kDa), respectively. These two results indicate the absence of a molecular weight-dependent trend at higher PVP concentrations. Concentration dependence also yielded trends.

In all concentration-dependent trends, a positive correlation was noted between PVP concentration and CI2 stability. Looking at results for individual residues, the trend was refined into three types. Figure 3.2 depicts an example of each trend using data from one representative backbone amide: Ile20 (in the α-helix), Asn56 (in a turn), and Trp5 (at the end of a short β-sheet). All three residues report an increase in stability from 0 g/L to 100 g/L of PVP. Ile20 shows the most pronounced increase with increasing PVP concentration. I call this trend “volume exclusion”. Asn56 exhibits no further stabilization with increasing PVP concentration. I call this trend “native-state binding”. Trp5 shows some additional increase as the PVP concentration is raised from 200 g/L to 300 g/L. I call this trend the “mixed effect”. The behaviors of these three residues were used to bin the other residues for which stability data were obtained. Figure 3.2 also shows

the backbone of the protein colored to indicate residues following each trend. We used R_1R_2 values and chemical shift changes to investigate soft interactions.

3.3.3 Soft Interactions

The variety in trends prompted us to probe soft interactions between PVP and CI2. R_1R_2 values were measured for backbone amide ^{15}N atoms of CI2 in solutions containing 100, 200, and 300 g/L PVP-40 at pH 5.4 and 25 °C. CI2 has the requisite correlation time of greater than 6 ns[36] under all these conditions because of the enhanced viscosity of the PVP solutions. A histogram of the results for 100 and 200 g/L PVP is shown in Figure 3.5. Note that 200 g/L PVP results in smaller R_1R_2 values than those acquired in 200 g/L BSA.[30] R_1R_2 values acquired in 300 g/L PVP cannot be compared to BSA results, because line broadening obviates the acquisition of R_2 values in 300 g/L BSA. These data were corroborated by examining changes in chemical shift.

In a 10 g/L solution of PVP-55 at pH 5.4 and 37 °C, chemical shift changes, compared to dilute solution (Figure 3.6), are smaller than our ability to measure them.[19] At 100 g/L, however, several significant changes are noted. The regions in which changes occur include the loop (Gly35-Ile44), the second β-sheet (Asp45-Asp52) and turns (Figure 3.5). The implications of these data are addressed below.

3.4 Discussion

3.4.1 PVP Crowding Trends

Volume exclusion theory predicts that crowding will increase stability if the crowder's size is close to that of the protein.[8] My observations are consistent with this prediction because PVP increases CI2 stability under all conditions (Figure 3.2). Given the polydispersity of PVP, I believe these values underestimate the effect of volume exclusion, because the results are more heavily influenced by short polymers present in the mixture. In addition, my residue-level interrogation yields stability trends as a function of PVP molecular weight and concentration (Figure 3.2).

3.4.2 Molecular Weight Trends

As mentioned in the Introduction, there are two volume exclusion regimes: hard particle exclusion and confinement.[8, 9] Above a certain polymer concentration, known as c^*, synthetic polymers begin to overlap, starting a transition from individual, independently moving molecules (dilute) to a series of overlapping polymers with cavities between (semidilute) to an entangled network of polymers (concentrated).[11] My calculations for PVP indicate that the transition to the semidilute region occurs at concentrations between 100 g/L and 200 g/L (Table 3.1). When solution conditions change from dilute to semidilute (*i.e.*, PVP concentration is above c^*), so does the model for volume exclusion. The change helps inform my interpretation of the molecular weight dependence.

As mentioned in Chapter 1, the change from the dilute to the semidilute regime is accompanied by a change in theoretical parameters, which are affected by crowder concentration and molecular weight in different ways. For hard particle exclusion, the key parameters are sphere size and number density. These parameters correspond to our experimental variables, molecular weight and concentration. The relationship between PVP particle size and molecular weight is consistent with a self-avoiding walk polymer,[11] and as the weight concentration increases, so does the number density.

The molecular weight dependence results from 100 g/L PVP are consistent with hard particle exclusion because they coincide with predictions of stability changes based on the size of independent hard sphere crowders. Specifically, $\Delta G_{op}^{0^*}$ increases with increasing PVP concentration, but higher molecular weight PVPs have less of a stabilizing effect.[10] The data for 200 g/L and 300 g/L PVP solutions are more consistent with confinement.

For confinement, the shape and size of the confining space should be independent of PVP molecular weight. At concentrations where PVP molecules are overlapping, changing the molecular weight of PVP should not drastically change the confining space. My observations point to confinement as a more appropriate model for 200 g/L and 300 g/L PVP solutions, because there is no consistent molecular weight dependence. Increasing the concentration, however, should decrease the average size of the confining space. As the space shrinks, protein stability should increase. This matches my results from experiments in 200 g/L and 300 g/L PVP, because stability increases with increasing PVP

concentration. In summary, the transition from the dilute to the semidilute regime of the polymer solution is accompanied by a change in the applicable model for crowding, from hard particle volume exclusion to confinement. Concentration trends yielded results that indicated both volume exclusion effects and soft interactions between the protein and crowder.

3.4.3 Concentration Trends

Stabilization by volume exclusion is expected to show a strong, consistent increase with crowding agent concentration, as shown by Leu8, Val9, Lys11, Val19, Leu21, Gln28, Ile30, Leu32, Val47, Leu49, Phe50, Val51, Ile57, Ala58, Glu59, and the exemplar, Ile20 (Figure 3.2). The $\Delta\Delta G_{op}^{0^*}$ values for these residues fall between 0.9 and 3.0 kcal/mol in 300 g/L PVP, which is also consistent with predictions for the magnitude of volume exclusion effects.[37]

Excepting Val9, residues in the volume exclusion regime are either involved in global unfolding, or are backbone hydrogen bond partners of global unfolders.[17] This result is expected, because volume exclusion increases protein stability through destabilization of the denatured ensemble. For residues on the global path, the exchange-competent unfolded states are most destabilized by volume exclusion, because the globally unfolded state creates the largest change in covolume. These results indicate a contribution to stability purely associated with volume exclusion. Some residues, as shown by Asn56 (Figure 3.2), indicated native-state binding trends that could not be explained with traditional exclusion models.

Native-state binding is expected to show saturation behavior. That is, an increase in stability is noted at lower PVP concentrations, with no increase upon further addition of PVP. This trend is exhibited by Val13, Asp55, Asn56, Arg62, Val63, and Gly64. These residues and those nearby in the primary structure also exhibit chemical shift changes (Val13,Leu54 and Arg62) and increased R_1R_2 values (Lys11, Glu15, Leu54, Asp55, Asn56, and Gly64; Figure 3.5), supporting the idea that native-state PVP binding plays a role in effecting stability. Consistent with the idea of weak native-state binding, these effects seem to be absent at the lowest PVP concentrations, because no significant chemical shift changes were noted in solutions containing 10 g/L 55 kDa PVP (Figure 3.6). Further implications of weak native-state binding are discussed in the next section.

These data point to weak native-state binding as the cause for this stability trend. Native-state binding, however, differs from another stabilizing soft interaction, the solvophobic effect.[38] This effect, as exemplified by TMAO and other osmolytes, continuously increases protein stability with increasing cosolute concentration. PVP, however, shows saturation. This set of residues does not show a dependence of $\Delta G_{op}^{0^*}$ on PVP concentration, ruling out the solvophobic effect as a source of the stability increase. The lack of PVP concentration dependence also rules out volume exclusion as a source of stabilization. I rationalize the lack of an excluded volume effect based on the fact that nearly all of these residues are surface exposed, and would have exchange-accessible states that require minimal rearrangement of the protein. As such, the minor

change in size of the protein from the closed to open state for these residues would lead to a minimal contribution from volume exclusion. All other residues exhibit properties of both native-state binding and volume exclusion. I call this trend, as represented by Leu49 (Figure 3.2), the mixed effect.

The mixed effect combines weak native-state binding with volume exclusion. A modest increase in stability is noted at lower crowder concentrations, with a plateau in stability that is only slightly surpassed in 300 g/L PVP. The majority of residues not implicated in global unfolding fall into this bin (Trp5, Gly10, Ala16, Lys17, Lys18, Gln22, Lys24, Val34, Arg46, Arg48, and Asp52). For the mixed effect, it is likely that weak native-state binding dominates the stabilizing effect of PVP at low concentrations. At higher concentrations, the roles are reversed, and volume exclusion becomes more important.

In summary, I find evidence for two types of interactions affecting the stability of CI2 when crowded by PVP: volume exclusion and native-state binding. Volume exclusion affects ~80% of the residues studied, while native-state binding affects ~50%. The fact that 80% of residues show effects from volume exclusion is expected; volume exclusion should affect all residues, albeit to different extents. Native-state binding affects 50% of the residues, yet this important effect is neglected in many studies of crowding. To investigate these weak native-state binding effects further, R_1R_2 values were used.

3.4.4 Soft Interactions

Large R_1R_2 values, indicative of binding,[30] can result from strong and weak soft interactions. We ruled out strong PVP-CI2 interactions because CI2 crosspeaks are not drastically broadened by PVP.[19] Backbone amide nitrogens from a "pure" species (*i.e.* 100% monomer, 100% dimer, …) that does not exhibit conformation exchange should have R_1R_2 values below a threshold known as the rigid limit line.[30] Mixtures yield larger values. The value for the rigid limit is approximately 20 s^{-2} for data acquired on a 600 MHz NMR spectrometer. We need only consider binding interactions involving monomers and dimers of CI2 for three reasons. First, Charlton *et al.*[19] used NMR-detected diffusion experiments to show that CI2 forms no more than a dimer in a 300 g/L solution of PVP-40 at pH 5.4 and 37 °C. Second, CI2 does not undergo significant conformation exchange in dilute solution.[30] Third, PVP decreases the amide proton exchange rate. This decrease in rate is only consistent with the absence of PVP−induced conformation exchange because an increase in conformation exchange would increase amide proton exchange.

In 300 g/L PVP-40 solution, the average R_1R_2 value, 26 s^{-2}, is essentially equal to the maximum theoretical value for a mixture of CI2 monomers and dimers (25 s^{-2}).[30] Taken together with the fact that this theoretical maximum only occurs at 50% homodimer formation and the conclusions of Charlton *et al.*,[19] this observation indicates that although limited CI2 self-association may occur, there are also weak soft interactions between PVP and CI2. My chemical shift analysis corroborates this information.

Chemical shift changes arise from changes in native-state chemical environment. This environmental effect could arise from PVP binding, or PVP-induced conformational changes. Shift changes occur at PVP concentrations of ≥100 g/L in tightly packed regions, including the second β-sheet (Asp45-Asp52). This observation leads me to invoke weak chemical interactions between PVP and the native state of CI2 as the cause of the chemical shift changes, because tightly packed regions are unlikely to undergo significant conformational changes. These weak native-state interactions, which account for the binding trend that stabilizes 50% of the residues studied, are distinct from nonspecific interactions, which are destabilizing.

Nonspecific interactions will destabilize proteins, as is the case with urea.[13] It was noted by Charlton *et al.* that the monomer model of PVP, N-ethyl pyrrolidone, destabilizes CI2.[19] This type of interaction is expected to persist in the polymer, although it should be attenuated because the polymer partially excludes access. The increase in R_1R_2 with increasing PVP concentration (Figure 3.5) is evidence for the persistence of nonspecific chemical interactions between the crowder and the protein. The weak destabilizing interaction mitigates the stabilizing effects in our system, resulting in an underestimate of contributions from volume exclusion and native-state binding interactions. The contribution of nonspecific interactions may be large in our experiments because of the low ionic strength used. Electrostatics should not be a major contributor, however, as PVP is uncharged. Proteins do, however, have electrostatic effects. As shown in Figure 3.5, the interactions of CI2 with PVP are weaker than interactions with

bovine serum albumin (BSA). I expect nonspecific binding to have a larger effect when proteins are used as crowders as opposed to synthetic polymers because of the increase in nonspecific interactions.[20]

3.5 Conclusions

I quantified both the effect of PVP molecular weight and concentration. Consistent with volume exclusion models, PVP never destabilizes the protein. I observe two trends for the molecular weight dependence and three trends for the concentration dependence. The molecular weight trends can be explained by the two regimes of volume exclusion, hard particle exclusion and confinement. The concentration dependence can be explained by two types of interactions, volume exclusion and soft interactions.

My study of molecular weight dependence on protein stability yielded two trends corresponding to two models of volume exclusion. At low PVP concentrations, there is a diminution of the stabilization effect with increasing molecular weight, as expected from hard sphere volume exclusion. At higher concentrations, there is no molecular weight dependence, signaling a shift from hard particle volume exclusion to confinement as the most predictive model as the polymer begins to overlap. Concentration trends yielded contributions from both volume exclusion and weak native-state binding.

Volume exclusion explains the concentration-dependent interaction for most of the globally unfolding residues. However, native-state binding is present for other residues where $\Delta G_{op}^{0^*}$ increases at lower concentrations with saturation.

Many residues exhibit effects from both volume exclusion and binding. Binding was investigated independently, and our results uncover soft interactions between PVP and CI2.

The most surprising conclusion is that soft interactions between the crowding agent and the native state of the protein play such a large role despite the fact that I purposely chose a system that minimizes soft interactions.[20] Weak nonspecific interactions mitigate the effects of volume exclusion, indicating that my analysis underestimates the effect of volume exclusion. We also find evidence for native-state interactions. Specifically, 50% of the residues show effects from weak native-state interactions. I expect soft interactions to play an even larger role in biological systems, where proteins are crowded by other proteins, which can have stabilizing or destabilizing soft interactions. In some cases, destabilizing nonspecific interactions could compete with the stabilizing volume exclusion effect. Such soft interactions will need to be addressed to understand the full effects of crowding in cells. In summary, although macromolecular crowding is often discussed solely in the context of volume exclusion, studies must be expanded to include soft interactions.

3.6 Figures and Tables

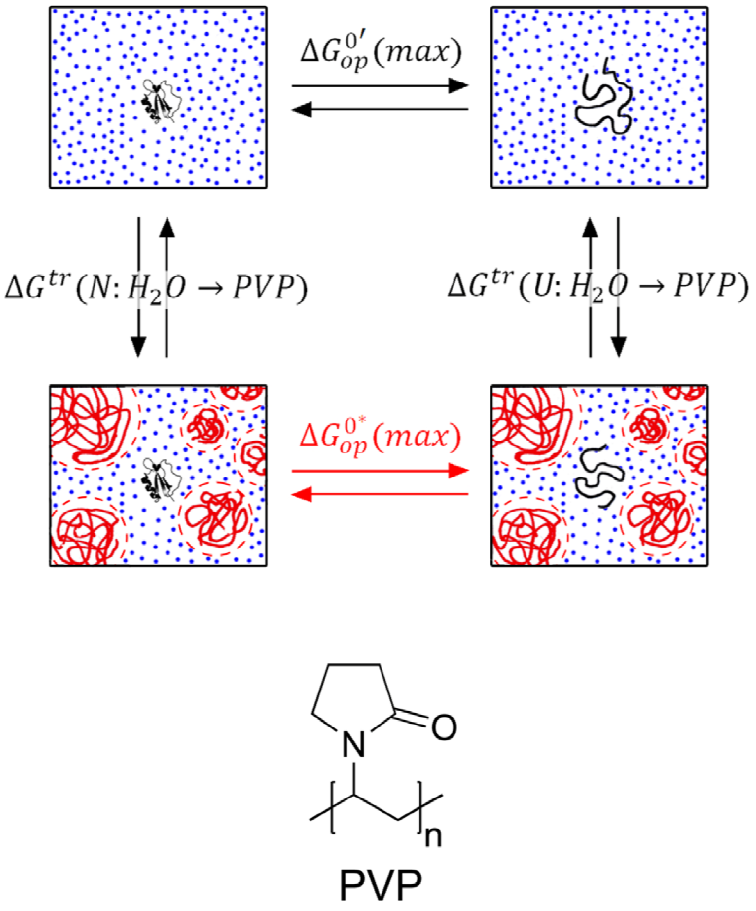

Figure 3.1 Diagram of stability relationships and the structure of PVP

$\Delta G^{0'}_{op}(max)$ presents dilute solution stability,and $\Delta G^{0^*}_{op}(max)$ represents stability under crowded conditions. ΔG_{tr} represents a transfer free energy between sets of solvent conditions.

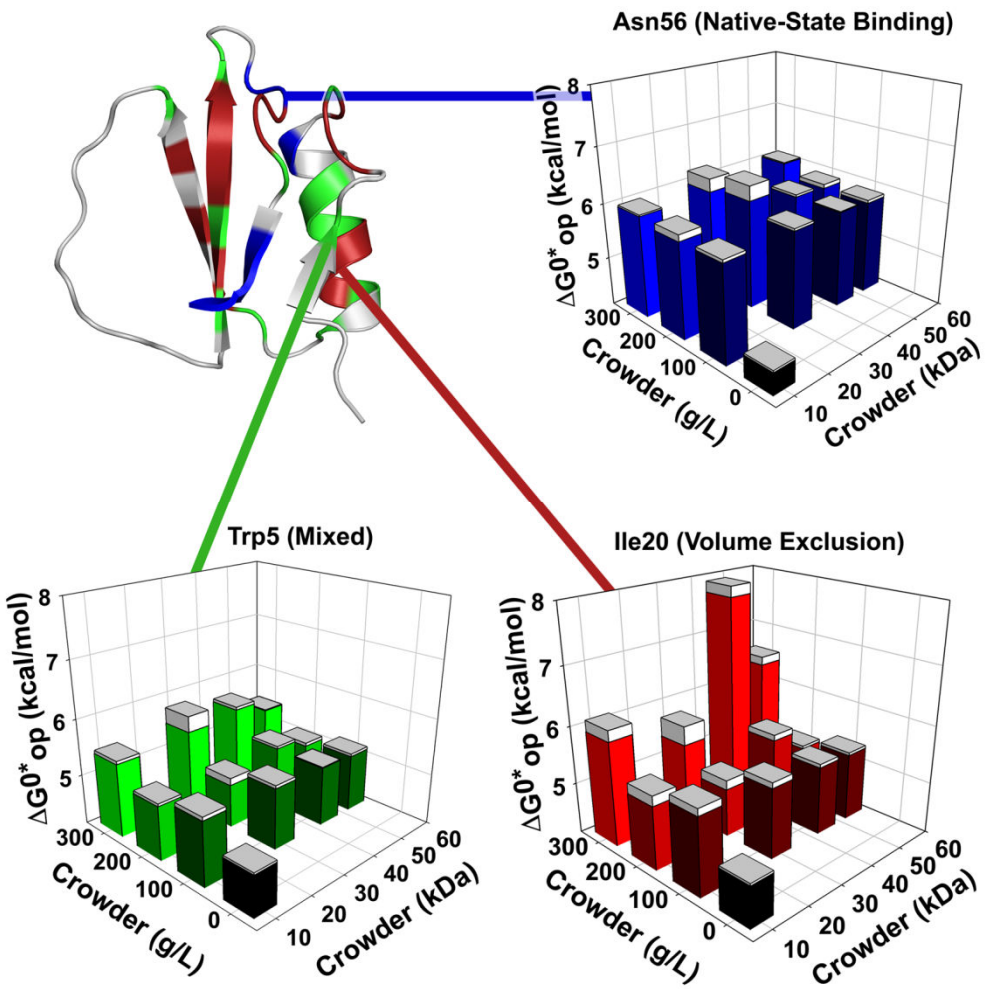

Figure 3.2 Structure of CI2 and stability histograms

Residues are colored by stability trends. Red, blue, and green residues exhibit trends consistent with volume exclusion, native-state binding, and the mixed effect, respectively. Residues for which stabilities could not be measured are shown in white. The mean $\Delta G_{op}^{0^*}$ from three trials is plotted for Ile20, Trp5, and Asn56 as a function of PVP molecular weight and concentration (50 mM sodium acetate, pH 5.4, 37 °C). The column caps represent the positive component of the standard errors. PyMol[39] was used to visualize the structure.

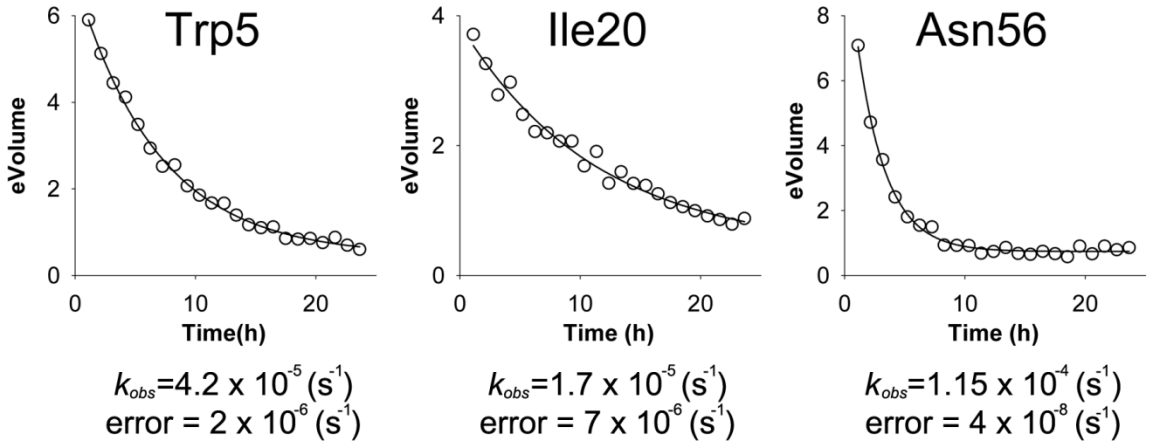

Figure 3.3 Amide proton exchange curves

Exchange curves are displayed for Trp5, Ile20, and Asn56 of CI2 in 300 g/L PVP-10, 50 mM sodium acetate buffer, pH 5.4, 37 °C with corresponding k_{obs} values and curve-fitting errors.

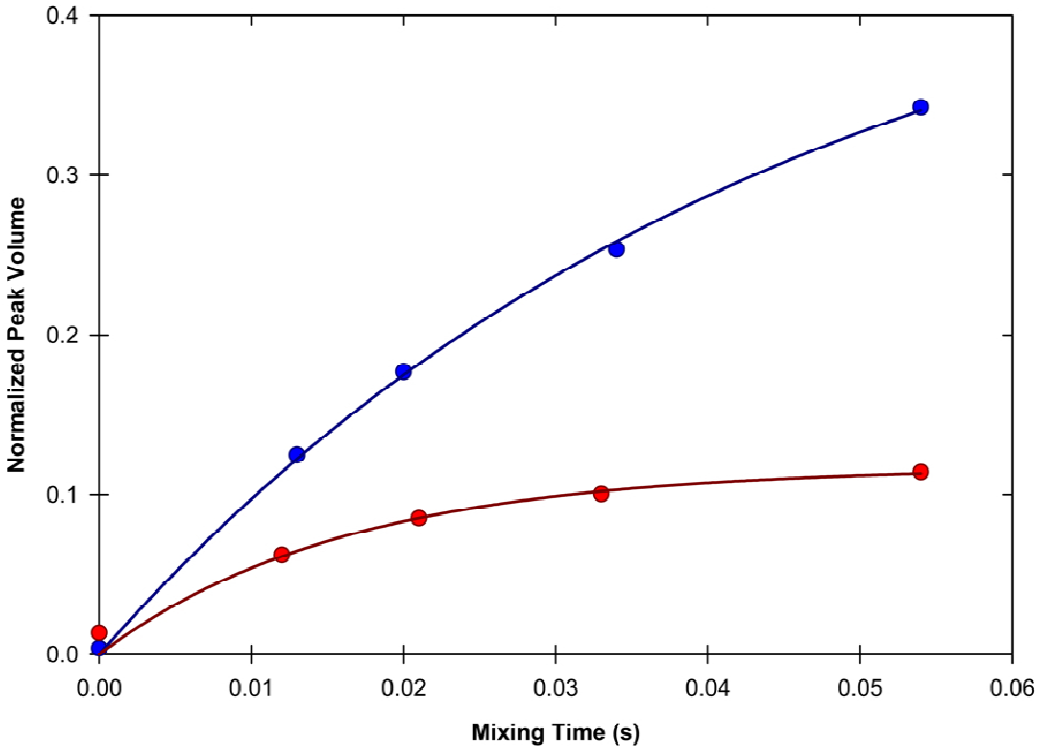

Figure 3.4 CLEANEX-PM curves

CLEANEX-PM buildup curves are shown for the His37 backbone amide proton of 1 mM CI2 (50 mM acetate, pH 5.4, 37° C) with 0 g/L (blue) and 300 g/L (red) PVP-40. Lines represent fits performed according to the method of Hwang *et al.*.[28] Because the water signal was invariate with mixing time, 0.1 s^{-1} was used as the value of R_{1Bapp} [29]. In dilute solution, k is 10 ± 2 s^{-1} and R_{1Aapp} is 11± 1 s^{-1}. In PVP, k is 7 ± 2 s^{-1} and R_{1Aapp} is 50 ± 10 s^{-1}. The value of k is unchanged between conditions, but R_{1Aapp} changes, because it is a function of R_1 and R_2 [28], which both change (see Figure 3.5).

Species	$\bar{M}_W$ (kDa)	$\bar{M}_N$ (kDa)	Polydispersity	R_H (nm)	$\bar{v}_2$ (mL/g)	c^* (g/L)
PVP-10	10.2	5.1	2.0	2.2	0.807	630
PVP-29	29.7	13.0	2.28	4.9	0.806	160
PVP-40	44.9	13.4	3.35	5.6	—	170
PVP-55	55.0	12.5	4.38	6.7	0.798	120

Table 3.1 Characterization of PVP-10, 29, 40, and 55

Residue(s)	k_{obs} NOESY ($s^{-1} \times 10^5$)	k_{obs} HSQC ($s^{-1} \times 10^5$)
Leu8	5	4
Val9	4	3
Leu8 + Val9[a]	9	7
Leu8 , Val9[b]	7	—
Ala58	5	4
Glu59	6	5
Ala58 + Glu59[a]	11	9
Ala58 , Glu59[b]	9	—

Table 3.2 NOESY-HEX results

k_{obs} values from NOESY-detected amide proton exchange and HSQC-detected amide proton exchange in 50 g/L PVP-10, 50 mM sodium acetate buffer, pH 5.4, 37 °C.

[a] Sum of values from individual crosspeak decays
[b] Exchange rate of amide-amide NOESY crosspeak

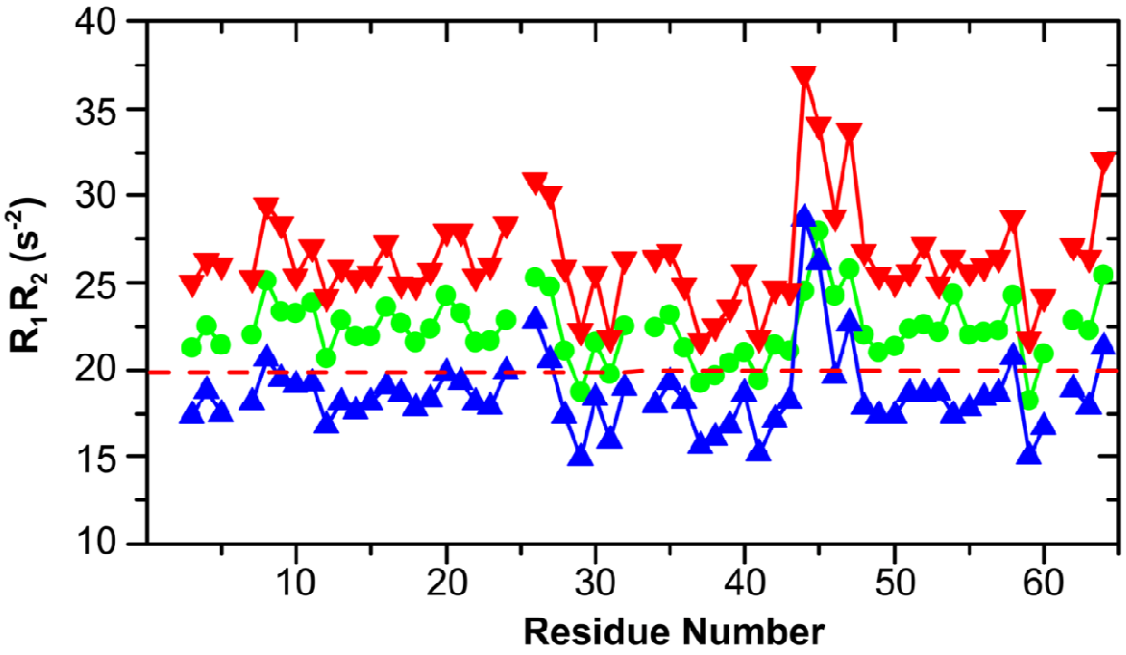

Figure 3.5 Histogram of R_1R_2 values

R_1R_2 values were determined for 0.4 mM CI2 (200 mM sodium acetate, pH 5.4, 25 °C) with 100 g/L PVP-40 (blue), 200 g/L PVP-40 (green), and 200 g/L BSA (red). The rigid limit is depicted as a dashed red line. Rigid limit value and data for 200 g/L BSA are from Li and Pielak [30].

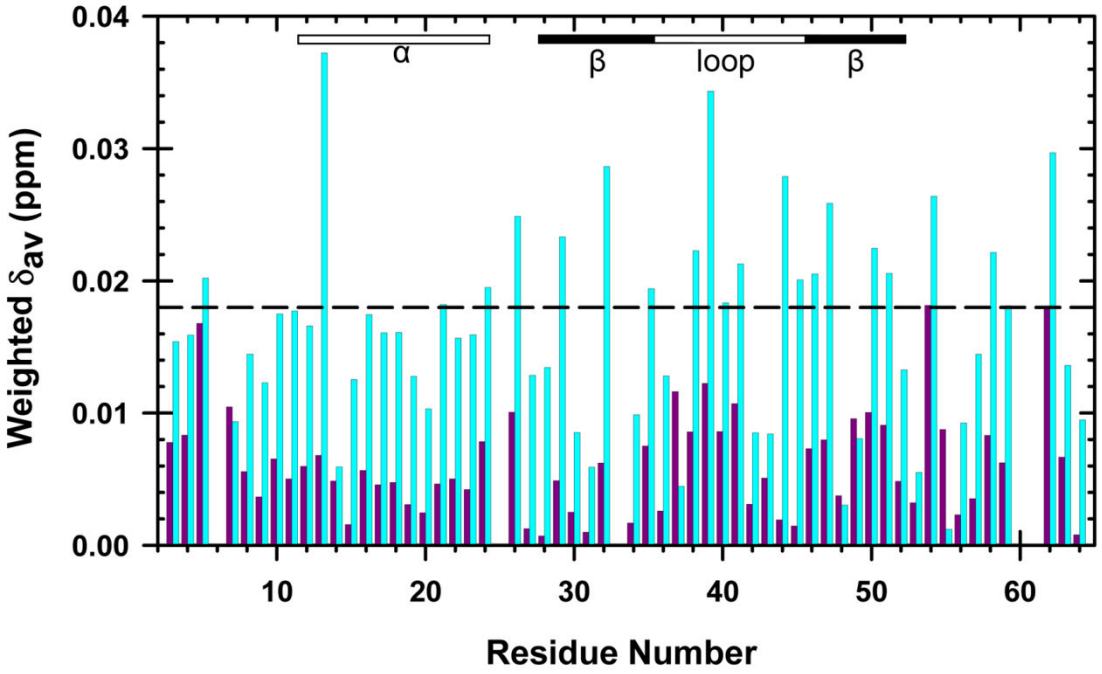

Figure 3.6 Chemical shift changes

A histogram of changes in backbone ^{15}N and ^{1}H chemical shifts for 1 mM CI2 upon adding 10 g/L PVP-55 (purple) and 100 g/L PVP-55 (cyan) in 50 mM sodium acetate buffer, pH 5.4, 37 °C. Elements of secondary structure are indicated above histogram. Values above the horizontal dashed line, as defined by Charlton *et al.* [19], represent statistically significant changes in chemical shift.

3.7 References

1. Capp, M. W., Cayley, D. S., Zhang, W. T., Guttman, H. J., Melcher, S. E., Saecker, R. M., Anderson, C. F., and Record, M. T. (1996) Compensating effects of opposing changes in putrescine (2^+) and K^+ concentrations on *lac* repressor-*lac* operator binding: *In vitro* thermodynamic analysis and *in vivo* relevance, *J. Mol. Biol.* **258**, 25-36.

2. Dedmon, M. M., Patel, C. N., Young, G. B., and Pielak, G. J. (2002) FlgM gains structure in living cells, *Proc. Natl. Acad. Sci. U.S.A.* **99**, 12681-12684.

3. Ignatova, Z., and Gierasch, L. M. (2004) Monitoring protein stability and aggregation *in vivo* by real-time fluorescent labeling, *Proc. Natl. Acad. Sci. U.S.A.* **101**, 523-528.

4. McGuffee, S. R., and Elcock, A. H. (2010) Diffusion, crowding & protein stability in a dynamic molecular model of the bacterial cytoplasm, *PLoS Comput. Biol.* **6**, e1000694.

5. Elcock, A. H. (2010) Models of macromolecular crowding effects and the need for quantitative comparisons with experiment, *Curr. Opin. Struct. Biol.* **20**, 196-206.

6. Lumry, R., Biltonen, R., and Brandts, J. F. (1966) Validity of the "two-state" hypothesis for conformational transitions of proteins, *Biopolymers* **4**, 917-944.

7. Clarke, J., and Itzhaki, L. S. (1998) Hydrogen exchange and protein folding, *Curr. Opin. Struct. Biol.* **8**, 112-118.

8. Zhou, H. X., Rivas, G. N., and Minton, A. P. (2008) Macromolecular crowding and confinement: Biochemical, biophysical, and potential physiological consequences, *Annu. Rev. Biophys.* **37**, 375-397.

9. Zhou, H. X., and Dill, K. A. (2001) Stabilization of proteins in confined spaces, *Biochemistry* **40**, 11289-11293.

10. Minton, A. P. (1983) The effect of volume occupancy upon the thermodynamic activity of protein: Some biochemical consequences, *Mol. Cell. Biochem.* **55**, 119-140.

11. Rubinstein, M., and Colby, R. (2003) *Polymer Physics*, Oxford University Press, New York, NY, USA.

12. Timasheff, S. N. (2002) Protein-solvent preferential interactions, protein hydration, and the modulation of biochemical reactions by solvent components, *Proc. Natl. Acad. Sci. U.S.A.* **99**, 9721-9726.

13. Lim, W. K., Rösgenc, J., and Englander, S. W. (2009) Urea, but not guanidinium, destabilizes proteins by forming hydrogen bonds to the peptide group, *Proc. Natl. Acad. Sci. U.S.A.* **106**, 2595-2600.

14. Vicky, D.-N., and Loria, J. P. (2007) The effects of cosolutes on protein dynamics: The reversal of denaturant-induced protein fluctuations by trimethylamine *N*-oxide, *Protein Sci.* **16**, 20-29.

15. Isom, D. G., Vardy, E., Oas, T. G., and Hellinga, H. W. (2010) Picomole-scale characterization of protein stability and function by quantitative cysteine reactivity, *Proc. Natl. Acad. Sci. U.S.A.* **107**, 4908-4913.

16. Jackson, S. E., and Fersht, A. R. (2002) Folding of chymotrypsin inhibitor 2. 1. Evidence for a two-state transition, *Biochemistry* **30**, 10428-10435.

17. Neira, J. L., Itzhaki, L. S., Otzen, D. E., Davis, B., and Fersht, A. R. (1997) Hydrogen exchange in chymotrypsin inhibitor 2 probed by mutagenesis, *J. Mol. Biol.* **270**, 99-110.

18. Molyneux, P. (1983) *Water-soluble synthetic polymers: properties and behavior*, Vol. **Volume 1**, CRC Press, Boca Raton, CA, USA.

19. Charlton, L. M., Barnes, C. O., Li, C., Orans, J., Young, G. B., and Pielak, G. J. (2008) Macromolecular crowding effects on protein stability at the residue level, *J. Am. Chem. Soc.* **130**, 6826-6830.

20. Wang, Y., Li, C., and Pielak, G. J. (2010) Effects of proteins on protein diffusion, *J. Am. Chem. Soc.*, 9392–9397.

21. Ladurner, A. G., and Fersht, A. R. (1999) Upper limit of the time scale for diffusion and chain collapse in chymotrypsin inhibitor 2, *Nat. Struct. Biol.* **6**, 28-31.

22. Güven, O., and Eltan, E. (1981) Molecular association in aqueous solutions of high molecular weight poly(N-vinyl-2-pyrrolidone), *Makromol. Chem.* **182**, 3129-3134.

23. Bai, Y. W., Sosnick, T. R., Mayne, L., and Englander, S. W. (1995) Protein folding intermediates: Native-state hydrogen exchange, *Science* **269**, 192-197.

24. Sadeghi, R., and Taghi Zafarani-Moattar, M. (2004) Thermodynamics of aqueous solutions of polyvinylpyrrolidone, *Journal of Chemical Thermodynamics* **36**, 665-670.

25. Kelly, A. E., Ou, H. D., Withers, R., and Dötsch, V. (2002) Low-conductivity buffers for high-sensitivity NMR measurements, *J. Am. Chem. Soc.* **124**, 12013-12019.

26. Delaglio, F., Grzesiek, S., Vuister, G. W., Zhu, G., Pfeifer, J., and Bax, A. (1995) NMRPipe: A multidimensional spectral processing system based on UNIX pipes, *J. Biomol. NMR* **6**, 277-293.

27. Johnson, B. A., and Blevins, R. A. (1994) NMR View: A computer program for the visualization and analysis of NMR data, *J. Biomol. NMR* **4**, 603-614.

28. Hwang, T.-L., van Zijl, P. C. M., and Mori, S. (1998) Accurate quantitation of water-amide exchange rates using the phase-modulated CLEAN chemical EXchange (CLEANEX-PM) approach with a fast-HSQC (FHSQC) detection scheme, *J. Biomol. NMR* **11**, 221-226.

29. Bertini, I., Ghosh, K., Rosato, A., and Vasos, P. R. (2003) A high-resolution NMR study of long-lived water molecules in both oxidation states of a minimal cytochrome *c*, *Biochemistry* **42**, 3457-3463.

30. Li, C., and Pielak, G. J. (2009) Using NMR to distinguish viscosity effects from nonspecific protein binding under crowded conditions *J. Am. Chem. Soc.* **131**, 1368–1369.

31. Davison, T. S., Nie, X., Ma, W., Lin, Y., Kay, C., Benchimol, S., and Arrowsmith, C. H. (2001) Structure and functionality of a designed p53 dimer, *J. Mol. Biol.* **307**, 605-617.

32. Frost, A. A., and Pearson, R. G. (1953) *Kinetics and Mechanism*, John Wiley & Sons, New York, NY, USA.

33. Wagner, G. (1980) A novel application of nuclear Overhauser enhancement (NOE) in proteins: Analysis of correlated events in the exchange of internal labile protons, *Biochem. Biophys. Res. Commun.* **97**, 614-620.

34. Miklos, A. C., Li, C., and Pielak, G. J. (2009) Using NMR-detected backbone amide ^{1}H exchange to assess macromolecular crowding effects on globular-protein stability, *Methods Enzymol.* **466**, 1-18.

35. Englander, S. W., and Kallenbach, N. R. (1983) Hydrogen exchange and structural dynamics of proteins and nucleic acids., *Q. Rev. Biophys.* **16**, 521-655.

36. Kneller, J. M., Lu, M., and Bracken, C. (2002) An effective method for the discrimination of motional anisotropy and chemical exchange, *J. Am. Chem. Soc.* **124**, 1852-1853.

37. Minton, A. P. (2000) Effect of a concentrated "inert" macromolecular cosolute on the stability of a globular protein with respect to denaturation by heat and by chaotropes: A statistical-thermodynamic model, *Biophys. J.* **78**, 101-109.

38. Auton, M., and Bolen, D. W. (2005) Predicting the energetics of osmolyte-induced protein folding/unfolding, *Proc. Natl. Acad. Sci. U.S.A.* **102**, 15065-15068.

39. DeLano, W. L. (2002) The PyMOL molecular graphics system.

4 Crowding by Giant Synthetic Polymers: Globular Protein Stability and Backbone Dynamics

4.1 Introduction

Having studied the polydisperse crowder, PVP, whose size is on the order of that of CI2, I decided to study crowders that are orders of magnitude larger than PVP. As discussed in Chapter 3, theory predicts that crowding effects diminish as the crowding agent's size surpasses the size of the test protein.[1] Studying the effects of particles vastly larger than CI2 would provide empirical proof about the upper boundary. Here, I used poly(*N*-isopropylacrylamide-*co*-acrylic acid) (*p*-NIPAm-*co*-AAc) microgels.

*p*NIPAm is of interest in pharmaceutical applications because it is one of a class of environmentally sensitive microgels.[2] Typically, NIPAm microgels absorb a large amount of water, resulting in highly swelled particles that exclude large amounts of solution volume (Figure 4.1). An increase in temperature causes the particle to shed water and shrink. This tunable uptake and release makes NIPAm microgels interesting for drug delivery applications. It also presents an interesting biological problem when considering possible interactions between the microgel and proteins. Transmission electron microscopy data show that our particular *p*-NIPAm-*co*-AAc particles (henceforth known simply as NIPAm-AAc) are

spherical.[3] The particle size is known to be both temperature and pH dependent. We thought that these properties would provide an opportunity to investigate the size dependence of crowding effects with a single polymer.

My PVP studies relied on multiple preparations of PVP for size differences. Although the PVP preparations were created from the same monomer, the lengths of the polymer chains were vastly different. Furthermore, these multiple preparations have different polydispersities, and impurities could be non-uniform. The NIPAm-AAc system had the potential to allow a single preparation whose size could be adjusted by adjusting pH or temperature.

4.2 Materials and Methods

^{15}N-enriched CI2 was expressed and purified as described in Chapter 3.

A general synthesis for NIPAm-AAc microgels is described by Jones and Lyon,[3] but variations yield products with different properties (size, temperature / pH dependence, *etc.*).[4-6] The microgels used here were prepared via aqueous, surfactant-free, free radical precipitation polymerization using 70 mM total monomer concentration. Briefly, *N*-isopropylacrylamide (0.6973 g) and *N,N'*-methylenebis(acrylamide) (0.0215 g) were dissolved in 99 mL of H2O and filtered through a 0.8 μm syringe filter into a round bottom flask. The mixture was bubbled with N_2 (g) and heated to 70 °C (±2 °C) over ~1 h. Acrylic acid (46 μL) was then added to the mixture. Polymerization was initiated by adding a solution of $(NH_4)_2S_2O_8$ (0.0226 g) dissolved in 1 mL of H_2O. This mixture was stirred at 70 °C (±2 °C) under a blanket of N_2 (g) for 4 h and was stirred and cooled overnight.

The mixture was filtered through Whatman #2 paper and stored. Aliquots of the resultant colloidal dispersion were purified with centrifugation at 15,422 x g, decanted, and resuspended in H_2O. This process was performed three times. The particles were then lyophilized to yield a white powder.

The microgels were characterized after suspension in sodium acetate (pH 5.4) and passage through a 0.8 μm filter. This solution was sonicated for 5 min, allowed to equilibrate for 30 min, then analyzed by using multi-angle laser light scattering (MALLS).[7]

HSQC-detected amide proton exchange, NOESY-HEX, and CLEANEX-PM[8] experiments were performed on samples comprising 1 mM CI2 and 10 g/L NIPAm-AAc particles in 50 mM acetate buffered solution, pH 5.4 at 37°C. Dilute solution samples are identical, but contain no NIPAm-AAc. Details of these NMR experiments are described in Chapter 2.

^{15}N T_1 and T_2 relaxation times and $^{15}N\{^1H\}$ NOEs were measured as described by Kay *et al*.[9] Experiments were performed on the 600 MHz spectrometer. Lipari-Szabo model free analysis[10] was performed with the software package Relaxn 2.2.[11] The majority of residues were fit with the original model-free formalism[12] to yield τ_m, S^2 and τ_e.

4.3 Results and Discussion

4.3.1 Polymer Characterization

The results of the polymer characterization are shown in Table 4.1. The microgels composed of NIPAm-AAc have an average hydrodynamic radius (R_H)

of 312 nm and an average polydispersity of 7.4%. The molecular weight of the microgels was estimated to be 1 GDa by MALLS.[7]

4.3.2 Controls for Amide Proton Exchange

To determine whether exchange from the open state (k_{int}) is rate limiting, I performed NOESY-HEX experiments (Chapter 2). The results are given in Table 4.2, along with individual backbone residue decay rates from HSQC-detected amide proton exchange.

To determine whether k_{int} values are changed by crowding, I used CLEANEX-PM experiments[8] to determine k_{int} for residues on the extended loop region of CI2. For His37, k_{int} values were 11 ±2 s^{-1} in dilute solution and 8 ±2 s^{-1} in 10 g/L NIPAm-AAc.

4.3.3 Dynamics

Analysis of the T_1, T_2, and NOE data acquired by Dr. Conggang Li in dilute solution and in 10 g/L NIPAm-AAc yielded the values for τ_m, S^2, and τ_e. The value of τ_m was the same (4.1 ns) in dilute solution and in 10 g/L NIPAm-AAc, and is consistent with the value obtained by Shaw *et al.* in dilute solution.[13] Histograms of S^2 and τ_e *versus* residue number are shown in Figure 4.2. Linear least squares analysis of a plot of S^2 in dilute solution *versus* S^2 in crowded solution gives a slope of 1.0 ±0.1, a y-intercept of 0.1 ±0.1 and an R^2 value of 0.80.

4.3.4 Amide Proton Exchange and Stability

Values for k_{obs} were determined in triplicate for solutions in the presence and absence of 10 g/L NIPAm-AAc. Exchange was slowed in 10 g/L NIPAm-AAc compared to dilute solution (Figure 4.3). Values of ΔG^{0*}_{op} were determined by using values for k_{int} calculated from SPHERE[14] and k_{obs} values from amide proton exchange experiments. A histogram of ΔG^{0*}_{op} *versus* residue number is shown in Figure 4.4.

4.4 Discussion

4.4.1 Polymer Characterization

The volume occupancy of NIPAm-AAc solutions defines the degree of crowding. Using a hydrodynamic radius of 312 nm and a molecular weight of 1 GDa, the microgel in a 10 g/L solution occupies ~70% of the solution volume at pH 5.4 and 37 °C (the conditions used in our experiments). The practical limit of spherical packing is 64% volume occupancy,[15] but soft materials such as microgels can be "overpacked."[16] My solutions, however, were still in the liquid state, meaning my value for volume occupancy is likely an overestimate. The high value does, however, suggest that experimental conditions were within the realm of crowding, as other systems show crowding effects at less than 20% volume occupancy.[17, 18]

4.4.2 Controls for Amide Proton Exchange

Although the microgel slowed exchange (Figure 4.3), it was necessary to perform NOESY-HEX and CLEANEX-PM control experiments (Chapter 2) to

ensure that stability values could be obtained under both sets of conditions. As shown in Table 4.2, the exchange rates observed for the amide-amide crosspeaks for CI2 in both dilute solution and in 10 g/L NIPAm-AAc are, within the uncertainty of the experiment, the sums of their respective individual exchange rates, indicating that the exchanges are uncorrelated. I concluded that exchange from the open state is rate limiting, allowing determination of stability from amide proton exchange rates.

It was also necessary to perform CLEANEX-PM experiments to ensure that k_{int} values calculated from SPHERE[14] were accurate. Measuring the exchange rate of the His37 amide proton, which is fully exposed in the flexible loop region of CI2 (residues 35-44), indicated that the intrinsic rate of exchange in 10 g/L NIPAm-AAc (8 ±2 s^{-1}) is within uncertainty of the value in dilute solution (11 ±2 s^{-1}). These results suggest that k_{int} values can be used without alteration. Having shown that it is valid to use k_{obs} and k_{int} values to obtain opening free energies, I constructed histograms of ΔG^{0*}_{op} values *versus* residue number (Figure 4.4).

4.4.3 Dynamics and Stability

Crowding involves two different types of effects on protein stability: volume exclusion and chemical interactions. Volume exclusion is expected to stabilize protein native states, whereas chemical interactions can be stabilizing or destabilizing (Chapter 3). Chemical interactions are also expected to impede rotational motion. Our data indicating that τ_m was unchanged from dilute to

crowded solution suggests no chemical interactions are present. Therefore, I only consider contributions from volume exclusion effects.

The patterns of ΔG^{0*}_{op} values along the amino acid sequence (Figure 4.4) are the same in dilute solution as they are in the microgel solution, suggesting that the microgel does not alter the open states of CI2. The ΔG^{0*}_{op} values in the microgel are uniformly larger than the values for dilute solution, indicating the polymer stabilizes the protein with a maximal stability increase of approximately 0.4 kcal/mol. Averaging the ΔG^{0*}_{op} values from residues known to be implicated in global unfolding[19] show that the microgel increases the overall stability from 4.9 kcal/mol to 5.2 kcal/mol. I cannot state with certainty that the increased stability arises from the polymeric nature of the microgel because its crosslinked nature makes determination of a suitable monomer unit difficult.

Considering the volume fraction estimate of ~70%, a 0.3 kcal/mol stability increase is quite small. This modest increase is anticipated, however, because the hydrodynamic radius of CI2 is only 1% that of the NIPAm-AAc microgels (Figure 4.5). In such a system, CI2 can occupy interstitial spaces between NIPAm-AAc microgels, putting CI2 in a dilute solution environment. Alternatively, the microgel particles probably have pores large enough to accommodate CI2 and water.

Next, I try to relate the stability change to the backbone dynamics data (Figure 4.2). The data indicate that the increased stability does not alter the ps-ns backbone dynamics. It has been proposed that stability changes are associated with alterations of ps-ns backbone dynamics.[20, 21] These results do not indicate a

connection, because we observe increased stability without a change in ps-ns timescale dynamics. The most straightforward conclusion is that stability is not linked to backbone ps-ns dynamics. It is possible, however, that stability is reflected in slower (ms-s) motions.[22]

4.5 Conclusions

Even though the 10 g/L solution of NIPAm-AAc microgels occupy ~70% of solution volume, these conditions do not affect the ps-ns timescale backbone dynamics of CI2. The microgel, however, does have a modest stabilizing effect on the protein. These conclusions are explained by the fact that the majority of the protein occupies a water-like environment in interstitial spaces of the microgel particles. In the context of NIPAm-AAc as a drug delivery tool, this is promising information, supporting the notion that these microgels are biocompatible materials. It seems likely, however, that larger crowding agents such as NIPAm-AAc can have more noticeable effects when present in mixed solutions that also contain multiple sizes of crowders.[23]

4.6 Figures and Tables

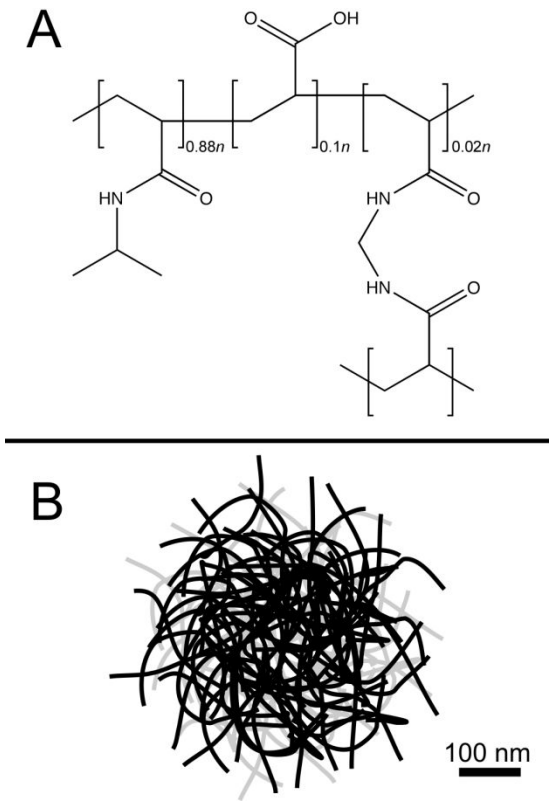

Figure 4.1 Structure and Size of *p*-NIPAm-*co*-AAc

A) The monomeric repeat of NIPAm. B) Overall shape and size of NIPAm-AAc microgels.

pH 5.4, 37 °C		pH 3.0, 23 °C	
R_H (nm)	Polydispersity (%)	R_H (nm)	Polydispersity (%)
310.9	9.1	254	13.0
311.4	8.3	261	10.1
309.4	4.1	254	10.3
321.5	10.7	255	14.5
308.2	5.0	253	12.5

Table 4.1 Characterization of NIPAm-AAc

Residue(s)	k_{obs} NOESY (s^{-1} x 10^5)	k_{obs} HSQC (s^{-1} x 10^5)
Leu8	3	3
Val9	2	2
Leu8 + Val9[a]	5	5
Leu8 , Val9[b]	5	N/A
Lys17	52	40
Lys18	20	15
Lys17 + Lys18[a]	72	55
Lys17 , Lys18[b]	50	N/A
Ala58	3	4
Glu59	3	3
Ala58 + Glu59[a]	6	7
Ala58 , Glu59[b]	7	—

Table 4.2 NOESY-HEX results

k_{obs} values from NOESY-detected amide proton exchange and HSQC-detected amide proton exchange for CI2 in 10 g/L NIPAm-AAc, 50 mM sodium acetate, pH 5.4, 37 °C.

[a] Sum of values from individual crosspeak decays
[b] Exchange rate of amide-amide NOESY crosspeak

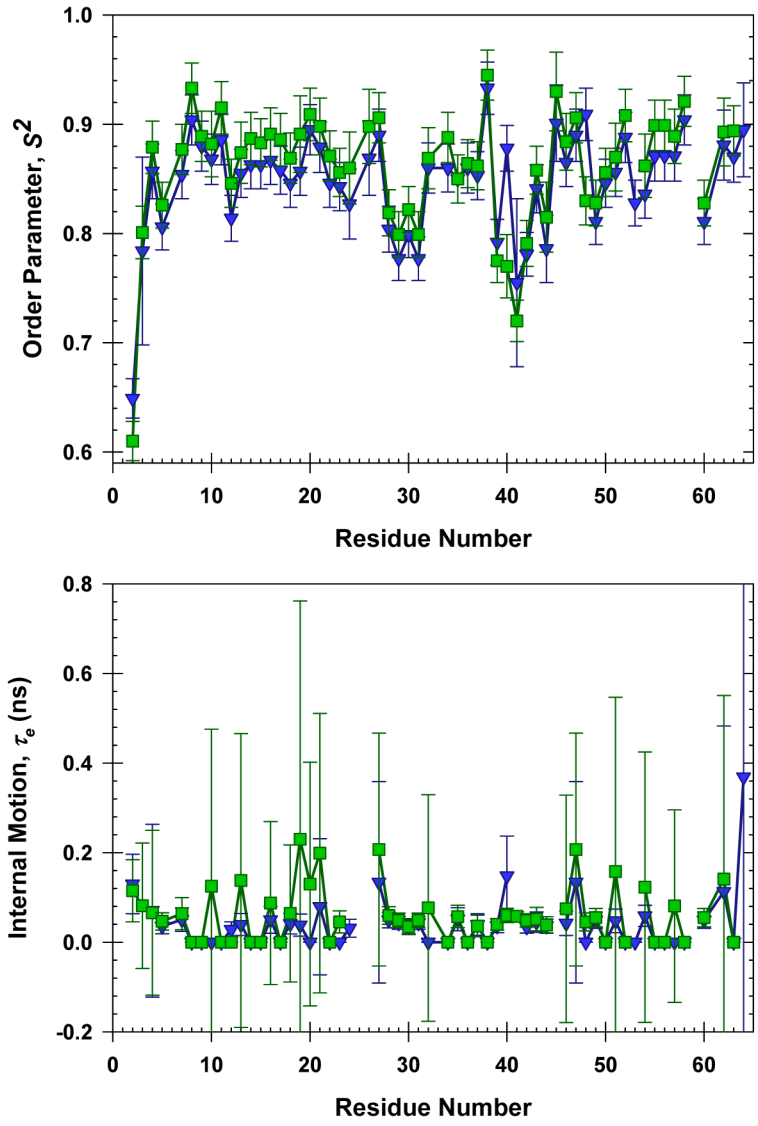

Figure 4.2 CI2 dynamics in NIPAm-AAc

Order parameters (upper panel) and timescales of internal motion (lower panel) for CI2 in dilute solution and in 10 g/L NIPAm-AAc.

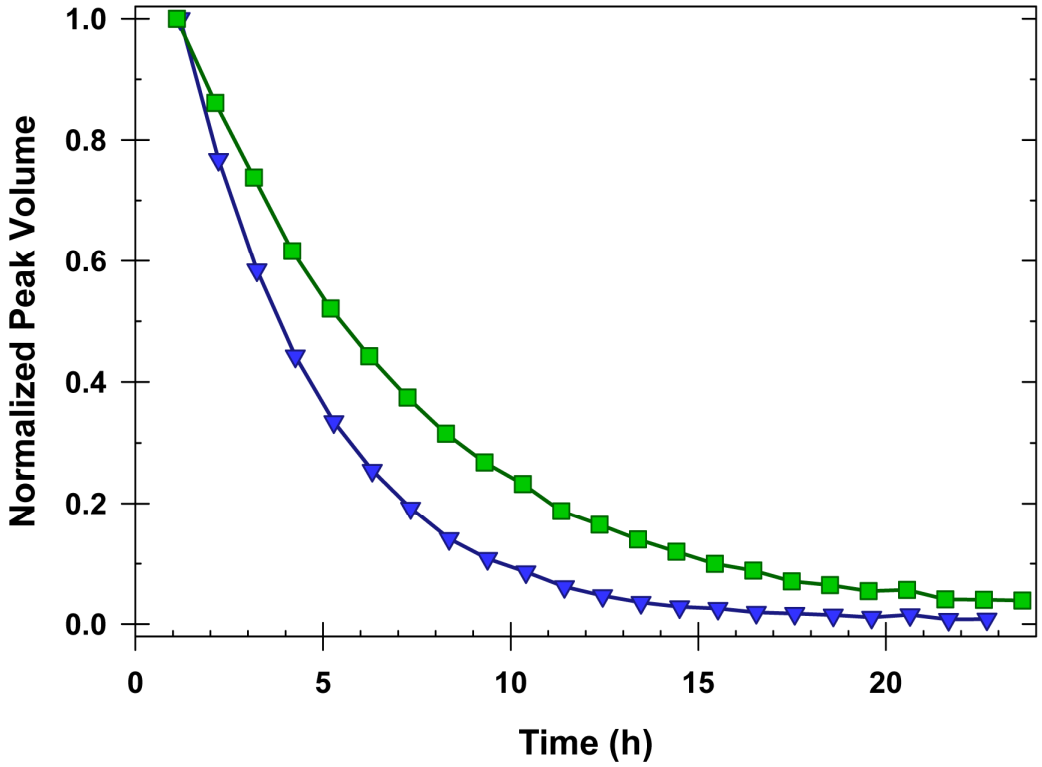

Figure 4.3 Exchange Curves

Amide proton exchange curves for Lys24 in dilute solution (blue triangles) and in 10 g/L NIPAm-AAc (green squares). Values for k_{obs} are 7.53 ±0.05 x 10^{-5} ± s^{-1} in dilute solution and 4.55 ±0.05 x 10^{-5} s^{-1} in 10 g/L NIPAm-AAc. These uncertainties are from non-linear least squares fitting and are smaller than the uncertainty from triplicate analysis.

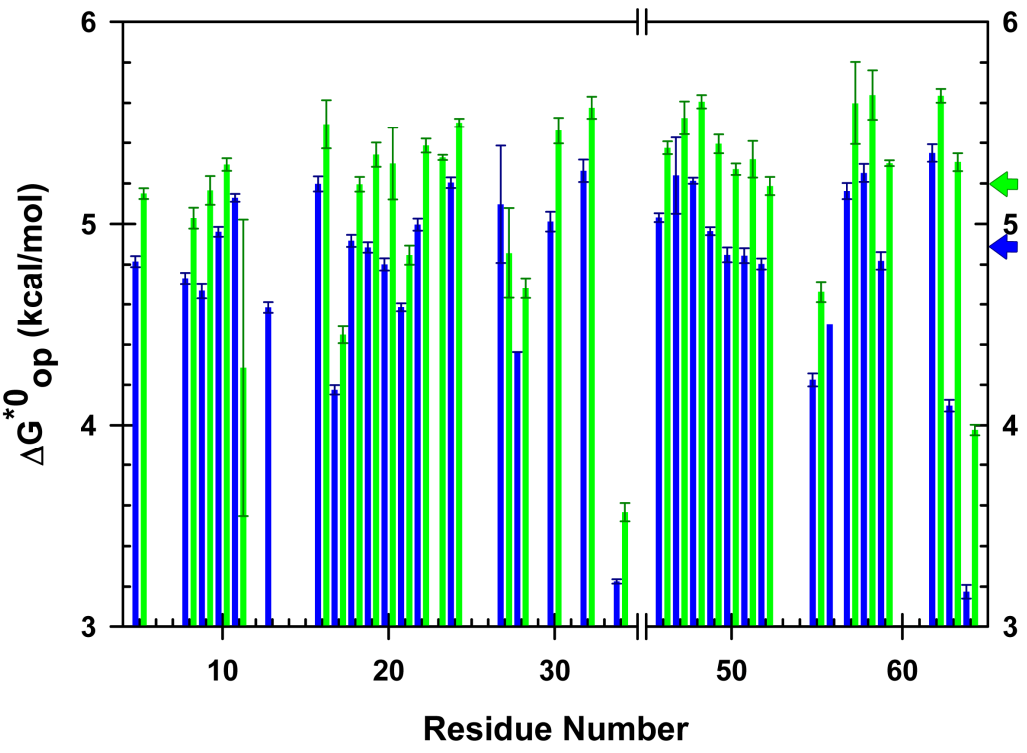

Figure 4.4 CI2 stability in NIPAm-AAc

Results are shown for dilute solution (blue) and 10 g/L NIPAm-AAc (green). Error bars reflect the standard error in k_{obs} values from three trials. Colored arrows indicate the average ΔG^{0*}_{op} values for globally exchanging residues[19] in crowded (5.2 kcal/mol) and dilute (4.9 kcal/mol) solution.

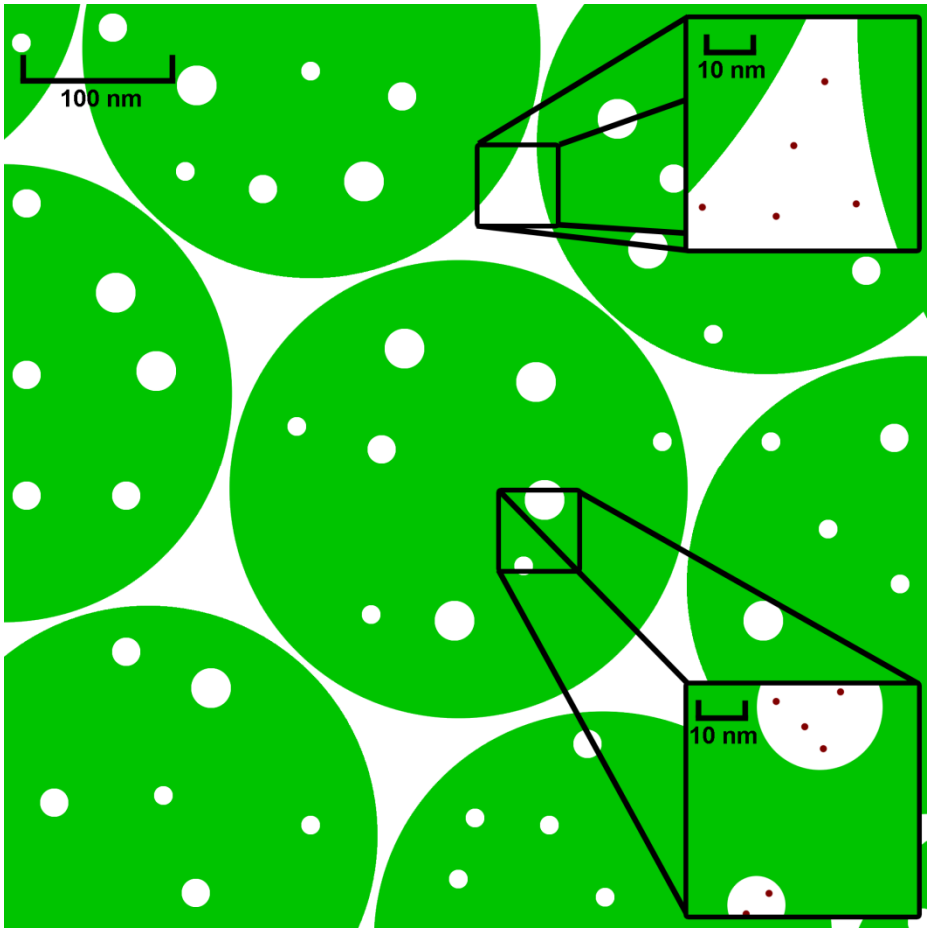

Figure 4.5 Interstitial Spaces in NIPAm-AAc

Depiction of the scale of microgel sizes for NIPAm-AAc (green) and CI2 (red). CI2 can exist in the spaces between crowder particles or within pores (of unknown size) without experiencing a change in environment compared to bulk water.

4.7 References

1. Minton, A. P. (1983) The effect of volume occupancy upon the thermodynamic activity of protein: Some biochemical consequences, *Mol. Cell. Biochem.* **55**, 119-140.

2. Pelton, R. (2000) Temperature-sensitive aqueous microgels, *Adv. Colloid Interface Sci.* **85**, 1-33.

3. Jones, C. D., and Lyon, L. A. (2000) Synthesis and characterization of multiresponsive core-shell microgels, *Macromolecules* **33**, 8301-8306.

4. Serpe, M. J., Jones, C. D., and Lyon, L. A. (2003) Layer-by-layer deposition of thermoresponsive microgel thin films, *Langmuir* **19**, 8759-8764.

5. Blackburn, W. H., and Lyon, L. A. (2008) Size-controlled synthesis of monodisperse core/shell nanogels, *Colloid and Polymer Science* **286**, 563-569.

6. Meng, Z. Y., Smith, M. H., and Lyon, L. A. (2009) Temperature-programmed synthesis of micron-sized multi-responsive microgels, *Colloid and Polymer Science* **287**, 277-285.

7. Sorrell, C. D., and Lyon, L. A. (2008) Deformation controlled assembly of binary microgel thin films, *Langmuir* **24**, 7216-7222.

8. Hwang, T.-L., van Zijl, P. C. M., and Mori, S. (1998) Accurate quantitation of water-amide exchange rates using the phase-modulated CLEAN chemical EXchange (CLEANEX-PM) approach with a fast-HSQC (FHSQC) detection scheme, *J. Biomol. NMR* **11**, 221-226.

9. Kay, L. E., Torchia, D. A., and Bax, A. (1989) Backbone dynamics of proteins as studied by ^{15}N inverse detected heteronuclear NMR spectroscopy: Application to staphylococcal nuclease, *Biochemistry* **28**, 8972-8979.

10. Lipari, G., and Szabo, A. (1982) Model-free approach to the interpretation of nuclear magnetic-resonance relaxation in macromolecules. 1. Theory and range of validity, *J. Am. Chem. Soc.* **104**, 4546-4559.

11. Lee, A. L., and Wand, A. J. (1999) Assessing potential bias in the determination of rotational correlation times of proteins by NMR relaxation, *J. Biomol. NMR* **13**, 101-112.

12. Jarymowycz, V. A., and Stone, M. J. (2006) Fast time scale dynamics of

protein backbones: NMR relaxation methods, applications, and functional consequences, *Chemical Reviews* **106**, 1624-1671.

13. Shaw, G. L., Davis, B., Keeler, J., and Fersht, A. R. (1995) Backbone dynamics of chymotrypsin inhibitor 2: Effect of breaking the active-site bond and its implications for the mechanism of inhibition of serine proteases, *Biochemistry* **34**, 2225-2233.

14. Zhang, Y.-Z. (1995) Protein and peptide structure and interactions studied by hydrogen exchange and NMR, in *Structural Biology and Molecular Biophysics*, University of Pennsylvania, PA, USA.

15. Aste, T., and Weaire, D. (2008) *The Pursuit of Perfect Packing*, Second Edition ed., Taylor & Francis, New York.

16. Lyon, L. A., Meng, Z. Y., Singh, N., Sorrell, C. D., and John, A. S. (2009) Thermoresponsive microgel-based materials, *Chemical Society Reviews* **38**, 865-874.

17. Homouz, D., Stagg, L., Wittung-Stafshede, P., and Cheung, M. S. (2009) Macromolecular crowding modulates folding mechanism of a/b protein apoflavodoxin, *Biophys. J.* **96**, 671-680.

18. Ping, G. H., Yang, G. L., and Yuan, H. M. (2006) Depletion force from macromolecular crowding enhances mechanical stability of protein molecules, *Polymer* **47**, 2564-2570.

19. Neira, J. L., Itzhaki, L. S., Otzen, D. E., Davis, B., and Fersht, A. R. (1997) Hydrogen exchange in chymotrypsin inhibitor 2 probed by mutagenesis, *J. Mol. Biol.* **270**, 99-110.

20. Boyer, J. A., and Lee, A. L. (2008) Monitoring aromatic picosecond to nanosecond dynamics in proteins via C-13 relaxation: Expanding perturbation mapping of the rigidifying core mutation, V54A, in eglin c, *Biochemistry* **47**, 4876-4886.

21. Vicky, D.-N., and Loria, J. P. (2007) The effects of cosolutes on protein dynamics: The reversal of denaturant-induced protein fluctuations by trimethylamine *N*-oxide, *Protein Sci.* **16**, 20-29.

22. Henzler-Wildman, K., and Kern, D. (2007) Dynamic personalities of proteins, *Nature* **450**, 964-972.

23. Jyotica, B., Ke, X., and Zhou, H-X. (2009) Nonadditive effects of mixed crowding on protein stability, *Proteins: Struct., Funct., Bioinf.* **77**, 133-138.

5 Protein Crowding and Protein Stability

5.1 Introduction

Over 70 years ago, Krebs espoused the idea that dilute solution data may fail to capture a full picture of protein chemistry in cells.[1] Nevertheless, there are only a small number of quantitative studies of protein properties under physiologically relevant conditions, and the few that have been conducted in living cells report a surprising result; proteins are either unaffected or destabilized.[2-4] One reason for the lack of progress is that the intracellular environment is difficult to manipulate, hampering systematic studies such as the effects of crowder concentration, size, and shape on stability. Reductionist stability studies (*e.g.,* Chapters 3 and 4) have been performed using synthetic polymers as crowders, but these "artificial" crowding agents are non-biological, and may not reveal relevant information.

Studies using physiologically relevant crowders have been hampered by the difficulty in detecting a test protein under crowded conditions when its mass is only a few percent of the total protein mass. Another reason involves the use of denaturants. Globular proteins have dilute-solution stabilities of 2 to 10 kcal/mol at room temperature, which means the native state for even the least stable proteins represents >99% of the population. Few methods can detect such low concentrations of the denatured state. Denaturants, including heat,

facilitate detection by increasing the population of the denatured state. Extrapolation to zero denaturant concentration, or lower T, is then used to determine the stability in the absence of denaturant. This approach is not reasonable for protein crowders because denaturants perturb the properties of both the test protein and the crowder.

NMR-detected amide proton exchange provides a means to detect a test protein surrounded by high concentrations of other proteins, while eliminating the need for denaturants. The ease of detection arises because the technique is highly sensitive to the low populations of non-native protein.[5] I have reported changes in the stability of the small (7.4 kDa) globular protein chymotrypsin inhibitor 2 (CI2) when crowded by the synthetic polymer, polyvinylpyrrolidone (PVP) (Chapter 3). Synthetic polymers, however, are not physiologically relevant. Here, I examine the effects of two globular proteins as crowding agents, bovine serum albumin (BSA) and lysozyme.

5.2 Materials and Methods

5.2.1 Expression and Purification

The plasmid containing our variant of CI2 is described in Chapter 3. The expression protocol used for these experiments, however, was altered for these studies. To generate ^{15}N enriched CI2, the plasmid is transformed into BL-21(DE3-Gold) competent *Escherichia coli* cells. All media contain 60 μg/mL kanamycin because the plasmid contains the kanamycin resistance gene. Transformants are spread onto Luria Broth (Fisher BioReagents) agar plates and

incubated at 37 °C overnight. A single colony is inoculated into 50 mL of Luria Broth and incubated at 37 °C overnight with shaking. The next morning, an 8-mL aliquot is transferred to 100 mL of 2xTY media (1.6 g tryptone, 1.0 g yeast extract, 0.5 g NaCl, 1 mM NaOH in 100 mL H_2O). The culture is incubated at 37 °C with shaking until its optical density at 600 nm reaches 0.8. This culture is spun at 1600 x g for 10 min, and the pellet is resuspended in 1 L of ^{15}N-enriched M9 media (13 g Na_2HPO_4, 4 g dextrose, 3 g KH_2PO_4, 0.5 g NaCl, 1 g $^{15}NH_4Cl$, 2 mM $MgSO_4$, 100 µM $CaCl_2$ in 1 L H_2O). This culture is incubated at 37°C with shaking until its optical density at 600 nm reaches 0.8, whereupon induction is initiated by adding isopropyl β-D-1-thiogalactopyranoside to a final concentration of 1 µM. Protein expression proceeds for 6 h, whereupon the culture is spun at 6500 x g, and the pellet is frozen. Purification is performed as described in Chapter 3.

5.2.2 NMR

Amide proton exchange experiments are performed on a 500 MHz Varian Inova spectrometer equipped with an HCN cold probe with a z-axis gradient at a ^1H sweep width of 8401.6 Hz and a ^{15}N sweep width of 2200 Hz. The ionic strength is kept low to exploit the full potential of the cold probe.[6] Sample preparation is altered compared to that described in Chapter 2.

Because they contain exchangeable protons, protein crowders are exchanged in D_2O prior to adding it to the exchange sample solution. 1-2 g of protein are suspended in 10 mL D_2O, pH 10. Exchange is allowed to occur for 2-

4 hours at room temperature, whereupon the solution is lyophilized overnight and resuspended a second time in 10 mL D_2O, pH 10. Another round of exchange is performed for 2-4 hours, whereupon the pH is readjusted to 7 with dilute HCl. This solution is lyophilized and used to prepare the exchange sample.

HSQC-detected amide proton exchange experiments are performed as described in Chapter 2. Experiments using 150 mM NaCl are conducted on a 600 MHz Varian Inova spectrometer equipped with a standard triple resonance HCN probe with three-axis gradients at a ^{1}H sweep of 11990 Hz and a ^{15}N sweep of 2500 Hz. This spectrometer was used because the cold probes lose sensitivity at high salt concentrations.[6]

The rate determining step of exchange is assessed by using HSQC-detected amide proton exchange and quantifying the exchange rate as a function of pH.[7] These experiments are identical to the amide proton exchange experiments described above, but experiments at pH 5.4 contain 50 mM sodium acetate buffer.

The rate determining step was also assessed by using NOESY-detected amide proton exchange.[7] The procedure is described in Chapter 2. Data are acquired on the 500 MHz spectrometer at a ^{1}H sweep width of 8401.6 Hz. Exchange samples were identical to samples prepared for HSQC-detected experiments.

The intrinsic exchange rates, k_{int}, were determined as described by Hwang *et al.*[8] for 1 mM I29A:I37H CI2 variant in 50 mM sodium phosphate buffer, pH 6.5, 37 °C containing 0 g/L and 100 g/L BSA or lysozyme. Experiments were

performed on the 600 MHz spectrometer at a ^{1}H sweep width of 10000 Hz and a ^{15}N sweep width of 2000 Hz. The water signal was unchanged with mixing times varying from 0 to 53 ms. $R_{1B,app}$ was thus chosen to be 0.01 s^{-1}. As expected,[9] the $R_{1B,app}$ values did not alter the results.

Relaxation experiments were performed by Yaqiang Wang on the 600 MHz spectrometer at 20 ^{o}C. The R_1R_2 data were acquired and processed as described.[10, 11] Briefly, the ^{1}H dimension was acquired with a sweep width of 12000 Hz and comprised 1024 complex points. The ^{15}N dimension was acquired with a sweep width of 2500 Hz and comprised 64 complex increments. For T_1 measurement, the relaxation delays were 0.01, 0.4, 0.6, 0.9, 1.2, and 1.5 s. For T_2 measurement, the delays were 0.01, 0.03, 0.07, 0.09, 0.15, and 0.21 s. Eight transients were acquired per spectrum. The data were processed with NMRPipe[12] and NMRViewJ.[13]

5.3 Results and Discussion

5.3.1 Controls

Linking amide proton exchange to stability requires the validity of three assumptions,[7] which I verified for my systems. First, the test protein must be stable; my CI2 variant has a stability of greater than 6 kcal/mol in dilute solution at pH 5.4, 37 °C.[14] Second, the rate-determining step is the exchange from the open state of CI2's backbone amide; the pH dependence of exchange and the NOESY-HEX experiment [7] are used to confirm this assumption. Finally, the

exchange rate from the open state must be the same in dilute and crowded solutions; CLEANEX-PM[8] is used to assess the validity of this assumption.

The pH dependence of exchange was assessed for both 100 g/L BSA (by myself) and 100 g/L lysozyme (by Mohona Sarkar) to assess. Because exchange from the open state is pH-dependent, if this step is rate-limiting, I expect to see a pH dependence of overall exchange (Chapter 2). If opening into the exchange-accessible state is rate-determining, no such dependence is expected.[5] There is a pH dependence for all conditions (Table 5.1), showing that exchange from the open state is rate determining and allowing interpretation in terms of stability. The difference in log k_{obs} values is slightly lower than the difference in pH, suggesting that CI2 stability is altered between conditions.

I also performed NOESY-detected amide proton exchange on 100 g/L BSA to confirm the result from the pH dependence experiments. NOESY-detected amide proton exchange was chosen as a means to confirm exchange limit because of the aforementioned pH-dependent stability of CI2 in crowded conditions. This is the preferred method for systems exhibiting pH-dependent stability because it requires no change in conditions to assess the rate-limiting step. Lysozyme was not studied by this method because interactions between lysozyme and CI2 resulted in line broadening that prevented analysis.

There are two possible outcomes from NOESY-detected exchange experiments.[7] If exchange from the open step is rate-limiting, then the combined amide-amide crosspeak decay (corresponding to an observation of both amide protons) for proximal amide protons should be equivalent to the sum of the

individual decays. If the opening step is rate-determining, then this combined decay should simply be equivalent to the individual decays, which should also be identical to one another. Table 5.2 displays results for two pairs of proximal amide protons. The data confirm my determination that exchange from the open state is rate-determining.

The overall rate of exchange for residues in the extended loop region of CI2 approximates exchange for an unstructured peptide, because these residues are highly solvent-exposed. Unprotected amide protons exchange quickly. It is therefore necessary to rely on CLEANEX-PM experiments,[8] which can measure fast exchange events. The resultant curves (Figure 5.1) can be analyzed to determine the rate of exchange from the open state. The different appearance of the curves is caused by changes to the second parameter, $R_{1A,app}$, which is expected to change because it is tied to the same properties that result in changes in R_1R_2 values. The results from these experiments can be analyzed to determine the rate of exchange from the open state (k_{int}). As shown in Table 5.3, k_{int} values are unchanged from dilute solution to 100 g/L of either crowder, confirming the final requirement for stability assessment.

5.3.2 Protein Crowding Effects on Stability

The results in 100 g/L BSA and lysozyme are distinctly different from those in PVP (Figure 5.2). Experiments in 100 g/L lysozyme were performed by Mohona Sarkar. Full tables of ΔG^{0*}_{op} values from amide proton exchange studies can be found in Appendix B. For PVP, all but one of the monitored residues are

stabilized, and the average stability increase compared to dilute solution ($\Delta\Delta G^{0*}_{op}$) for global exchangers[15] is +0.3 ±0.1 kcal/mol. For the protein crowders, however, the majority of residues are slightly destabilized, with an average stability decrease for global exchangers of -0.2 ±0.1 kcal/mol for 100 g/L BSA and -0.6 ±0.2 kcal/mol for 100 g/L lysozyme. Increasing the BSA concentration from 100 g/L to 200 g/L (Figure 5.3) had minimal effects on stability compared to 100 g/L BSA, but resulted in poorer quality spectra, thus increasing the uncertainty in $\Delta\Delta G^{0*}_{op}$. Amide proton exchange experiments could not be performed in 200 g/L lysozyme, because a combination of peak broadening due to interactions and faster exchange resulted in sparingly few backbone amides that could be subjected to analysis.

These results contradict *in vitro* observations of crowding effects on stability, but those studies used non-physiological synthetic polymers as crowding agents. Differences are expected because synthetic polymers and proteins have differing effects on protein diffusion[11] and enzyme activity.[16] My results show that this trend is also true for stability, and are consistent with in-cell results, which show either no stability change[2] or destabilization of the test protein.[3, 4] My data also agree with findings obtained with carboxyamidated RNase T1 in 400 g/L BSA[17] and simulations of protein stability in cellular environments.[18] Unlike the in-cell studies, *in vitro* experiments with protein crowders allow tight control of conditions, which allows me to investigate the source of destabilization.

5.3.3 Weak Destabilizing Interactions

To ensure that the observations arise from the macromolecular nature of the protein crowders, I examine CI2 in the presence of a model of the protein backbone. Favorable interprotein interactions, probably involving H-bonding, have been observed under crowded conditions.[11] I predict that these favorable, nonspecific interactions between backbone residues will destabilize CI2 under crowded conditions. I chose urea as a model for protein backbone monomer because it lacks end effects exhibited by individual amino acids and it interacts favorably with the protein backbone.[19] As expected, a large destabilization occurred for 100 g/L urea. The average destabilization for global exchangers is -1.7 ±0.1 kcal/mol in 100 g/L urea (Figure 5.2). It is known that urea slows amide proton exchange in unstructured peptides,[19] which means that my values underestimate urea's ability to destabilize CI2.

My results indicate that crowding by proteins is a competition between stabilizing volume exclusion effects and destabilizing nonspecific interactions. The destabilization induced by lysozyme and BSA, however, is not a simple combination of my model systems (PVP and urea). Unlike PVP, globular proteins behave more like hard spheres. Unlike urea, globular proteins mitigate their nonspecific interactions by burying most of their backbone. This interpretation not only explains the effects of protein crowders in general, but also explains the stability changes brought about by different protein crowders.

As stated above, 100 g/L lysozyme is more destabilizing than 100 g/L BSA. This observation could be the result of increased nonspecific interactions.

Typical NMR relaxation parameters are sensitive to not only nonspecific interactions, but also viscosity. We used a viscosity-independent method involving the product of longitudinal and transverse relaxation rates to assess the degree of weak interaction between protein and crowder.[10, 11] Our data (Table 5.4) report a stronger interaction between lysozyme and CI2 than between BSA and CI2. In summary, destabilization is increased as the strength of interaction increases between CI2 and crowding agent.

Spitzer and Poolman suggest that electrostatics play a large role in cells, because the intracellular surface-to-surface distance between proteins is less than the Debye screening length.[20] To test this idea, Mohona Sarkar performed amide proton exchange experiments with 100 g/L BSA in 50 mM sodium phosphate with either 0 or 150 mM NaCl. As shown in Figure 5.4, BSA exerts a stabilizing effect at higher ionic strengths. NaCl was used to ensure the effect did not arise from a Hofmeister effect.[21]

These results are consistent with the idea that electrostatics plays a role in destabilization, in agreement with a simulation-based suggestion of electrostatic-mediated destabilization.[22] When the ionic strength increases, the favorable nonspecific interaction between CI2 and the protein crowder diminishes, and the stabilizing effect of volume exclusion dominates. The electrostatic nature of this interaction is also suggested in our pH jump experiments and previous studies of the interactions between BSA and CI2.[10]

5.4 Conclusions

Despite the fact that volume exclusion can only stabilize globular proteins, when proteins act as the crowding agent, stability can be increased, unaffected, or even decreased. My key finding is that the presence of nonspecific crowder-protein interactions can be destabilizing. These nonspecific interactions are modulated by pH and ionic strength, indicating that they are driven by electrostatics.

The results shown here indicate that under physiologically relevant conditions, protein stability is a competition between stabilizing and destabilizing interactions. The net effect is that stability in crowded solutions is mildly destabilizing, similar to that observed in dilute solution.

These observations have several important biological implications. First, proteins act as “good neighbors” in crowded conditions by not perturbing each other. Second, the variation in stability with changing conditions suggests that the tunable nature of protein stability in a crowded environment can be exploited in biological systems (*e.g.* the interior of mitochondria has a different chemical environment from the cytoplasm). Third, the heterogeneity of the cellular interior can create regions where proteins are stabilized or destabilized depending on the degree of volume exclusion and the extent of nonspecific interactions. This can result in proteins being stabilized in one region of a cell, but destabilized in another. This granularity of environment could also account for the “noisiness” of bacterial protein expression.[23]

5.5 Tables and Figures

	-log(k_{obs}*) for Lysozyme						-log(k_{obs}*) for BSA		
Residue	pH 5.4	pH 6.5	pH 7.5	5.4 - 6.5	6.5 - 7.5	5.4 - 7.5	pH 5.4	pH 6.5	5.4 - 6.5
9	—	4.81	3.90	—	0.91	—	—	—	—
10	—	—	—	—	—	—	4.74	3.74	1.00
13	7	4.48	3.69	3	0.79	3	—	—	—
16	—	4.63	3.92	—	0.71	—	—	—	—
17	—	—	—	—	—	—	4.27	3.33	0.94
18	3.54	3.82	—	-0.28	—	—	4.99	3.87	1.12
21	—	4.9	4.21	—	0.69	—	—	—	—
22	—	4.41	3.74	—	0.67	—	—	—	—
24	—	4.47	3.82	—	0.65	—	—	—	—
27	4.86	3.86	—	1.00	—	—	4.99	3.95	1.04
34	4.32	3.6	4.08	0.7	-0.5	0.24	4.32	3.44	0.88
46	7	4.44	3.74	3	0.70	3	—	—	—
47	—	4.7	4.08	—	0.6	—	—	—	—
50	—	4.6	4.00	—	0.6	—	—	—	—
51	4.1	4.7	4.2	-0.6	0.5	-0.1	—	—	—
52	—	4.77	3.92	—	0.85	—	—	—	—
56	4.75	4.41	3.92	0.34	0.49	0.83	4.58	3.52	1.06
57	—	4.9	4.0	—	0.9	—	—	—	—
59	—	5.0	4.13	—	0.9	—	—	—	—
62	—	4.28	3.78	—	0.5	—	—	—	—
63	—	4.64	4.11	—	0.53	—	—	—	—
64	—	5.1	4.4	—	0.7	—	—	—	—

*k_{obs} in s^{-1}

Table 5.1 Dependence of overall exchange on pH value

The logarithms of exchange rates (k_{obs} in s^{-1}) are compared between conditions. The difference in values corresponds to the difference in pH when the exchange step is rate-limiting. Amide proton exchange experiments were performed at different pH values for 100 g/L lysozyme and 100 g/L BSA. For experiments performed at pH 6.5 and 7.5, solutions contained 50 mM sodium phosphate.

Residue(s)	k_{obs} NOESY ($s^{-1} \times 10^5$)	k_{obs} HSQC ($s^{-1} \times 10^5$)
Leu8	—	1.2
Val9	—	1.3
Leu8 + Val9[a]	—	2.5
Leu8, Val9[b]	2.5	—
Ala58	—	1.4
Glu59	—	0.4
Ala58 + Glu59[a]	—	1.8
Ala58 , Glu59[b]	2.0	—

Table 5.2 NOESY-detected Amide Proton Exchange

The exchange rates of the amide-amide crosspeaks correspond directly to the sum of the exchanges observed by HSQC-detected amide proton exchange experiments. Experiments were performed in 100 g/L BSA with 50 mM sodium phosphate, pH 6.5, 20 °C.

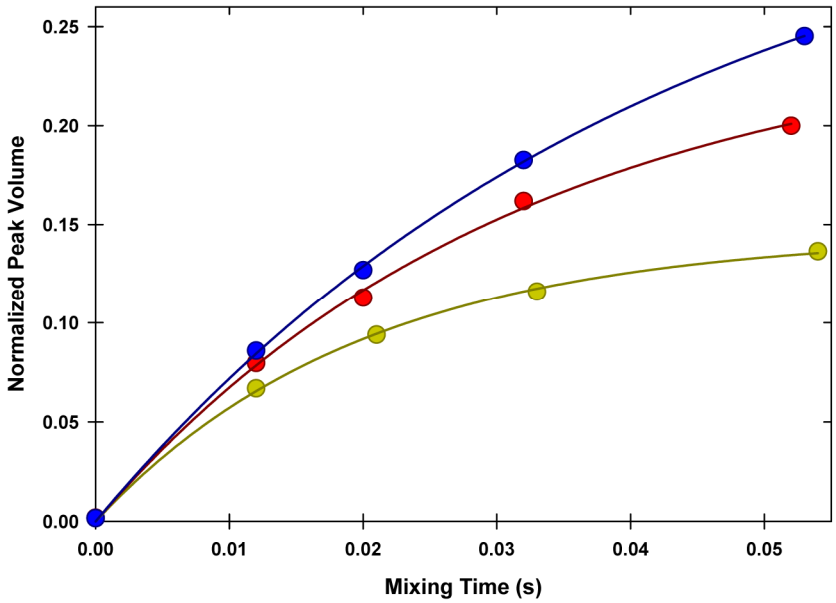

Figure 5.1 CLEANEX-PM Results

CLEANEX-PM values and corresponding exponential-rise-to-maximum fitting curves for CI2 in dilute solution (blue), 100 g/L BSA (red), and 100 g/L lysozyme (yellow). Fits yielded (k_{int}, $R_{1A,app}$) values of (8 ±1 s^{-1}, 14 ±1 s^{-1}), (8 ±1 s^{-1}, 24 ±2 s^{-1}), and (7 ±1 s^{-1}, 43 ±5 s^{-1}) for dilute solution, 100 g/L BSA, and 100 g/L lysozyme, respectively. Experiments were performed in 50 mM sodium phosphate, pH 6.5, 20 °C.

		k_{int} values (s^{-1})		
Residue	SPHERE	Dilute Solution	100 g/L BSA	100 g/L Lysozyme
37	8.0	12 ±1	8 ±1	10 ±1
38	1.4	1 ±1	1 ± 0.4	2 ± 1
39	1.7	1 ±1	1 ±1	—
41	1.1	1 ±1	0.9 ± 0.1	2 ±1
42	1.0	0.8 ±0.2	0.9 ± 0.2	—
45	0.8	—	1.0 ±0.2	—
53	1.6	2 ±1	—	1.4 ±0.1

Table 5.3 Values from CLEANEX-PM Experiment

Rates of exchange from the open state (k_{int}) were measured using buildup curves from CLEANEX-PM[8] data. Values of k_{int} were unchanged from dilute solution, and matched values calculated with SPHERE.[24]

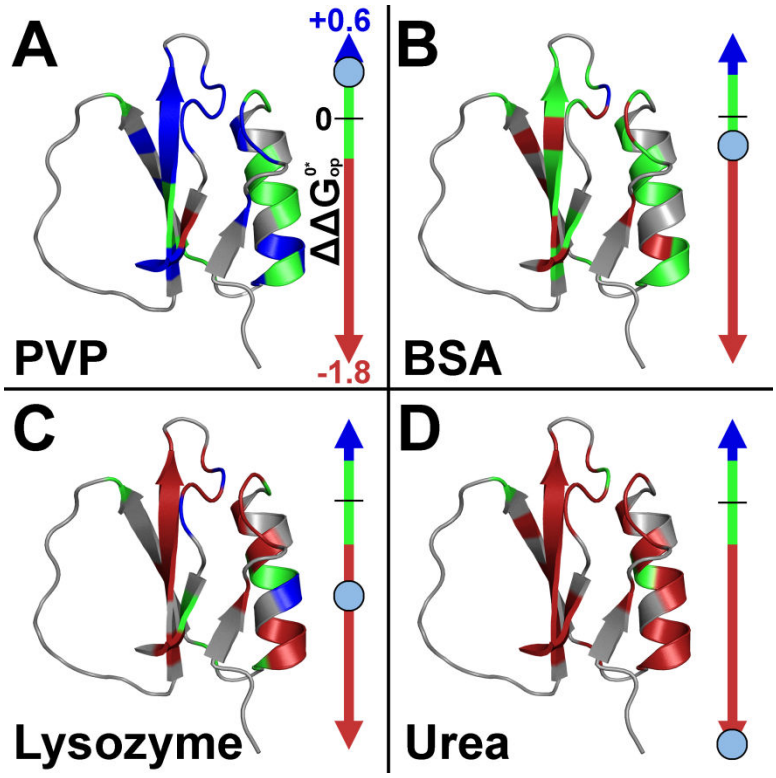

Figure 5.2 Stability Changes

The structure of CI2 (PDB ID: 2CI2) colored by changes in stability compared to dilute solution ($\Delta\Delta G^{0*}_{op}$). Stabilization greater than 0.3 kcal/mol is indicated in blue, no effect (between -0.3 and 0.3 kcal/mol) is indicated in green, and destabilization by greater than 0.3 kcal/mol is indicated in red. White residues could not be observed. On the right of each structure is an indication of the average $\Delta\Delta G^{0*}_{op}$ value for globally exchanging residues.[15] Results are shown for A) 100 g/L PVP-40 (+0.3 ± 0.1 kcal/mol), B) 100 g/L BSA (-0.2 ± 0.1 kcal/mol), C) 100 g/L lysozyme (-0.6 ± 0.2 kcal/mol), D) 100 g/L urea (-1.72 ± 0.1 kcal/mol).

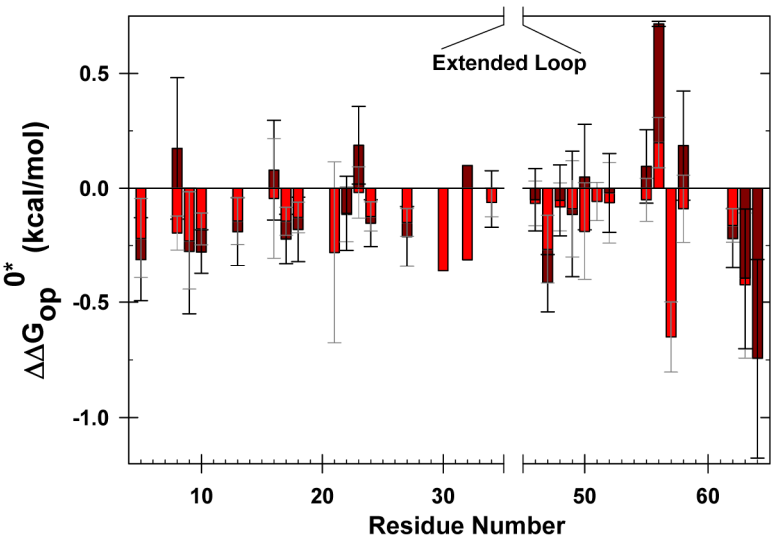

Figure 5.3 Crowding by BSA

Results are shown for 100 g/L BSA experiments (red) and 200 g/L BSA experiments (dark red). Error bars represent the standard error from three trials. Amide proton exchange experiments were performed in 50 mM sodium phosphate, pH 6.5, 20 °C.

Solution	pH	Average R_1R_2 (s^{-2})
Glycerol	6.5	14.5
100 g/L BSA	6.5	20.7
100 g/L Lysozyme	6.5	31.1

Table 5.4 Interactions between CI2 and Protein Crowders

The value of R_1R_2 exceeds the rigid limit value[10] of 19 s^{-2} in crowded conditions, indicating the presence of protein-protein interaction. Results indicate a higher degree of interaction between lysozyme and CI2 than that between BSA and CI2. Experiments were performed at 20 °C in 50 mM sodium phosphate, pH 6.5.

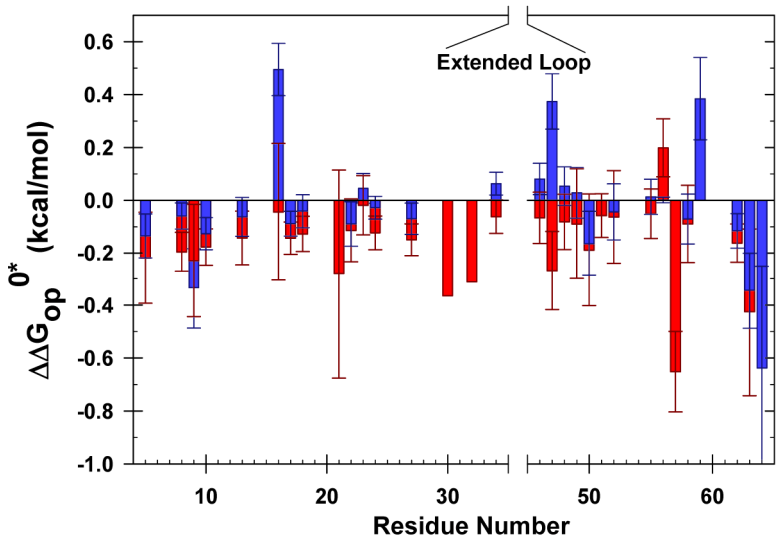

Figure 5.4 Ionic Strength Effects

Histogram of $\Delta\Delta G^{0*}_{op}$ *versus* residue number for CI2 in 100 g/L BSA with no added NaCl (red) or upon adding 150 mM NaCl (blue). Adding NaCl mitigates the destabilizing effects of BSA. Experiments were performed in 50 mM phosphate buffer, pH 6.5, 20 °C.

5.6 References

1. Krebs, H. A., and Henseleit, K. (1932) Untersuchungen über die harnstoffbildung im tierkörper, *Z. Physiol. Chem.* **210**, 33-66.

2. Ghaemmaghami, S., and Oas, T. G. (2001) Quantitative protein stability measurement *in vivo*, *Nat. Struct. Biol.* **8**, 879-882.

3. Ignatova, Z., and Gierasch, L. M. (2004) Monitoring protein stability and aggregation *in vivo* by real-time fluorescent labeling, *Proc. Natl. Acad. Sci. U.S.A.* **101**, 523-528.

4. Sakakibara, D., Sasaki, A., Ikeya, T., Hamatsu, J., Hanashima, T., Mishima, M., Yoshimasu, M., Hayashi, N., Mikawa, T., Walchli, M., Smith, B. O., Shirakawa, M., Guntert, P., and Ito, Y. (2009) Protein structure determination in living cells by in-cell NMR spectroscopy, *Nature* **458**, 102-105.

5. Englander, S. W., and Kallenbach, N. R. (1983) Hydrogen exchange and structural dynamics of proteins and nucleic acids., *Q. Rev. Biophys.* **16**, 521-655.

6. Kelly, A. E., Ou, H. D., Withers, R., and Dötsch, V. (2002) Low-conductivity buffers for high-sensitivity NMR measurements, *J. Am. Chem. Soc.* **124**, 12013-12019.

7. Miklos, A. C., Li, C., and Pielak, G. J. (2009) Using NMR-detected backbone amide ^{1}H exchange to assess macromolecular crowding effects on globular-protein stability, *Methods Enzymol.* **466**, 1-18.

8. Hwang, T.-L., van Zijl, P. C. M., and Mori, S. (1998) Accurate quantitation of water-amide exchange rates using the phase-modulated CLEAN chemical EXchange (CLEANEX-PM) approach with a fast-HSQC (FHSQC) detection scheme, *J. Biomol. NMR* **11**, 221-226.

9. Bertini, I., Ghosh, K., Rosato, A., and Vasos, P. R. (2003) A high-resolution NMR study of long-lived water molecules in both oxidation states of a minimal cytochrome *c*, *Biochemistry* **42**, 3457-3463.

10. Li, C., and Pielak, G. J. (2009) Using NMR to distinguish viscosity effects from nonspecific protein binding under crowded conditions *J. Am. Chem. Soc.* **131**, 1368–1369.

11. Wang, Y., Li, C., and Pielak, G. J. (2010) Effects of proteins on protein diffusion, *J. Am. Chem. Soc.*, 9392–9397.

12. Delaglio, F., Grzesiek, S., Vuister, G. W., Zhu, G., Pfeifer, J., and Bax, A. (1995) NMRPipe: A multidimensional spectral processing system based on UNIX pipes, *J. Biomol. NMR* **6**, 277-293.

13. Johnson, B. A., and Blevins, R. A. (1994) NMR View: A computer program for the visualization and analysis of NMR data, *J. Biomol. NMR* **4**, 603-614.

14. Charlton, L. M., Barnes, C. O., Li, C., Orans, J., Young, G. B., and Pielak, G. J. (2008) Macromolecular crowding effects on protein stability at the residue level, *J. Am. Chem. Soc.* **130**, 6826-6830.

15. Neira, J. L., Itzhaki, L. S., Otzen, D. E., Davis, B., and Fersht, A. R. (1997) Hydrogen exchange in chymotrypsin inhibitor 2 probed by mutagenesis, *J. Mol. Biol.* **270**, 99-110.

16. Derham, B. K., and Harding, J. J. (2006) The effect of the presence of globular proteins and elongated polymers on enzyme activity, *Biochim. Biophys. Acta* **1764**, 1000-1006.

17. Qu, Y. X., and Bolen, D. W. (2002) Efficacy of macromolecular crowding in forcing proteins to fold, *Biophys. Chem.* **101**, 155-165.

18. McGuffee, S. R., and Elcock, A. H. (2010) Diffusion, crowding & protein stability in a dynamic molecular model of the bacterial cytoplasm, *PLoS Comput. Biol.* **6**, e1000694.

19. Lim, W. K., Rösgenc, J., and Englander, S. W. (2009) Urea, but not guanidinium, destabilizes proteins by forming hydrogen bonds to the peptide group, *Proc. Natl. Acad. Sci. U.S.A.* **106**, 2595-2600.

20. Spitzer, J. J., and Poolman, B. (2005) Electrochemical structure of the crowded cytoplasm, *Trends Biochem. Sci.* **30**, 536-541.

21. Tadeo, X., Lopez-Mendez, B., Castano, D., Trigueros, T., and Millet, O. (2009) Protein stabilization and the Hofmeister effect: The role of hydrophobic solvation, *Biophys. J.* **97**, 2595-2603.

22. Tanizaki, S., Clifford, J., Connelly, B. D., and Feig, M. (2008) Conformational sampling of peptides in cellular environments, *Biophys. J.* **94**, 747-759.

23. Cai, L., Friedman, N., and Xie, X. S. (2006) Stochastic protein expression in individual cells at the single molecule level, *Nature* **440**, 358-362.

24. Zhang, Y.-Z. (1995) Protein and peptide structure and interactions studied by hydrogen exchange and NMR, in *Structural Biology and Molecular Biophysics*, University of Pennsylvania, PA, USA.

6 Conclusions and Implications for Biology

6.1 Conclusions

My research focused on protein stability under crowded conditions. The crowding agents comprised synthetic polymers both large and gigantic as well as protein crowders. The studies were designed to answer questions about the biological significance of crowding studies and the applicability of theoretical models. My results provide compelling support for paying increased attention to weak interactions, which can be both stabilizing and destabilizing. My findings with PVP highlight the importance of two underappreciated aspects of crowding by synthetic polymers: polymer overlap and interactions between native-state protein and polymers. My work with NIPAm-AAc provides an upper boundary on size effects. Finally, my work with protein crowders provides the first in-depth look at protein stability under physiological conditions, and showcases the differences between polymeric and protein crowders.

The studies I performed on systems crowded by PVP pointed to two major findings with implications for biological systems. First, the detection of weak interactions that affect stability shows that volume exclusion alone cannot fully explain crowding effects in cells. Second, polymeric crowders can act as either individual excluding particles or overlapping particles that confine proteins. Such behavior is rarely noted, but should be considered in all studies where polymeric

crowders are present in excess of the overlap concentration. Even Ficoll, a standard in crowding experiments due to its relative sphericity, has an overlap concentration near 100 g/L,[1] and most studies use concentrations of 200 to 300 g/L. Modeling these polymers as individual hard spheres is not an accurate assessment of physical reality. Although an excellent model system due to the ease of creating samples and relative ease of data collection, my work suggests that the crowding community needs to move away from synthetic polymers to understand crowding as it occurs in cells.

My experiments with NIPAm-AAc polymers were conceived to investigate size effects with a tunable system. I determined that stability was only modestly increased, showing an upper limit for crowder size effects. Although large assemblies of proteins may not strongly affect smaller proteins by volume exclusion, the interior of a cell comprises many different-sized molecules. Multiple sizes of crowding agents act synergistically,[2] meaning that extremely large molecules can contribute to crowding when intermediate-sized crowding molecules are also present. In other words, larger complexes can relay larger volume exclusion effects even though they do not have strong direct effects on smaller proteins.

The work involving polymeric crowders elucidated volume exclusion factors, but cells are not filled with PVP or pNIPAm-AAc. A physiologically relevant study should include the use of crowders present in biological systems. My work using globular proteins as crowders is not only the first such quantitative study of protein stability, but also it shows the inherent difference between

proteins and other polymers as crowding agents. Namely, while synthetic polymer crowders had a stabilizing effect on proteins, protein crowders can be destabilizing. These results, compared to studies of protein stability in cells,[3-5] show that proteins are more physiologically relevant crowders than synthetic polymers.

In addition to establishing these important differences between proteins and synthetic polymers, my work has important implications for biology. Specifically, the fact that proteins increase, decrease or maintain stability makes proteins an "ideal crowder." Many protein-mediated events in biology require reversibility. For instance, systems where a signaling protein binds its target irreversibly, an enzyme does not release its product, or a transport protein does not shuttle its molecule of interest are, at the least, of limited usefulness, and at the most, toxic to cells.[6] If crowding were to strongly favor one state over another, these equilibria could be shifted to such an extent that reversibility would be lost. The ability of the protein crowders to mitigate volume exclusion with nonspecific interactions also provides a means for maintaining globular protein stability in a range that assures a high concentration of the active form while allowing relatively low expenditure of energy to recycle the components.

The tunability of electrostatic interactions could also provide an explanation for the "noise" associated with protein expression.[7] The heterogeneity of the cellular interior can facilitate regions where proteins are stabilized or destabilized depending on the degree of volume exclusion and the extent of nonspecific interactions. The fact that a protein could be stabilized or

destabilized based on location could result in differential activation and deactivation of transcription, translation and protein-mediated processes. In situations where there exist only a few complexes, local variation could drastically increase the noise, resulting in unpredictable expression behavior from cell to cell.

In summary, the work presented in this thesis advances the field of macromolecular crowding in the following ways:

1) I have developed a regimen that allows residue-level quantification of protein stability under crowded conditions.
2) I used this technique to establish that weak interactions are an important, but overlooked, factor that can affect globular protein stability in crowded conditions.
3) I observed a distinct difference between synthetic polymer and protein crowders.

I hope this work will encourage theoretical treatments of crowding that include factors explicitly addressing weak interactions. This work overcomes a major hurdle in determining protein stability under physiologically relevant conditions. The results also highlight a difference between synthetic polymer crowders and protein crowders, suggesting that proteins are more physiologically relevant. I hope these findings will guide others away from synthetic polymers, which may not approximate cellular conditions, and towards biologically relevant crowding macromolecules. Having completed this work, we are one step closer to the ability to study proteins directly as they function in their native environment.

6.2 References

1. Lavrenko, P. N., Mikriukova, O. I., and Okatova, O. V. (1987) On the separation ability of various ficoll gradient solutions in zonal centrifugation, *Anal. Biochem.* **166**, 287-297.

2. Zhou, H. X. (2008) Effect of mixed macromolecular crowding agents on protein folding, *Proteins: Struct., Funct., Bioinf.* **72**, 1109-1113.

3. Ghaemmaghami, S., and Oas, T. G. (2001) Quantitative protein stability measurement *in vivo*, *Nat. Struct. Biol.* **8**, 879-882.

4. Ignatova, Z., and Gierasch, L. M. (2004) Monitoring protein stability and aggregation *in vivo* by real-time fluorescent labeling, *Proc. Natl. Acad. Sci. U.S.A.* **101**, 523-528.

5. Sakakibara, D., Sasaki, A., Ikeya, T., Hamatsu, J., Hanashima, T., Mishima, M., Yoshimasu, M., Hayashi, N., Mikawa, T., Walchli, M., Smith, B. O., Shirakawa, M., Guntert, P., and Ito, Y. (2009) Protein structure determination in living cells by in-cell NMR spectroscopy, *Nature* **458**, 102-105.

6. Rodkey, F. L., Oneal, J. D., Collison, H. A., and Uddin, D. E. (1974) Relative affinity of hemoglobin s and hemoglobin a for carbon monoxide and oxygen, *Clin. Chem.* **20**, 83-84.

7. Cai, L., Friedman, N., and Xie, X. S. (2006) Stochastic protein expression in individual cells at the single molecule level, *Nature* **440**, 358-362.

Appendix A
Supplementary Materials for Chapter 3

Table A.1 PVP-55 Stabilities

$\Delta G_{op}^{0^*}$ values, and standard errors from three trials (both in kcal/mol) for CI2 residues at 0, 100, 200, and 300 g/L **PVP-55**, 50 mM sodium acetate buffer, pH 5.4, 37 °C. Values without error reflect a single datum.

	Dilute	Error	100 g/L	Error	200 g/L	Error	300 g/L	Error
Trp5	4.81	0.03	5.13	0.04	5.00	0.05	5.41	0.01
Leu8	4.73	0.03	5.14	0.03	5.03	0.06	5.5	—
Val9	4.66	0.04	4.99	0.06	4.88	0.06	5.5	0.1
Gly10	4.96	0.02	5.18	0.04	5.00	0.07	5.42	0.06
Lys11	5.12	0.02	5.267	0.004	5.27	0.06	5.7	0.1
Val13	4.58	0.03	5.17	0.04	5.02	0.06	5.3	0.1
Ala16	5.19	0.04	5.49	0.01	5.3	0.1	5.7	0.1
Lys17	4.17	0.02	—	—	—	—	—	—
Lys18	4.91	0.03	5.01	0.04	4.78	0.07	5.04	0.03
Val19	4.88	0.03	5.21	0.04	5.05	0.05	5.85	0.07
Ile20	4.80	0.03	5.29	0.04	5.10	0.04	6.4	—
Leu21	4.58	0.02	5.0	0.1	4.83	0.07	5.4	0.1
Gln22	4.99	0.03	5.29	0.03	5.12	0.07	5.58	0.05
Asp23	—	—	5.5	0.1	5.8	0.1	5.56	0.07
Lys24	5.20	0.03	5.49	0.03	5.35	0.06	5.2	0.7
Ala27	5.0	0.3	5.02	0.03	4.8	0.1	5.1	—

	Dilute	Error	100 g/L	Error	200 g/L	Error	300 g/L	Error
Gln28	4.3636	0.0004	4.5	—	4.57	0.04	4.7	—
Ile30	5.01	0.05	5.42	0.06	5.2	0.1	6.0	0.2
Leu32	5.26	0.06	5.59	0.03	5.52	0.04	6.4	0.4
Val34	3.22	0.01	3.33	0.04	3.1	0.1	3.45	0.07
Arg46	5.03	0.02	5.28	0.04	5.14	0.06	5.51	0.04
Val47	5.2	0.2	5.28	0.03	5.14	0.05	5.3	0.3
Arg48	5.21	0.01	5.46	0.04	5.32	0.06	5.77	0.04
Leu49	4.96	0.02	5.25	0.05	5.12	0.06	5.66	0.04
Phe50	4.84	0.04	5.18	0.03	5.07	0.06	5.63	0.07
Val51	4.84	0.04	5.19	0.05	5.10	0.05	5.5	0.1
Asp52	4.80	0.03	5.20	0.02	5.06	0.05	5.6	0.1
Asp55	4.22	0.03	3.9	0.1	—	—	4.9	—
Asn56	4.5	—	5.85	0.03	5.83	0.07	6.1	—
Ile57	5.16	0.04	5.6	0.1	5.49	0.05	6.0	0.2
Ala58	5.25	0.04	5.57	0.04	5.56	0.06	6.0	0.1
Glu59	4.81	0.04	5.34	0.04	5.22	0.07	5.77	0.05
Arg62	5.35	0.04	5.18	0.04	4.88	0.05	5.1	0.1
Val63	4.09	0.03	5.31	0.07	5.16	0.04	5.64	0.06
Gly64	3.17	0.03	4.11	0.03	4.00	0.03	4.4	0.1

Table A.2 PVP-40 Stabilities

$\Delta G_{op}^{0^*}$ values, and standard errors from three trials (both in kcal/mol) for CI2 residues at 100, 200, and 300 g/L **PVP-40**, 50 mM sodium acetate buffer, pH 5.4, 37 °C. Values without error reflect a single datum.

	100 g/L	Error	200 g/L	Error	300 g/L	Error
Trp5	5.163	0.007	5.18	0.04	5.62	0.05
Leu8	5.18	0.02	5.20	0.03	4.9	0.1
Val9	5.05	0.01	5.1	0.1	6.02	0.2
Gly10	5.18	0.02	5.20	0.02	5.58	0.05
Lys11	5.25	0.07	5.4	0.1	7.55	0.6
Val13	5.21	0.02	5.24	0.04	5.3	0.1
Ala16	5.48	0.05	5.53	0.02	5.93	0.04
Lys17	4.25	0.02	4.5	—	4.43	0.03
Lys18	5.024	0.006	5.02	0.04	5.33	0.04
Val19	5.19	0.02	5.31	0.02	6.4	0.3
Ile20	5.31	0.05	5.5	0.1	7.7	0.2
Leu21	5.0	0.1	5.11	0.07	5.7	0.1
Gln22	5.30	0.02	5.31	0.04	5.74	0.05
Asp23	5.46	0.04	5.8	0.2	—	—
Lys24	5.51	0.02	5.54	0.03	5.82	0.03
Ala27	4.99	0.02	5.05	0.06	5.2	0.1
Gln28	4.469	0.008	4.58	0.07	4.85	0.04

	100 g/L	Error	200 g/L	Error	300 g/L	Error
Ile30	5.43	0.07	5.49	0.07	6.4	0.1
Leu32	5.67	0.04	5.8	0.1	7.5	0.4
Val34	3.32	0.01	3.38	0.03	3.65	0.03
Arg46	5.31	0.02	5.31	0.03	5.67	0.04
Val47	5.34	0.05	5.5	0.1	5.5	0.2
Arg48	5.47	0.01	5.52	0.05	5.94	0.04
Leu49	5.26	0.01	5.32	0.05	5.8	0.1
Phe50	5.23	0.01	5.25	0.05	5.8	0.1
Val51	5.30	0.02	5.33	0.05	6.3	0.2
Asp52	5.22	0.02	5.24	0.04	5.51	0.04
Asp55	4.7	—	—	—	4.74	0.02
Asn56	5.87	0.01	5.86	0.04	4.72	0.01
Ile57	5.6	0.05	5.65	0.01	6.7	0.3
Ala58	5.65	0.07	5.65	0.03	6.6	0.2
Glu59	5.37	0.01	5.42	0.03	5.61	0.08
Arg62	4.8	0.4	5.0	0.1	6.30	0.07
Val63	5.36	0.06	5.31	0.05	6.1	0.1
Gly64	4.10	0.03	4.0	0.1	3.69	0.05

Table A.3 PVP-29 Stabilities

$\Delta G_{op}^{0^*}$ values, and standard errors from three trials (both in kcal/mol) for Cl2 residues at 100, 200, and 300 g/L **PVP-29**, 50 mM sodium acetate buffer, pH 5.4, 37 °C. Values without error reflect a single datum.

	100 g/L	Error	200 g/L	Error	300 g/L	Error
Trp5	5.19	0.05	4.9	0.1	5.5	0.3
Leu8	5.2	0.1	4.9	0.1	5	1
Val9	5.1	0.1	4.7	0.1	5.0	0.6
Gly10	5.25	0.06	4.9	0.1	5.6	0.1
Lys11	4.8	—	5.2	0.1	4.2	0.3
Val13	5.3	0.1	4.9	0.1	5.0	0.4
Ala16	5.52	0.07	5.2	0.1	5.8	0.3
Lys17	4.4	—	4.2	—	4.6	0.06
Lys18	5.10	0.06	4.7	0.1	5.4	0.1
Val19	5.25	0.07	4.9	0.2	5.3	0.6
Ile20	5.3	0.1	4.9	0.2	5.4	0.4
Leu21	5.2	0.3	4.6	0.2	5.9	0.6
Gln22	5.36	0.07	5.0	0.1	5.6	0.3
Asp23	5.5	0.1	5.9	0.2	5.6	0.2
Lys24	5.57	0.07	5.2	0.1	5.7	0.2
Ala27	5.1	0.1	4.7	0.2	5.2	0.3
Gln28	4.56	0.05	4.5	0.1	4.95	0.06

	100 g/L	Error	200 g/L	Error	300 g/L	Error
Ile30	5.5	0.1	5.1	0.1	5.5	0.4
Leu32	5.7	0.1	5.4	0.1	5.5	—
Val34	3.42	0.06	3.17	0.05	3.9	0.1
Arg46	5.37	0.06	5.0	0.1	5.6	0.2
Val47	5.4	0.1	5.0	0.1	6	1
Arg48	5.6	0.1	5.2	0.1	5.9	0.3
Leu49	5.34	0.07	5.0	0.1	5.9	0.3
Phe50	5.27	0.07	4.9	0.1	5.8	0.4
Val51	5.24	0.07	5.0	0.1	5.7	0.4
Asp52	5.27	0.06	5.0	0.1	5.6	0.2
Asp55	3.9	0.1	4.3	0.2	4.6	0.2
Asn56	5.89	0.04	6.1	0.3	6.0	0.2
Ile57	5.70	0.03	5.3	0.1	5.7	0.4
Ala58	5.7	0.1	5.4	0.1	5.8	0.6
Glu59	5.42	0.07	5.1	0.1	5.8	0.3
Arg62	5.26	0.06	4.7	0.1	6.2	0.5
Val63	5.38	0.02	5.0	0.1	5.8	0.4
Gly64	4.16	0.07	3.9	0.1	4.6	0.3

Table A.4 PVP-10 Stabilities

$\Delta G_{op}^{0^*}$ values, and standard errors from three trials (both in kcal/mol) for CI2 residues at 50 (one trial), 100, 200, and 300 g/L **PVP-10**, 50 mM sodium acetate buffer, pH 5.4, 37 °C. Values without error reflect a single datum.

	50 g/L	100 g/L	Error	200 g/L	Error	300 g/L	Error
Trp5	5.2	5.23	0.06	5.06	0.04	5.41	0.05
Leu8	5.2	5.21	0.05	4.7	0.5	4.6	0.3
Val9	5.0	5.17	0.05	4.95	0.07	5.6	0.2
Gly10	5.2	5.31	0.06	5.12	0.04	5.49	0.02
Lys11	—	4.7	0.3	5.2	0.1	4.9	—
Val13	5.2	4.8	0.2	4.6	0.2	4.6	—
Ala16	5.5	5.56	0.04	5.4	0.1	5.71	0.02
Lys17	4.3	4.41	0.05	4.16	0.02	4.35	0.07
Lys18	5.1	5.17	0.05	4.99	0.04	5.27	0.04
Val19	5.2	5.32	0.05	5.1	0.1	6.1	0.2
Ile20	5.3	5.4	0.1	5.2	0.2	5.9	0.2
Leu21	5.1	5.01	0.04	4.8	0.1	5.44	0.07
Gln22	5.4	5.41	0.05	5.19	0.06	5.59	0.03
Asp23	5.2	5.4	0.1	5.5	0.1	5.7	0.3
Lys24	5.5	5.60	0.03	5.45	0.03	5.74	0.03
Ala27	5.0	5.13	0.06	5.0	0.1	5.6	0.3
Gln28	—	4.64	0.03	4.49	0.05	5.3	0.5

	50 g/L	100 g/L	Error	200 g/L	Error	300 g/L	Error
Ile30	5.5	5.5	0.1	5.3	0.1	5.7	0.1
Leu32	5.7	5.8	0.1	5.6	0.1	6.22	0.05
Val34	5.4	3.49	0.05	3.37	0.03	3.73	0.04
Arg46	5.3	5.40	0.07	5.2	0.1	5.60	0.04
Val47	5.3	5.8	0.4	5.4	0.1	6.3	0.6
Arg48	5.5	5.58	0.05	5.42	0.04	5.85	0.05
Leu49	5.3	5.36	0.06	5.20	0.03	5.68	0.07
Phe50	5.2	5.29	0.04	5.12	0.04	5.60	0.06
Val51	5.3	5.35	0.06	5.19	0.07	5.57	0.07
Asp52	5.2	5.27	0.04	5.13	0.03	5.46	0.03
Asp55	—	—	—	5.3	0.4	3.6	0.4
Asn56	5.9	5.89	0.02	5.9	0.1	5.97	0.02
Ile57	5.6	5.68	0.07	5.5	0.1	5.87	0.05
Ala58	5.8	5.8	0.1	5.52	0.02	6.2	0.1
Glu59	5.3	5.4	0.1	5.17	0.07	5.56	0.05
Arg62	5.2	5.7	—	5.52	0.04	6.5	0.4
Val63	5.4	5.42	0.08	5.16	0.04	5.50	0.04
Gly64	4.2	4.18	0.02	4.02	0.04	4.5	0.1

Table A.5 CLEANEX-PM Results

k_{int} values for CI2 at pH 5,4m 37 °C. Values were calculated by SPHERE, values with an asterisk (*) were confirmed by CLEANEX-PM.

Residue	k_{int} (s^{-1})	Residue	k_{int} (s^{-1})
Trp5	0.232	**Val34**	0.941
Leu8	0.157	**Gly35**	1.09*
Val9	0.101	**His37**	5.88*
Gly10	1.09	**Glu41**	0.339*
Lys11	1.09	**Arg46**	0.677
Val13	0.322	**Val47**	0.268
Ala16	0.593	**Arg48**	0.702
Lys17	0.735	**Leu49**	0.353
Lys18	0.968	**Phe50**	0.287
Val19	0.213	**Val51**	0.187
Ile20	0.110	**Asp52**	0.315
Leu21	0.126	**Asp55**	0.268
Gln22	0.571	**Asn56**	1.74
Asp23	0.687	**Ile57**	0.315
Lys24	0.514	**Ala58**	0.475
Ala27	0.593	**Glu59**	0.263
Gln28	0.925	**Arg62**	0.558
Ile30	0.152	**Val63**	0.268
Leu32	0.155	**Gly64**	0.0194

Appendix B
Supplementary Materials for Chapter 5

Table B.1 Stabilities at low salt concentration

$\Delta G_{op}^{0^*}$ values, and standard errors from three trials (both in kcal/mol) for CI2 residues in 50 mM sodium phosphate buffer, pH 5.4, 37 °C with 0, 100, and 200 g/L of BSA and lysozyme. Values without error reflect a single datum.

	Dilute	Error	100 g/L BSA	Error	200 g/L BSA	Error	100 g/L Lysozyme	Error
Trp5	6.7	0.1	6.5	0.1	6.4	0.1	6.2	0.1
Leu8	6.43	0.05	6.24	0.02	6.6	0.3	6.0	0.2
Val9	6.2	0.2	6.0	0.1	5.9455	0.1	5.79	0.01
Gly10	6.0	0.1	5.78	0.01	5.68	0.04	1.8	—
Lys11	—	—	—	—	—	—	6.7	0.1
Val13	6.5	0.1	6.36	0.03	6.3	0.1	5.81	0.02
Ala16	7.0	0.1	6.9	0.2	7.1	0.1	6.59	0.02
Lys17	5.14	0.05	5.00	0.01	4.9	0.1	5.0	0.1
Lys18	6.0	0.1	5.868	0.005	5.8	0.1	5.87	0.03
Val19	7.0	—	—	—	—	—	8	1
Ile20	—	—	—	—	6.3	—	—	—
Leu21	6.6	0.2	6.4	0.1	—	—	2.0	—
Gln22	6.8	0.1	6.65	0.04	6.7	0.1	6.4	0.1
Asp23	6.9	0.1	6.8	0.1	7.1	0.1	2.1	—
Lys24	6.55	0.04	6.44	0.02	6.4	0.1	6.34	0.04
Ala27	5.8	0.1	5.677	0.001	5.6	0.1	5.60	0.03

	Dilute	Error	100 g/L BSA	Error	200 g/L BSA	Error	100 g/L Lysozyme	Error
Gln28	—	—	—	—	5.4	—	—	—
Ile30	7.0	—	6.6	—	—	—	2.2	—
Leu32	6.8	—	6.4	—	6.9	—	—	—
Val34	3.96	0.04	3.90	0.02	3.9	0.1	4.02	0.04
Arg46	6.8	0.1	6.72	0.04	6.7	0.1	6.40	0.04
Val47	7.0	0.1	6.74	0.04	6.59	0.02	—	—
Arg48	7.0	0.1	6.89	0.03	6.9	0.1	6.5	0.1
Leu49	7.0	0.1	6.9	0.1	6.8	0.2	6.16	0.03
Phe50	6.9	0.1	6.7	0.1	7.0	0.1	6.0	0.2
Val51	6.81	0.05	6.75	0.04	—	—	6.2	0.1
Asp52	6.8	0.1	6.7	0.1	6.8	0.1	6.3	0.1
Asp55	6.3	0.1	6.29	0.03	6.4	0.1	5.84	0.03
Asn56	5.46	0.01	5.7	0.1	6.2	—	6.94	0.03
Ile57	7.6	—	6.9	0.2	—	—	2.2	—
Ala58	6.9	0.1	6.8	0.1	7.1	0.1	2.2	—
Glu59	7.2	0.2	—	—	—		8	1
Arg62	6.5	0.1	6.35	0.01	6.3	0.1	6.37	0.03
Val63	7.2	0.1	6.8	0.2	6.8	0.2	6.4	0.2
Gly64	5.5	0.4	—	—	4.72	0.04	—	—

Table B.2 Stabilities at high salt concentrations

$\Delta G_{op}^{0^*}$ values, and standard errors from fitting (both in kcal/mol) for CI2 residues in 50 mM sodium phosphate buffer with 150 mM NaCl, pH 6.5, 20 °C with 0 and 100g/L of BSA. Also are results from CI2 in 50 mM sodium phosphate buffer, pH 6.5, 20 °C with 100 g/L urea. These experiments were performed once, and errors reflect errors in fitting.

	Dilute	Error	100 g/L BSA	Error	100 g/L Urea	Error
Trp5	6.44	0.04	6.5	0.1	5.227	0.003
Leu8	6.26	0.05	6.4	0.1	5.069	0.002
Val9	5.79	0.03	5.89	0.03	5.044	0.003
Gly10	5.84	0.003	5.83	0.01	5.506	0.003
Lys11	—	—	—	—	5.72	0.01
Ser12	—	—	—	—	5.83	0.01
Val13	6.04	0.01	6.45	0.01	5.339	0.002
Ala16	6.86	0.03	—	—	5.515	0.001
Lys17	5.07	0.01	5.05	0.02	5.083	0.003
Lys18	5.945	0.002	5.954	0.004	5.548	0.001
Val19	6.5	0.1	—	—	5.244	0.004
Ile20	—	—	—	—	5.098	0.004
Leu21	5.87	0.02	—	—	4.878	0.003
Gln22	6.59	0.01	6.67	0.03	5.409	0.002
Asp23	6.75	0.02	6.91	0.03	5.76	0.02
Lys24	6.45	0.01	6.52	0.01	5.728	0.004

	Dilute	Error	100 g/L BSA	Error	100 g/L Urea	Error
Ala27	5.773	0.002	5.756	0.003	5.349	0.001
Gln28	—	—	—	—	4.96	0.01
Ile30	—	—	—	—	5.350	0.005
Leu32	—	—	—	—	5.560	0.005
Val34	4.03	0.01	4.02	0.01	4.021	0.002
Arg46	6.73	0.02	6.86	0.03	5.476	0.002
Val47	—	—	—	—	5.307	0.003
Arg48	6.92	0.02	7.02	0.04	5.590	0.002
Leu49	6.75	0.04	7	0.1	5.246	0.002
Phe50	6.66	0.04	7	0.1	5.140	0.002
Val51	6.36	0.05	—	—	5.091	0.002
Asp52	6.55	0.04	7	0.1	5.293	0.003
Leu54	—	—	—	—	4.16	0.01
Asp55	6.17	0.02	6.36	0.03	4.90	0.01
Asn56	5.48	0.03	5.5	0.1	5.602	0.001
Ile57	6.9	0.1	—	—	5.502	0.003
Ala58	6.65	0.03	6.85	0.05	5.718	0.004
Glu59	6.7	0.1	—	—	5.349	0.003
Arg62	6.69	0.02	6.39	0.03	5.443	0.001
Val63	6.61	0.05	6.9	0.1	5.324	0.003
Gly64	—	—	—	—	4.57	0.01